Alma Mater Studiorum – Università di Bologna

DOTTORATO DI RICERCA IN

CHIMICA

Ciclo XXVII

Settore Concorsuale di afferenza: 03/C1

Settore Scientifico disciplinare: CHIM/06

SYNTHETIC STRATEGIES OF NEW SPIN-LABELLED SUPRAMOLECULAR SYSTEMS

Presentata da: **Roberta Manoni**

Coordinatore Dottorato

Prof. Aldo Roda

Relatore

Prof. Marco Lucarini

Esame finale anno 2015

ABSTRACT

Molecular recognition and self-assembly represent fundamental issues for the construction of supramolecular systems, structures in which the components are held together through non-covalent interactions. The study of host-guest complexes and mechanical interlocked molecules, important examples in this field, is necessary in order to characterize self-assembly processes, achieve more control over the molecular organization and develop sophisticated structures by using properly designed *building blocks*. The introduction of paramagnetic species, or spin labelling, represents an attractive opportunity that allows their detection and characterization by the Electron Spin Resonance spectroscopy, a valuable technique that provides additional information to those obtained by traditional methods.

In this Thesis, recent progresses in the design and the synthesis of new paramagnetic host-guest complexes and rotaxanes characterized by the presence of nitroxide radicals and their investigation by ESR spectroscopy are reported. In Chapter 1 a brief overview of the principal concepts of supramolecular chemistry, the spin labelling approach and the development of ESR methods applied to paramagnetic systems are described. Chapter 2 and 3 are focused on the introduction of radicals in macrocycles as Cucurbiturils and Pillar[n]arenes, due to the interesting binding properties and the potential employment in rotaxanes, in order to investigate their structures and recognition properties. Chapter 4 deals with one of the most studied mechanical interlocked molecules, the bistable [2]rotaxane reported by Stoddart and Heath based on the ciclobis (paraquat-p-phenylene) $CBPQT^{4+}$, that represents a well known example of molecular switch driven by external stimuli. The spin labelling of analogous architectures allows the monitoring by ESR spectroscopy of the switch mechanism involving the ring compound by tuning the spin exchange interaction. Finally, Chapter 5 contains the experimental procedures used for the synthesis of some of the compounds described in Chapter 2-4.

TABLE OF CONTENTS

Chapter 1.	Introduction	1
Part 1.	Supramolecular Chemistry	2
1.1.	Concepts	2
1.2.	Host-guest Chemistry	2
1.3.	Self-assembly	3
Part.2.	Spin labelling	5
2.1.	Sensitivity of the method	6
2.2.	Distances between radical centers	8
2.3.	ESR studies of spin-labelled macrocycles	8
2.4.	Mechanical Interlocking Molecules and Free Radicals	10
2.5.	Conclusions	14
References		15
Chapter 2.	Spin labelled macrocycles: Cucurbiturils	17
2.1.	Introduction	18
2.2.	Hystorical background	18
2.3.	Synthesis of CB[n]	19
2.4.	Properties of CB[n]	20
2.5.	Recognition properties of CB[6]	21
2.6.	Control over the recognition processes	23

2.7. Functionalization of CB[n] 24

2.8. Conclusions 31

References 32

Chapter 3. Spin labelled macrocycles: Pillar[n]arenes 34

3.1. Introduction 35

3.2. Synthesis 36

3.3. Functionalization 38

3.4. Host-guest binding properties 40

3.5. Spin labelling 41

3.6. Conclusions 49

References 50

Chapter 4. Spin labelled rotaxanes 51

4.1. Introduction 52

4.2. Spin labelling of rotaxanes 53

4.3. [2]Rotaxanes containing tetrathiafulvalene or 1,5-dioxynaphtalene molecular stations 53

4.3.1. Synthesis and ^{1}H NMR characterization 53

4.3.2. ESR characterization 58

4.4. Supramolecular Control of Spin Exchange in a Spin-Labelled [2]Rotaxane Incorporating a Tetrathiafulvalene Units 59

4.5. Conclusions 66

References 68

Chapter 5. Experimental Section 69

5.1. General information 70

5.2. Synthetic procedures 70

5.2.1. Chapter 2 70

5.2.2. Chapter 3 74

5.2.3 Chapter 4 79

References 92

Introduction

Part 1. Supramolecular Chemistry

1.1 Concepts

Molecular chemistry is concerned with strong interactions called covalent bonds that link atoms together to create ever more sophisticated molecules.
Supramolecular chemistry, defined as 'chemistry beyond the molecule' by Jean-Marie Lehn,[1] who received the Nobel Prize in 1987 for his related studies, introduced the predominant role of non-covalent intermolecular interactions in the construction of molecular assemblies.
Concepts and perspectives of supramolecular chemistry have been well delineated in the last forty years.[2]
It deals with molecular aggregates held together by a variety of non-covalent interactions such as electrostatic forces, hydrogen bonds, π-π stacking interactions, Van der Waals forces and hydrophobic effects.[3]
These interactions are weaker than covalent bonds but all together determine the formation of stable molecular assemblies or complexes. This field has known a great development, starting from the basis of molecular recognition, controlled by the molecular information stored in the interacting species to the application of these ideas in programming ever more complex chemical systems via self-organization processes.[2]
Inspiration came from natural molecules,[4] such as proteins, oligonucleotides, lipids and related self-assembled structures like deoxyribonucleic acid (DNA).
Effectively, molecular recognition is a primary step in any biological process. Enzyme catalysis, protein-protein association, reactant transport and the non-covalent binding of a receptor with a ligand, for instance, implicate the recognition process between two or more molecular binding compounds, leading to their association or rejection. Molecular association is widely investigated, as it generally leads to biological function.[5]

1.2 Host-guest chemistry

Molecular recognition, which is the selective non covalent binding of a specific substrate (or guest) by a receptor molecule (or host) is a key issue in supramolecular chemistry.
In 1967 Donald Cram said that *The host component is defined as an organic molecule or ion whose binding sites converge in the complex… The guest component is any molecule or ion whose binding sites diverge in the complex*.[6]
A *binding site* is a region of the host or guest that is of the correct size, geometry and chemical nature to interact with the other species. In Figure 1 the covalently synthesised host has four binding sites that converge on a central guest binding pocket.
Thus, the host is described as a molecule significantly large that can encircle a smaller molecule termed guest.

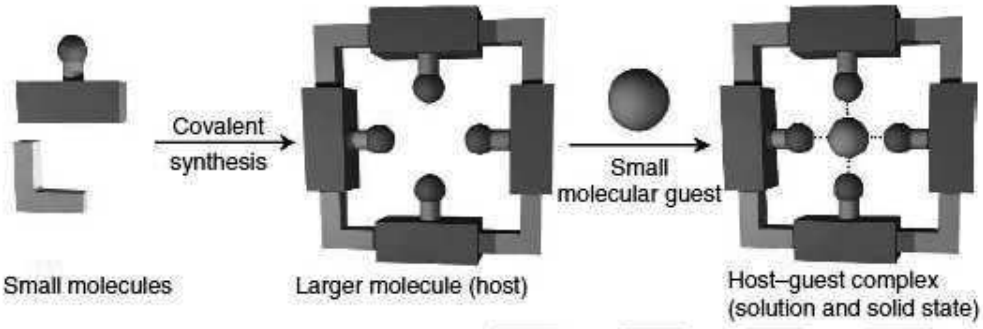

Figure 1. Host-guest complexation.[3]

Rigid host compounds with permanent binding cavities and fixed interacting sites show enhanced complexation properties than flexible receptors, both in solution and in the solid state.
Otherwise the presence of host-guest complexes only as crystalline solids where the guest is bound to a cavity formed in the packing of the host lattice at the solid state can be detected.
Such compounds are termed clathrates from the greek klethra, meaning bars (Figure 2).

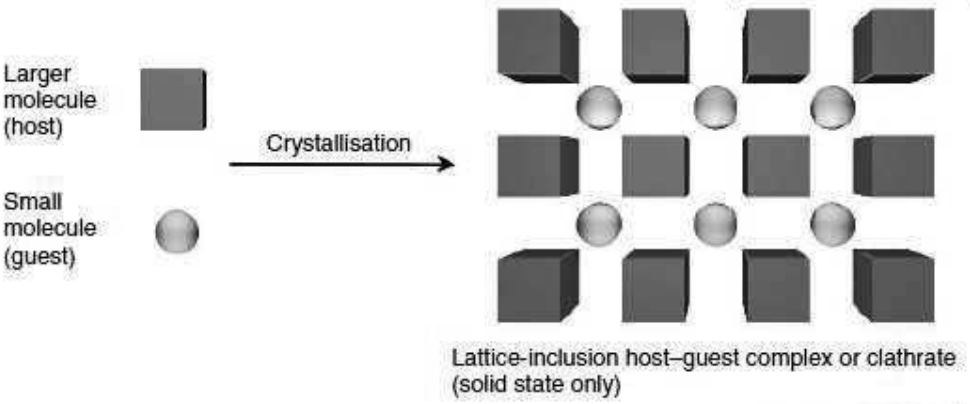

Figure 2. Lattice inclusion.[3]

Selectivity is determined by complementarity of shape and interacting sites between host and guest, according to Emil Fischer that, in 1894, compared the mechanism of interaction between enzyme and substrate to the key and lock model, suggesting that this is a fundamental prerequisite for molecular recognition.[3]
Several receptors able to selectively bind specific substrates have been developed; they perform molecular recognition, based on the molecular information stored in the interacting compounds.[1]
Examples of host molecules are crown ethers, cryptands, calixarenes, cyclodextrins, cucurbiturils, cyclophanes and pillararenes.

1.3 Self-assembly

The further step is represented by supramolecular self-assembly, the spontaneous and reversible association of molecular components in complex ordered architectures through non covalent forces (Figure 3).

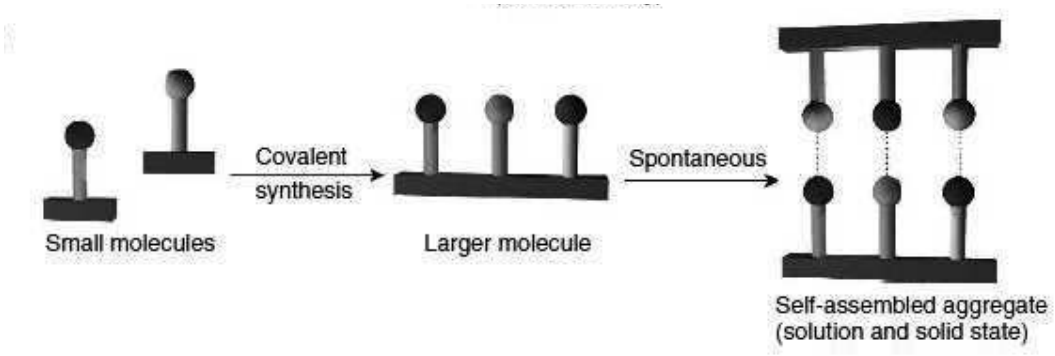

Figure 3. Self-assembly between complementary molecules.[3]

Because of these weak interactions the amount of energy required for creating or destroying self-assembled structures is relatively small compared to covalent interactions.
Thus, one important characteristic of these systems is the dynamic nature that allows the preparation of functional smart materials with properties that can be tuned and modulated by external stimuli such as light or temperature.
Self-organization[2] process may be directed via the molecular information stored in the covalent framework of the components and read out at the supramolecular level. The implementation of molecular information in programming chemical structures towards self-organization processes can be obtained by careful design or selection of specific components.
Thus self-assembly takes place by combining properly designed subunits that contain in themselves the information necessary to create the self-assembled architecture in terms of position and directionality of their binding sites, distribution of electron density over their surfaces or their oxidation states.
DNA is an important example of self-assembled biological system.
Mechanical interlocked molecules such as rotaxanes and catenanes are important example of supramolecular self-assembly driven by non-covalent interactions in which the components are kinetically trapped and can not be separated without breaking covalent bonds.

Figure 4. Schematic representation of a rotaxane and a catenane.

Species that are linked in this way are said to be topologically connected. The great interest in such systems derives from their use as nanoscale molecular machines and molecular electronic devices, considering also their potential use for the storage of information.
Rotaxanes consist of a macrocycle encircling an axle that is blocked at the ends by bulky groups that prevent the macrocycle from unthreading.
According to one of the synthetic strategies commonly used, the macrocycle, driven by non-covalent interactions, first encircles the thread and then bulky stoppers at the ends are covalently linked in order to avoid the dissociation of the complex and allow the creation of the rotaxane.
Catenanes show two or more interlocked macrocycles and can be prepared exploiting the supramolecular preorganization of the precursors through non-covalent interactions.
Design and synthesis of novel supramolecular architectures and a high level of control over their shape and size have, therefore, become the goal for many scientists both in biologic and chemical fields.[4]
In particular, an in-depth knowledge in host-guest systems and mechanical interlocked molecules (MIM) is required in order to explain the mechanism of self-assembly, gain progressive control over the organization of matter and develop new sophisticated structures by the spontaneous but controlled arrangement of suitably instructed and functional *building blocks*.[7]

Part 2. Spin labelling[8,9]

The reversible and dynamic nature of host-guest complexes matches with only a few methods suitable for their characterization, in particular for measuring the kinetics of association and dissociation processes, which occur in the microsecond and submicrosecond time range.[10]
Remarkable changes observed in the spectrum upon the complexation process make NMR spectroscopy one of the most important methods for the investigation of such complexes. In general, the replacement of the original peaks with only one signal at an intermediate mean-weighted position between the signals of free and complexed molecules can be detected.[11] This because fast exchange is common for complexation processes and this technique operates at a time scale relatively slow.
On the other hand, ESR spectroscopy makes possible to extend the time range of supramolecular kinetics accessible to resonance methods to the microsecond region[10b] and to recognize different modes of complexation, allowing the investigation of usually undetectable (by NMR) microequilibria.
This technique operates at a shorter time scale compared to that of complexation processes, originating discrete signals from free and complexed species when the radical involved is sensitive to the environmental changes with a subsequent modification of the spectroscopic parameters upon complexation.[10b]
The sensitivity of the method, the possibility of obtaining kinetic information on the formation of complexes in the microsecond range[12] and the ability to measure distances between radical moieties at the nanometer scale[13] are important features of this technique.
Unfortunately, most of supramolecular structures do not contain paramagnetic fragments, and in order to obtain an ESR signal a free radical must be introduced in the system. Although any free radical or paramagnetic metal ion or even a group with an accessible triplet state,[14] could be used, most of the reported spin labelling studies exploit organic nitroxide radicals as spin labels.[15]

They can be introduced either covalently (spin labels) or non-covalently (spin probes).
Nitroxides represent an important class of radicals, enclosing stable structures such as the popular 2,2,6,6-tetramethylpiperidine-*N*-oxyl (TEMPO) **1** (Scheme 1) and its derivatives.

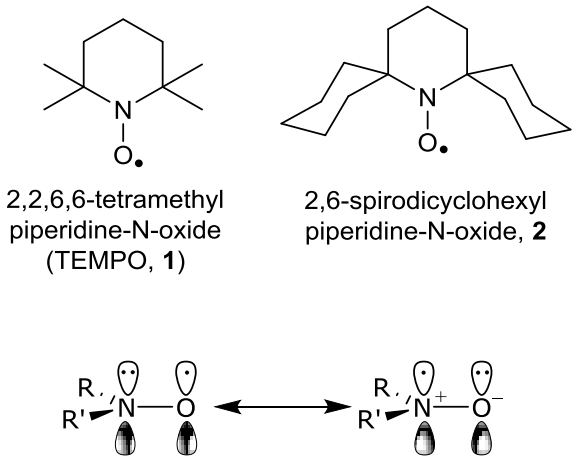

Scheme 1. Some representative nitroxide radicals and their resonance structures.

The electronic structure shows that three π electrons are distributed over two atomic centers and, as a result, nitroxides do not undergo dimerization.
Moreover, their lifetime is determined by the ability to react with themselves by disproportionation to afford the corresponding hydroxylamine and nitrone (Scheme 2) and the lack of hydrogens at the beta position in sterically hindered nitroxides prevents this reaction.

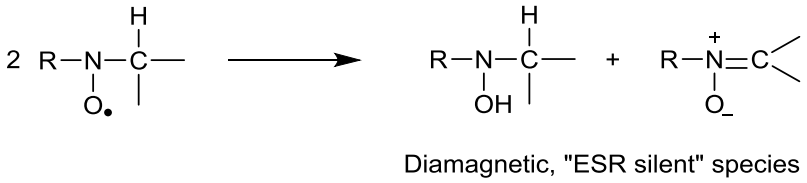

Scheme 2. Disproportionation decay for a dialkyl nitroxide containing a hydrogen atom at β-position.

The versatility of these radicals is due to the opportunity of behaving like diamagnetic compounds, with the possibility, mostly, of performing organic reactions on molecules carrying a nitroxide group without affecting the radical site itself.

2.1 Sensitivity of the method

ESR spectra depend on the motional dynamics of the radical and on various parameters such as polarity, molecular oxygen concentration, pH, etc. that characterize the free radical microenvironment.
Nitroxides are characterized by a hyperfine interaction between the unpaired electron and the ^{14}N nucleus (I =1) that gives rise to a splitted ESR signal in three lines whose distance is related to the corresponding isotropic nitrogen hyperfine splitting constant, a_N (Figure 5a).

The nitrogen coupling constant a_N is known to be very sensitive to the nature of the environment, in particular increases when the radical center is in a polar medium[16] and decreases in a hydrophobic environment, that is what happens in the complexation process.
Therefore, changes of a_N generally give evidence of the formation of a complex between nitroxide radicals and host compounds.

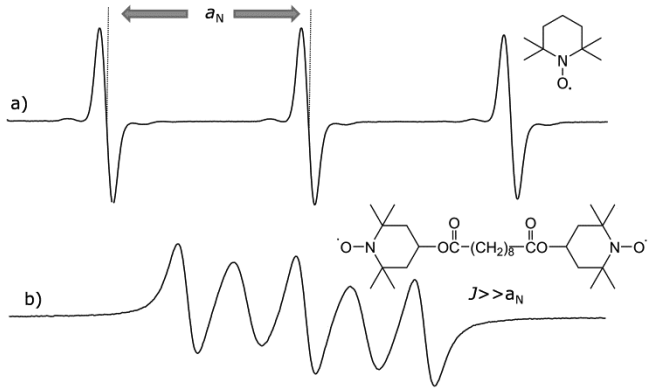

Figure 5. ESR spectra of TEMPO (a) and a bis(nitroxide) (b) showing an exchange interaction (*J*).

As mentioned before, nitroxides in terms of spectroscopic parameters are affected by changes in the surrounding medium. In particular, the complexation process, when a nitroxide probe is employed, induces a considerable modification in the medium that surrounds the radical moiety because the distribution of the nitroxide probe from the solvent into the hydrophobic environment of the host occurs and consequently a modification of the hyperfine coupling constant is observed.
As mentioned before, ESR spectroscopy is usually characterized by a shorter time scale compared to that of complexation processes and, accordingly, spectra are characterized by separate signals for free and complexed compounds when the nitroxide used shows different a_N values for the two species[10b] thus, it is possible to obtain kinetic information on different host–guest complexation events.[17]
Finally, ESR spectra reflect the probe's motional dynamics which depends mainly on the local viscosity,[8, 18-20] on the tumbling of the macromolecule and the flexibility of the backbone of the whole structure. Therefore, another important evidence of the formation of the spin-labelled complex is represented by the analysis of the correlation time, τ_c, the parameter generally used for describing mobility in ESR studies, namely the characteristic time during which a molecule turns over ca. 1 radian. Effectively, a decrease in the tumbling rate and mobility of the nitroxide upon the inclusion in the host compound is reliable and expected.

2.2 Distances between radical centers

ESR technique is a sensitive method that allows to get spatial information as well (distance between radical moieties).
In particular, the degree of through-space spin exchange coupling (*J*) between two nitroxides can be investigated: CW-ESR spectra carry relevant information on structures containing two radicals relatively close in space.[21] An insignificant spin exchange interaction between the two radical fragments originates a spectrum characterized by three lines. On the contrary, if the spin exchange coupling is large enough ($J >> a_N$), the spectrum exhibits five signals (see Figure 5b), due to the short distance between the two spins.
In particular, the spectra can show a simple three-line spectrum (1:1:1 intensities) or a five-line spectrum (1:2:3:2:1 intensities) when the spin system is completely delocalized.[19,22,23] It is possible, for example, to follow the binding process of a guest, analyzing changes in the distance between the spin centers.
If two or more nitroxide labels are located in a supramolecular assembly at distances from 1.5 to 8 nm, measurements of distances between the nitroxide labels are possible by using pulsed ESR techniques like PELDOR (pulse electron double resonance).[24]
Beside to this analysis, ESR spectroscopy can be exploited for concentration measurements. The absorption of microwave energy in a sample is directly proportional to the number of spin labels present. Thus the total number of spin labels (and the purity of the spin labelled sample) may be measured by integration of the ESR signals.[23]

2.3 ESR studies of spin-labelled macrocycles

As mentioned above, when a radical probe is employed as the included species in a specific host (Scheme 3), changes of its spectroscopic parameters allow to gain significant information about the complexation process. For example, the decrease in the nitrogen hyperfine splitting a_N related to the less polar environment of the host cavity gives evidence of the formation of the complex.

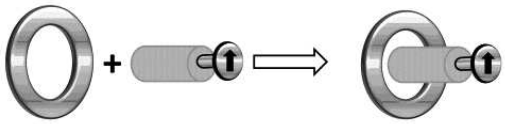

Scheme 3. Schematic representation of spin-labelled host-guest complex employing the nitroxide as a probe.

Besides, spin labelled hosts have attracted great attention in order to investigate complexes including diamagnetic guests, therefore, persistent nitroxide units have been covalently attached to macrocycles, such as cyclodextrins.

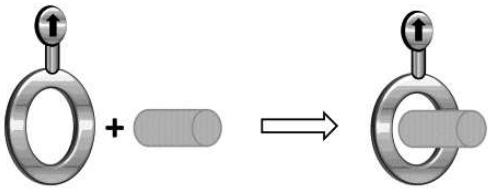

Scheme 4. Schematic representation of spin-labelled host-guest complex having the nitroxide covalently bound to the macrocycle.

Cyclodextrins (CDs) are a well-known family of natural cyclic oligosaccharides made up of 6, 7, or 8 D-glucose units, characterized by a chiral hydrophobic internal cavity and a hydrophilic external surface.

They are able to form in water a wide range of inclusion complexes with suitable guest molecules, consequently, their functionalization with radical moieties has been investigated (Scheme 4) and several examples are known in literature.[25-28]

Unlike the inclusion of the nitroxide inside the host cavity, when the radical is located at the rim of the macrocycle, it does not experience remarkable changes in terms of environment, especially when the included guest is a small molecule. However, considerable information can be obtained analyzing larger host-guest complexes because the ESR technique is able to detect a substantial reduction in the rate of tumbling. In particular, spectra of spin-labelled CDs in water show a broadening of the high field line due to the restricted tumbling.

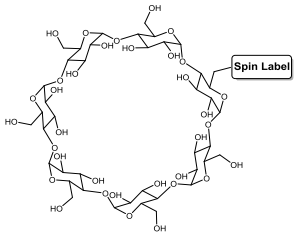

Scheme 4. Spin labelled cyclodextrins at 6-position.

Several studies performed on spin-labelled CDs, for example, made possible to monitor recognition events in which large molecules such as polymers[29] or hydrogels[30] are involved.

Tordo's group also reported the synthesis of a mono spin-labelled permethylated CD (β-CD-1 **Scheme 5**) and analysed the self-inclusion process of the paramagnetic moiety covalently attached to the CD core.[31]

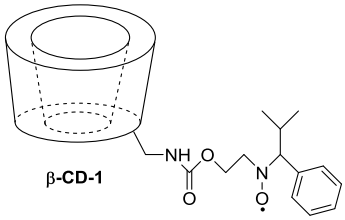

Scheme 5. Structure of **β-CD-**

In aqueous solution, the ESR spectrum of β-CD-1 shows asymmetric shape due to a strong broadening of the two lines resonating at higher magnetic field. A good simulation of this spectrum could be achieved only by assuming the presence of a fast exchange between two nearly equally populated species, one with the nitroxide moiety outside of the cavity and the other showing a self-, weak inclusion of the aromatic group inside the cavity.[32] The reported examples are just a few of the investigations focused on spin-labelled macrocycles and, in the next chapters, studies on different macrocycles, such as cucurbiturils, pillararenes, cyclophanes and related supramolecular structures will be presented.

2.4 Mechanical Interlocking Molecules and Free Radicals

Probably, one of the most attractive aspects of self-assembly is represented by mechanical interlocked architectures, in which two or more molecules are kinetically trapped not through covalent bonds, but as a result of their topology, their shape, through weak non covalent interactions.[33,34] In particular, a chemical bond must be broken in order to separate the individual components of the assembly from each other, therefore, they are defined as topologically connected. As mentioned before, rotaxanes represent an interesting example of interlocked structures in which a linear molecule is threaded through a macrocycle and two large units called stoppers, located at the opposite ends of the thread, prevent the components from dissociation. Another example of topologically connected species is represented by catenanes that are mechanically interlocked macrocycles.
Thus, the possibility of using ESR spectroscopy for detecting these systems is attractive in order to extend the current knowledge on rotaxanes or catenanes in addition to other traditional techniques. Effectively, several information can be gained from ESR spectra.
In 2006, our group reported the first example of a spin-labelled rotaxane consisting of a complex between the dumbbell component and α-CD as the wheel, locked by TEMPO units (**Rot-1**, Scheme 6).[35]

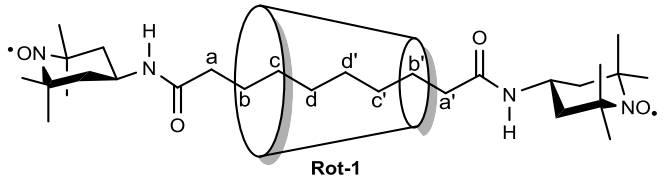

Scheme 6. Synthesis and structure of **Rot-1**.

In this paramagnetic architecture ESR spectroscopy was clearly able to confirm the rotaxane structure comparing the spectrum of the dumbbell with that of the corresponding rotaxane **Rot-1** (Figure 5). The typical spectrum of a diradical with five lines is detected for the dumbbell, while the rotaxane shows the three-lines spectrum of a mononitroxide, because it takes an extended conformation reducing the probability of interactions between the TEMPO moieties.

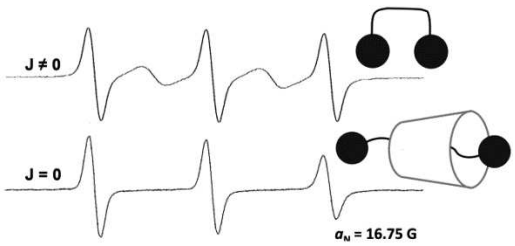

Figure 5. ESR spectra of **Rot-1** (bottom) and of the corresponding free thread (up) recorded in water.

In 2008 a [1]rotaxane-type[27] based on a β-cyclodextrin and a nitroxide probe was prepared. In this molecule, the self-inclusion of the nitroxide group - covalently bound to one of the CD rim - inside the cavity is detected .

In particular, as showed in Scheme 7, treatment of nitroxide **3a** and **3b** with 6-mercapto-β-cyclodextrin **6-SH-β-CD** in alkaline water generates two different forms of TEMPO-functionalized CD, one locating the paramagnetic side arm outside the cavity **β-CD-2** and the other showing the trapped radical **β-CD-3**.

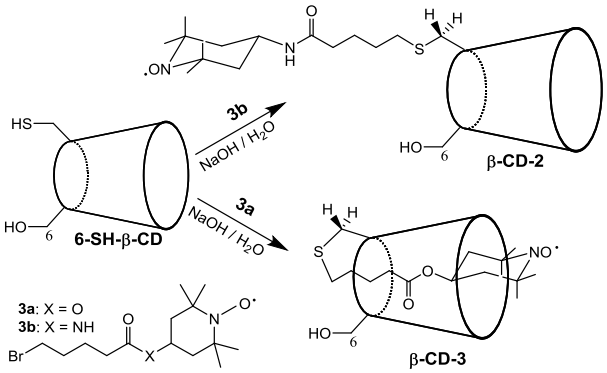

Scheme 7. Synthesis and structure of **β-CD-2** and **β-CD-3**.

ESR spectra of the two radical species exhibit peculiar features. Comparing the spectrum of the free linear nitroxide **3a** to the paramagnetic **β-CD-3**, a considerable decrease of a_N in water revelead the presence of a complexation process, thus, it was assigned to a geometry in which the piperidine ring was strongly self-included within the hydrophobic cavity of the β-CD. On the other hand, the smaller variation of the nitrogen coupling constant between the open **β-CD-2** and the free dumbbell was not compatible with an interlocked radical species but with a weak self-complexing nitroxide. In order to evaluate the effective presence of the interlocked structure, addition of sodium dodecyl sulphate, a competitive guest for **β-CD,** able to displace the nitroxide from the internal cavity, was performed. In these experiments, however, the spectrum of **β-CD-3** did not change in the presence of the competing species, confirming the irreversible nitroxide trapping inside the CD cavity (see Figure 6).

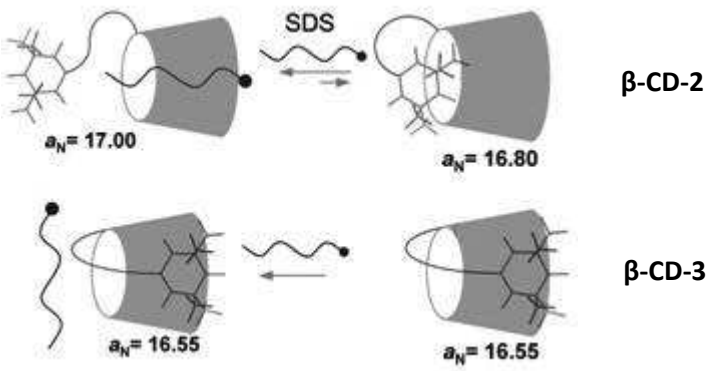

Figure 6. Schematic representation of equilibria involving **β-CD-2** and **β-CD-3**.

Moreover, spin-labelling in which the radical moiety is located both on the macrocycle and the guest compound has been explored (Scheme 8).

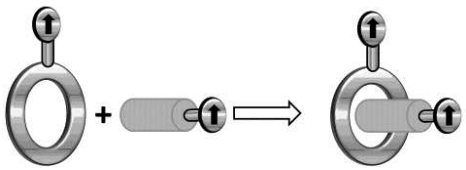

Scheme 8. Schematic representation of a double spin-labelled host-guest complex in which both guest and host are spin labelled.

Recently, a double spin-labelled α-CD-based [2]rotaxane showing two persistent nitroxide radicals at the wheel and the dumbbell was synthesized.[28]
As shown in Scheme 9, taking into account the unsymmetrical structure of both the ring and the axle, on the base of the orientation of the CD along the thread upon the rotaxanation process a mixture of isomers could be predicted, defined as 'close' and 'far' isomers relatively to the distance between the two radical moieties.

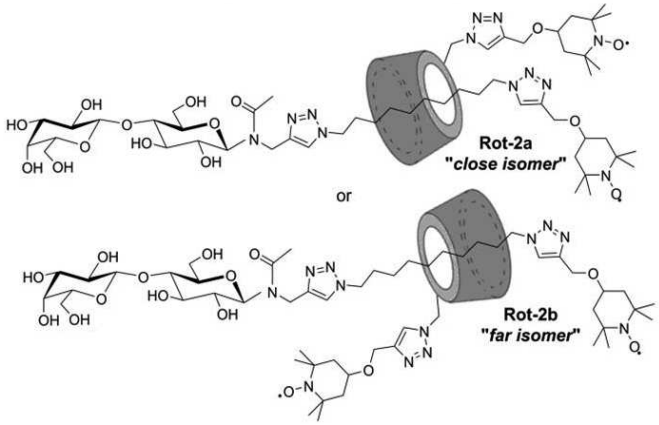

Scheme 9. Structure of bis-labelled rotaxanes.

^{1}H NMR studies revealed that only one isomer was isolated but they did not allow to assign the correct geometry of the complex. This information was achieved, on the contrary, by combining the information extracted from the ESR spectrum (characterized by the presence of spin exchange) and molecular dynamic calculations that identified the isolated isomer as the "*close isomer*" (Figure 7).

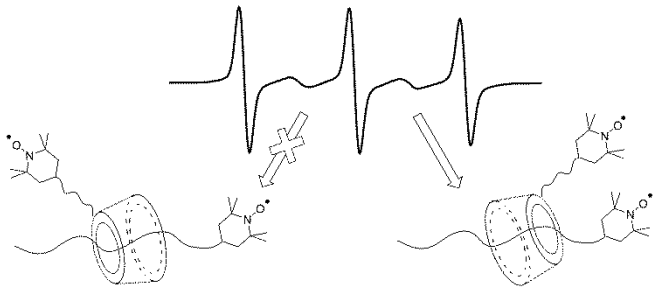

Figure 7. ESR spectrum of **Rot-2a** recorded in water at 328 K.

Interesting information were obtained also through the PELDOR technique, a pulsed ESR spectroscopy based on dipolar interactions that can be used to estimate distances between radical centers in a range of 1.4-8 nm, compatible with supramolecular architectures.
In particular, a rotaxane based on the macrocycle cucurbit[6]uril was investigated by our group in 2012 (Figure 8).[36]

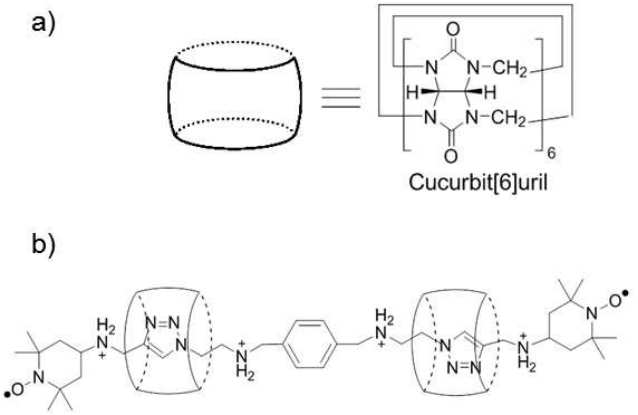

Figure 8. a) Structure of a Cucurbit[6]uril and b) structure of the rotaxane employing this macrocycle as the wheel.

Thanks to the introduction of the two terminal nitroxide units in a quite rigid structure, it was possible to obtain, for the first time, the exact distance between paramagnetic centers using PELDOR technique. In this case, the PELDOR trace, recorded at the Max Planck Institute for Biophysical Chemistry of Gottingen was in agreement with a distance of 3.06 nm.
Accordingly, spin-labelling in rotaxanes is a powerful tool also to investigate the behavior of molecular devices.
Rotaxanes, actually, are attractive, for example, as potential molecular machines[37-39].

Developments in this field are allowed by a specific design of the thread with the introduction of two or more different binding sites for the macrocycle along the axle. This architecture makes possible to move the ring back-and-forth along the thread, driven by external factors, either chemically,[40] electrochemically,[41] or photochemically[42], achieving a structure so called 'molecular shuttle'.
In particular, a π-electron-deficient tetracationic cyclophane ring, cyclobis(paraquat-*p*-phenylene) $(CBPQT)^{4+}$, is one of the most versatile host involved in the preparation of molecular devices proposed by the Stoddart's group[43] (Figure 8).
In the next chapters one of the most promising candidates for a programmable molecular switch, the "Stoddart–Heath type" bistable [2]rotaxane will be reported and investigated.

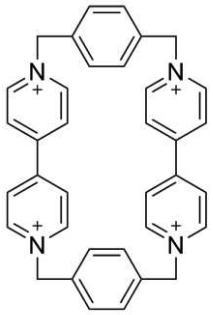

Figure 8. Structures of cyclobis(paraquat-*p*-phenylene) $(CBPQT)^{4+}$.

2.5 Conclusions

Specific design criteria are necessary in order to obtain control over the molecular assembly.
Great targets of modern chemistry, thus, involve the reproducibility in supramolecular synthesis and the design and construction of synthetic systems able to store and transfer information at the supramolecular level through molecular recognition processes.
Moreover, the introduction of paramagnetic centers in different supramolecular structures, like rotaxanes, makes the ESR spectroscopy a suitable method to detect these systems.
Nowadays a wide set of spin-labelled macrocyclic hosts have been synthesized and characterized. Interesting topic is the continuous development in this field employing spin-labelling in mechanically interlocked molecules as molecular machines because this can represent a first step towards a new generation of nanoscale magnetic switches that may be of interest for information and communication technology applications.

References

[1] J. M. Lehn, *Pure and Applied Chemistry*, **1978**, *50*, 871-892.

[2] J. M. Lehn, *Angew. Chem., Int. Ed. Engl*., **1988**, *27*, 89-112.

[3] J. W. Steed, D. R. Turner, K. J. Wallace, *Core Concepts in Supramolecular Chemistry and Nanochemistry*, Wiley & Sons, Ltd, Chichester, UK, **2007**.

[4] D. A Uhlenheuer, K. Petkau, L. Brunsveld, *Chem. Soc. Rev.*, **2010**, *39*, 2817-2826.

[5] R. Baron, J. A. McCammon, *Annu. Rev. Phys. Chem.*, **2013**, *64*, 151-75.

[6] D. J. Cram, *Angew. Chem. Int. Ed. Engl*., **1986**, *25*, 1039-1134.

[7] J. M. Lehn, *Angew. Supramolecular Chemistry: Concepts and Perspectives*, VCH, Weinheim, **1995**.

[8] M. Lucarini, *Encyclopedia of Radicals in Chemistry, Biology and Materials*, Vol. 2 (Eds. C. Chatgilialoglu, A. Studer), John Wiley & Sons Ltd, Chichester, **2012**, pp 229-248.

[9] E. Mezzina, R. Manoni, F. Romano, M. Lucarini, *Asian Journal of Organic Chemistry*, **2015**, doi: 10.1002/ajoc.201402286

[10] a) M. Eigen, *Pure Appl. Chem*., **1963**, *6*, 97-115; b) W. M. Nau, X. Wang, *ChemPhysChem*., **2002**, *3*, 393-398.

[11] H. J. Schneider, F. Hacket, V. Rüdiger, *Chem. Rev.*, **1998**, *98*, 1755-1786.

[12] P. Franchi, M. Lucarini, G. F. Pedulli, *Curr. Org. Chem.*., **2004**, *8*, 1831-1849.

[13] R. E. Martin, M. Pannier, F. Diederich, V. Gramlich, M. Hubrich, H. W.Spiess, *Angew. Chem., Int. Ed. Engl.*, **1998**, *37*, 2833-2837.

[14] M. Di Valentin, M. Albertini, E. Zurlo, M. Gobbo, D. Carbonera, *J. Am. Chem. Soc.*, **2014**, *136*, 6582-6585.

[15] D. Bardelang, M. Hardy, O. Ouari, P. Tordo, *Encyclopedia of Radicals in Chemistry, Biology and Materials, Vol. 4* (Eds. C. Chatgilialoglu, A. Studer), John Wiley & Sons Ltd, Chichester, **2012**, pp 1-51.

[16] P. Franchi, M. Lucarini, P. Pedrielli, G. F. Pedulli, *ChemPhysChem*., **2002**, *3*, 789-793.

[17] M. Lucarini, L. Pasquato, *Nanoscale*, **2010**, *2*, 668-676.

[18] M. Lucarini, E. Mezzina, *Electron Paramagnetic Resonance: (Specialist Periodical Reports)*, *Vol. 22.*, (Eds. B. C. Gilbert, V. Chechick, D. M. Murphy), RSC Publishing, Cambridge, UK, **2010**, pp. 41-70.

[19] J. A. Weil, J. R. Bolton, J. E. Wertz, *Electron Paramagnetic Resonance: Elementary Theory and Practical Applications*, John Wiley & Sons Inc., New York, **1994**.

[20] V. Chechik, A. Caragheorgheopol in *Electron Paramagnetic Resonance (Specialist Periodical Reports), Vol. 20*. (Eds. B. C. Gilbert, M. J. Davies D. M. Murphy), RSC Publishing, Cambridge, **2007**, pp. 96-130.

[21] M. Abe, *Chem. Rev.*, **2013**, *113*, 7011-7088.

[22] N. M. Atherton, *Principles of Electron Spin Resonance*, Ellis Horwood and Prentice Hall, Chichester, **1993**.

[23] *Electron Paramagnetic Resonance: a practitioner's toolkit*, (Eds. M. Brustolon, E. Giamello), John Wiley & Sons Inc., Hoboken, New Jersey, **2009**.

[24] M. Pannier, S. Veit, A. Godt, G. Jeschke, H. W. Spiess, *J. Magn. Reson.*, **2000**, *142*, 331-340.

[25] G. Ionita, V. Chechik, *Org. Biomol. Chem.*, **2005**, *3*, 3096-3098.

[26] R. K. Strizhakov, E. V. Tretyakov, A. S. Medvedeva, V. V. Novokshonov, V. G. Vasiliev, V. I. Ovcharenko, O. A. Krumkacheva, M. V. Fedin, E. G. Bagryanskaya, *Appl. Magn. Reson.*, **2014**, *45*, 1087-1098.

[27] P. Franchi, M. Fanì, E. Mezzina, M. Lucarini, *Org. Lett.*, **2008**, *10*, 1901-1904.

[28] C. Casati, P. Franchi, R. Pievo, E. Mezzina, M. Lucarini, *J. Am. Chem. Soc.*, **2012**, *134*, 19108-19117.

[29] V. Chechik, G. Ionita, *Org. Biomol. Chem.*, **2006**, *4*, 3505-3510.

[30] a) G. Ionita, V. Chechik, *Chem. Commun.*, **2010**, *46*, 8255–8257; b) G. Ionita, M. Florent, D. Goldfarb, V. Chechik, *J. Phys. Chem. B,* **2009**, *113*, 5781-5787.

[31] a) D. Bardelang, A. Rockenbauer, L. Jicsinszky, J.-P. Finet, H. Karoui, S. Lambert, S. R. A. Marque, P. Tordo, *J. Org. Chem.,* **2006**, *71*, 7657-7667; b) D. Bardelang, J. P. Finet, L. Jicsinszky, H. Karoui, S.R.A. Marque, A. Rockenbauer, R. Rosas, L. Charles, V. Monnier, P. Tordo, *Chem. Eur. J.*, **2007**, *13*, 9344-9354.

[32] O. A. Krumkacheva, M. V. Fedin, D. N. Polovyanenko, L. Jicsinszky, S. R. A. Marque, E. G. Bagryanskaya, *J. Phys. Chem. B*, **2013**, *117*, 8223-8231.

[33] D. H. Rouvray, R. B. King, eds., *Topology in Chemistry-Discrete Mathematics of Molecules*, Horwood Publishing, Chichester, **2002**.[34] J. P. Sauvage and C. Dietrich-Buchecker, eds., *Molecular Catenanes, Rotaxanes and Knots-A Journey Through the World of Molecular Topology*, Wiley-VCH Verlag GmbH, Weinheim, **1999**.

[35] E. Mezzina, M. Fanì, F. Ferroni, P. Franchi, M. Menna, M. Lucarini, *J. Org. Chem.*., **2006**, *71*, 3773-3777.
[36] R. Pievo, C. Casati, P. Franchi, E. Mezzina, M. Bennati, M. Lucarini, *ChemPhysChem*., **2012**, *13*, 2659-2661.
[37] L. Raehm, J. P. Sauvage, *Struct. Bonding*, **2001**, *99*, 55-78.
[38] J. F. Stoddart, H. M. Colquhoun, *Tetrahedron*, **2008**, *64*, 8231-8263.
[39] J. F. Stoddart, *Chem. Soc. Rev.*, **2009**, *38*, 1802-1820.
[40] M. C. Jìmenéz, C. Dietrich-Buchecker, J. P. Sauvage, *Angew. Chem. Int. Ed.*, **2000**, *39*, 3284-3287.
[41] A. Altieri, F. G. Gatti, E. R. Kay, *et al*., *J. Am. Chem. Soc.*, **2003**, *125*, 8644-8653.
[42] A. Livoreil, J. P. Sauvage, N. Armaroli, *et al*., *J. Am. Chem. Soc.*, **1997**, *119*, 12114-12124.
[43] V. Balzani, A. Credi, F. M. Raymo, J. F. Stoddart, *Angew. Chem., Int. Ed.*, **2000**, *39*, 3349-3391.

Spin labelled macrocycles: Cucurbiturils

Chapter 2. Spin labelled macrocycles: Cucurbiturils

2.1 Introduction

Cucurbit[n]urils[1,2] are a family of synthetic cyclic molecules consisting of 5 to 10 glycoluril units characterized by a hydrophobic cavity accessible through two identical carbonyl portals. The peculiar name came out from the similarity of their shape to a pumpkin, member of the Cucurbitaceae family.
Similarly to cyclodextrins, in water the rigid structure and the hydrophobic cavity of cucurbiturils provides a potential site for inclusion of many organic molecules, including pharmaceuticals, through a wide range of non-covalent interactions.
Great interest in the supramolecular community have been generated thanks to the exciting recognition properties in aqueous medium.
In addition, specific chemical modifications can provide useful properties to be exploited, extending their potential employment, and from this point of view, the functionalization with a radical moiety represents a target that includes the ESR spectroscopy among the analytical methods available for their characterization.

2.2 Hystorical background

The first discovery of these molecules dates back to more than 100 years ago.
In 1905, Behrend and coworkers performed under strongly acidic conditions the condensation of glycoluril (**1,** Figure 1) and formaldehyde, obtaining ‘‘white, amorphous compounds, which are weakly soluble in dilute acid and base, and absorb large quantities of water without losing their dusty powdery character’’.[3]
Nevertheless, they were identified as macrocyclic molecules only in 1981 by Mock and co-workers that, revisiting Behrend’s studies, achieved the crystallization of a hydrated macrocycle complexed with calcium sulfate, leading to the exact structure that consists of six glycoluril units and twelve methylene bridges, interacting with the calcium cations via its two carbonylated portals.[4]
This structure is known as cucurbit[6]uril, generally abbreviated CB[6], in which ‘6’ represents the number of glycoluril units in the macrocycle.
In this study, they also found out that CB[6] is able to bind alkylammonium cations.
Aside from CB[6], others CB[n] analogs should have been identified in the mixture under the conditions reported by Mock[5], but only 20 years later, performing reactions under milder and kinetically controlled conditions, the isolation and characterization of three new members of the CB[n] family were reported by Kim and coworkers (CB[5], CB[7] and CB[8]).[6]
Moreover, Day et al. identified[5] and crystallized[7] the interlocked complex CB[5] ⊂ CB[10].
Consequently to these developments, a great interest in this new macrocyclic family has grown fast, related with the great advances in many areas of fundamental and applied science as chemistry, biology, materials science, and nanotechnology, that rely on the ability to employ and control non-covalent interactions between molecules.

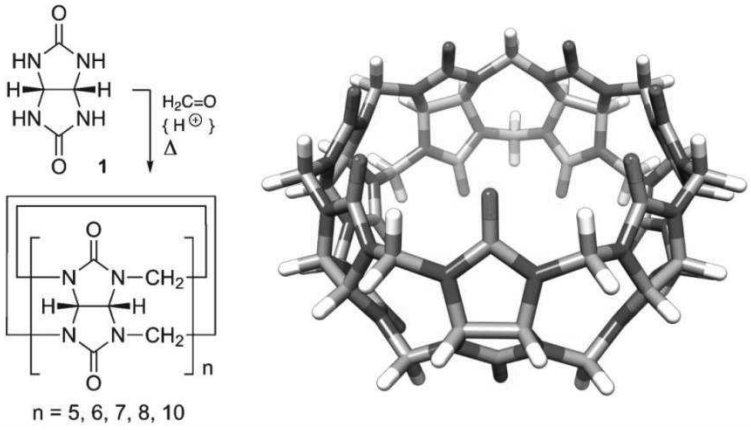

Figure 1. Preparation of CB[n]s from glycoluril (**1**) and formaldehyde under acidic conditions. Structure of CB[7] from X-ray diffraction (carbon atoms in grey, hydrogens in white, nitrogens in blue and oxygens in red).

2.3 Synthesis of CB[n]

The general scheme for the preparation of these compounds is based on Day,[5] Kim[6] and Isaacs[8] works.

Glycoluril reacts with aqueous formaldehyde or paraformaldehyde, and hydrochloric or sulfuric acid (concentrated, or diluted to approximately 5 M) at 80-100°C during 10-100 h. A mixture of CB[n] (n = 5–8, mostly CB[6]) and small amounts of CB[5] ⊂ CB[10], and other oligomers are reported. Purification of each compound is based on their differential solubility in water, water/methanol and diluted hydrochloric acid solutions (see Figure 2a).[8]

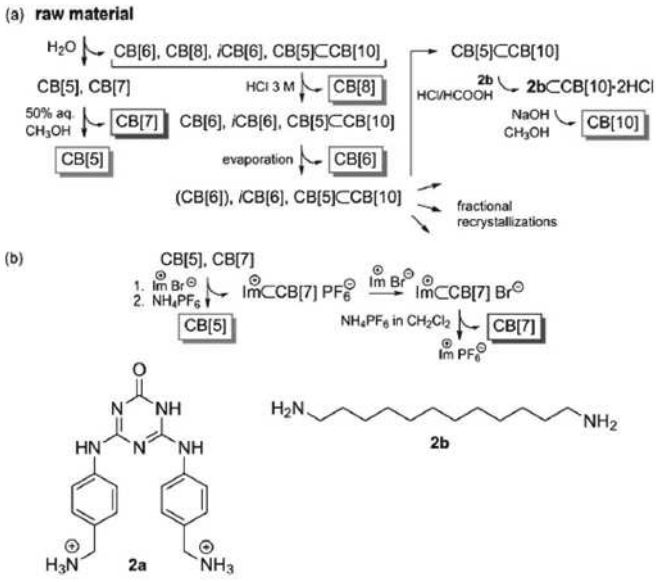

Figure 2. Purification of CB[n]s: (a) General procedure;[8] (b) alternate method for the separation of CB[5] and CB[7].[9] Curved arrows indicate precipitation.

Day[5] was able to separate CB[7] from the mixture of CB[n] by using a hot 20% aqueous solution of glycerol with good selectivity. Scherman, instead, reported a different method to separate CB[5] from CB[7] (see Figure 2b): CB[7] could be complexed in water with 1-alkyl-3 methylimidazolium bromides (Im^+Br^- in Figure 2b) and subsequent anion exchange with ammonium hexafluorophosphate ($NH_4^+PF_6^-$) allows its selective precipitation, while CB[5] can be recrystallized from the aqueous phase.[9]
In 2005 Isaacs obtained also free CB[10] by treating CB[5] ⊂ CB[10] with an excess amount of melamine derivative **2a** that led to a ternary complex consisting of CB[10] and two molecules of **2a**; the elimination of the first guest was achieved using methanol and the second one with acetic anhydride.[10] In 2009 the crystal structure was reported.[11]
Recently the treatment with 1,12-dodecanediamine (**2b**) at low pH and several washing with a hot ethanolic solution of sodium hydroxide to obtain free CB[10] has been reported.[12]

2.4 Properties of CB[n]

CB[*n*] are synthetic cyclic oligomers consisting of glycoluril units linked by methylene bridges.
In Figure 3 the X-ray crystal structures for CB[5]-CB[8] and CB[5]⊂CB[10] are reported.
They all exhibit two hydrophilic carbonylated portals and a hydrophobic cavity characterized by a common depth *c* ($9{,}1x10^{-9}$ m).
However, as a result of a different amount of glycoluril units from CB[5] to CB[10], each compound is characterized by a specific width and volume (Table 1).
The diameter of the CB[n] portal is approximately 2 Å narrower than the cavity of the macrocycle, resulting in a steric barrier to guest inclusion processes.[12]

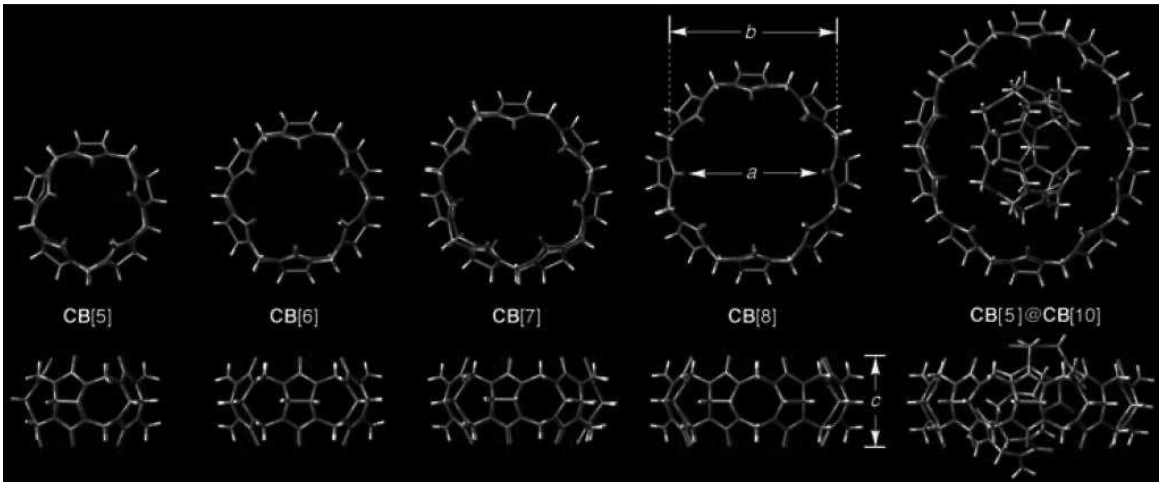

Figure 3. Top and side views of the X-ray crystal structures of CB[5],[6] CB[6],[4] CB[7],[6] CB[8],[6] and CB[5]⊂CB[10].[7] The various compounds are drawn to scale.

	M_r	a [Å][a]	b [Å][a]	c [Å][a]	V [Å^3]	s_{H_2O} [mM]	Stability [°C]	pK_a
CB[5]	830	2.4[5]	4.4[5]	9.1[5]	82[5]	20–30[5]	>420[5]	
CB[6]	996	3.9[5]	5.8[5]	9.1[5]	164[5]	0.018[61]	425[62]	3.02[63]
CB[7]	1163	5.4[5]	7.3[5]	9.1[5]	279[5]	20–30[5]	370[5]	
CB[8]	1329	6.9[5]	8.8[5]	9.1[5]	479[5]	<0.01[5]	>420[5]	
CB[10][b]	1661	9.0–11.0	10.7–12.6	9.1	–	–	–	–

[a] The values quoted for a, b, and c for CB[*n*] take into account the van der Waals radii of the relevant atoms. [b] Determined from the X-ray struc the CB[5]@CB[10] complex.[9]

Table 1. Dimensions and physical properties of CB[n].

CB[*n*] family is characterized by a relatively poor solubility in water: in particular CB[5] and CB[7] are much more water-soluble than CB[6] and CB[8] (20-30 mM vs. less than 0.01 mM in pure water, see Table 1).[13]

CB[n] are insoluble in all organic solvents, but some exceptions are reported in which hexafluorophosphate is employed as the counterion to the positively charged guest of CB.[14,15]

The carbonylic portals of CB[n] are weak bases: the pKa value of the conjugate acid of CB[6] is 3.02. The pKa values for CB[5], CB[7], and CB[8], not yet measured, should be similar to that of CB[6]. Consequently, the solubility of CB[n] increases in concentrated aqueous acid (for example, 61 mM for CB[6] in HCO_2H/H_2O (1:1), about 60 mM for CB[5], about 700 mM for CB[7], and about 1.5 mM for CB[8] in 3M HCl).[16-18] Moreover CB[n] show high thermal stability, exceeding 370°C.

Another key issue in molecular recognition events in both aqueous and organic solution[19] is the electrostatic potential.

In particular, CB[*n*] show a remarkable preference to interact with cationic guests due to the negative electrostatic potential near the portals and within the cavity.[13]

2.5 Recognition properties of CB[6]

CB[6] is a weak base (pKa=3.02) that can be protonated in acidic media, therefore, the potential inclusion of the guest in strongly acidic media as HCO_2H/H_2O (1:1) is affected by the competition with H^+ ions (Scheme 1, red equilibria).

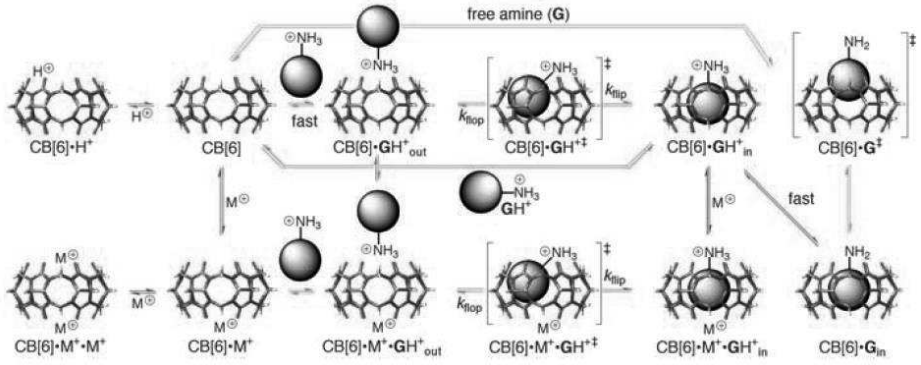

Scheme 1. Comprehensive mechanistic scheme for molecular recognition by CB[6]. Red arrow: protonation; Blue arrow: cation binding, green arrow: ammonium ion binding, light blue arrow: amine binding.

Similarly to the ability of binding protons at the carbonyl groups of the portals, CB[6] also binds alkali-metal, alkaline-earth, transition-metal, and lanthanide cations in homogenous solution (Scheme 1, blue equilibria).[16,17,20-25] Table 3 shows the binding constants determined by Buschmann et al. for CB[6] with a variety of monovalent and divalent cations.

	Li^+	Na^+	K^+	Rb^+	Ca^{2+}	Sr^{2+}	Ba^{2+}
CB[6]	2.38	3.23	2.79	2.68	2.80	3.18	2.83

Table 2. Calorimetrically determined log K values for the complexation of monovalent and divalent cations with CB[6] in HCO_2H/H_2O (1:1) at 25°C.[16]

Consequently, metals (Scheme 2, blue equilibria) compete with protons (red equilibrium) in the binding event and, as the acidity of the solution is increased, the metal binding should decrease.
One of the most interesting features of CB[n]s is their extreme affinity towards selected organic guests, and in most cases, the complexation process can be investigated by ^1H NMR spectroscopy.
In particular Mock and co-workers observed by a series of ^1H NMR experiments that alkylammonium ions bind tightly to CB[6] in HCO_2H/H_2O (1:1) and measured binding constants of 10^1-10^7 M^{-1}.
Effectively, upon the complexation process it is possible to detect a strong upfield shift for the hydrogen atoms near the center of the CB[n] cavity,[26] a moderate upfield shift for decentered hydrogens,[27] and a significant downfield shift for the hydrogens outside the cavity.[28]
The peculiar rigidity of CB[6], the location of two opposite binding regions that can accomodate positively charged groups and the cavity that favors hydrophobic fragments provides high selectivity to the binding of CB[6] (Figure 4).
As noticed by Mock thus, CB[n] are ideal hosts for positively charged amphiphilic guests, with the positive charges interacting with the carbonylated portals through ion-dipole stabilization, and the hydrophobic moiety located inside the CB[n] cavity; affinities of $1.3 \cdot 10^7$ M^{-1} were measured at that time in the case of spermine and CB[6] in a 50% formic acid solution.[27]

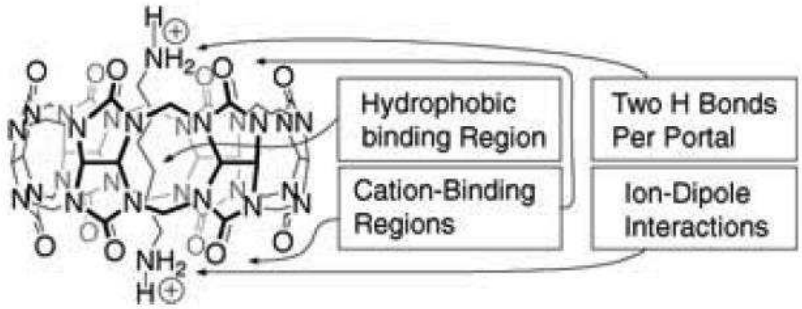

Figure 4. Representation of the different binding regions of CB[6] and the geometry of the complex between CB[6] and the hexanediammonium ion.

In 2005 the Isaacs group measured affinities exceeding 10^{12} M^{-1},[29] and two years later, Kaifer, Isaacs, Gilson, Kim and Inoue reported the value of $3.0 \cdot 10^{15}$ M^{-1} with CB[7] and ferrocene derivative **3a**.[30] Recently, a $5.0 \cdot 10^{15}$ M^{-1} binding constant[31] was measured by Kim, Inoue and

Gilson between guest **3b**[32] and CB[7]. These affinities represent very strong non-covalent interactions.

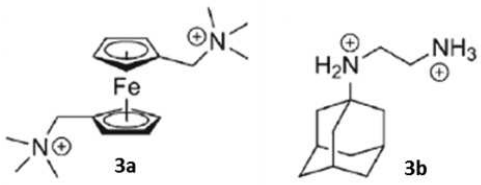

Figure 5. Structures of guest compound **3a** and **3b**.

Binding properties of CB[6] have been largely studied and several guests have been tested.[1]

2.6 Control over the Recognition Processes

The outstanding binding properties of CB[n] and the rigid cyclic shape have promoted the rapid development of applications in the supramolecular, synthetic, medicinal and material science fields, in particular as synthetic receptors, but also as building blocks in the design of supramolecular assemblies as rotaxanes, catenanes and molecular machines, in which external stimuli, such as pH or temperature, light irradiation, etc. can modulate the system between two different states.
Tuncel and coworkers exploited the CB[6]-catalyzed [3 + 2] cycloaddition preparing a rotaxane in which two CB[6] are threaded along the polyaminated axle **4**, through the interactions between the carbonyl portals and the positive charged moieties on the thread. The switch is performed by pH variations that induce deprotonation of the axle and subsequent reprotonation, forcing the macrocycles to shuttle from the charged recognition sites to the same 1,12-dodecanediamine station (Figure 6).[33]

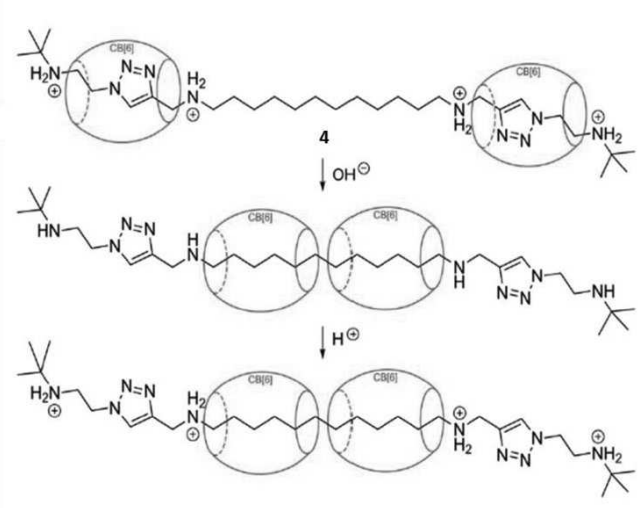

Figure 6. Two CB[6] units locked along the 1,12-dodecanediammonium station of axle **4**.[33]

Kaifer reported that CB[7] is able to bind the carboxyalkyl substituent of methylviologen (MV) derivative **5** at low pH, while at higher pH, when negative carboxylate units are formed, the macrocycle shuttles to the central bipyridine station, due to the resulting repulsion (Figure 7).[34,35]

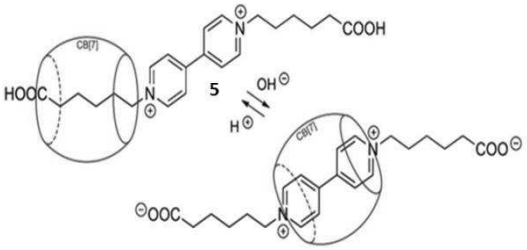

Figure 7. Example of pH-controlled CB[7] switch.

Tian and coworkers monitored the behavior of CB[7] as a function of the pH as well; CB[7] interacts with the protonated aniline moiety of the dye **6** at pH 4–6, and moves to the dimethylaniline at pH 8–11 (Figure 8). Changes of the dye color give evidence of the pH-dependent switch (yellow under acidic conditions, red at high pH).[36]

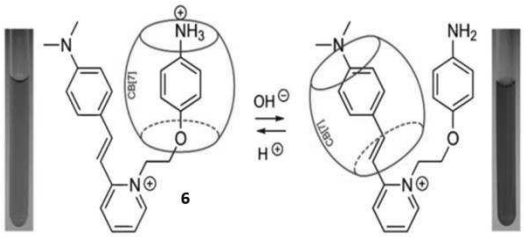

Figure 8. Color changes in a pH-dependent switch.

Kaifer and coworkers achieved a fully reversible switch monitoring the CB[7] moving between two recognition sites by electrochemical oxidation, in particular from the ferrocenyl station of axle **7** to the central xylylene station upon formation of the ferrocenium cation that shows a weaker affinity towards CB[7] (Figure 9).[37]

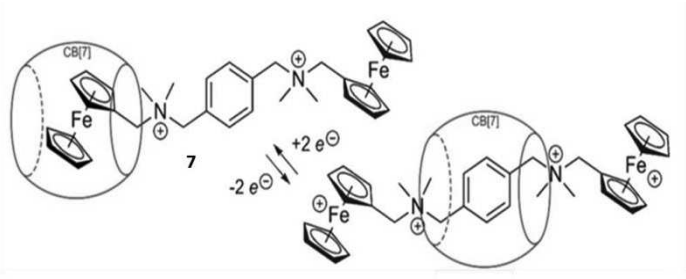

Figure 9. Redox-controlled shuttling of CB[7] along a ferrocene derivative.[37]

CB[n] have also been incorporated into promising novel materials, for example the inclusion of these macrocycle in the preparation of polymers and hydrogels is reported.[38-46]

2.7 Functionalization of CB[n]

The synthesis of cucurbiturils showed how self-assembly is able to generate a rigid, hollow structure consisting of six glycoluril units linked by pairs of methylene groups.

Moreover, a real interest for synthetic strategies to obtain CB[n] derivatives carrying new functional groups that could be suitable for further functionalization reactions and incorporation into more complex systems, is observed.[47]
In particular, the introduction of radical moieties, or spin labelling, could be achievable in order to investigate cucurbiturils with ESR spectroscopy.
Different approaches to functionalize CB[n] are reported in literature.
The first example (Scheme 2) shows the use of a functionalized glycoluril unit in the synthesis, in particular the dimethylglycoluril **8** in order to obtain CB[n] derivatives.[48]

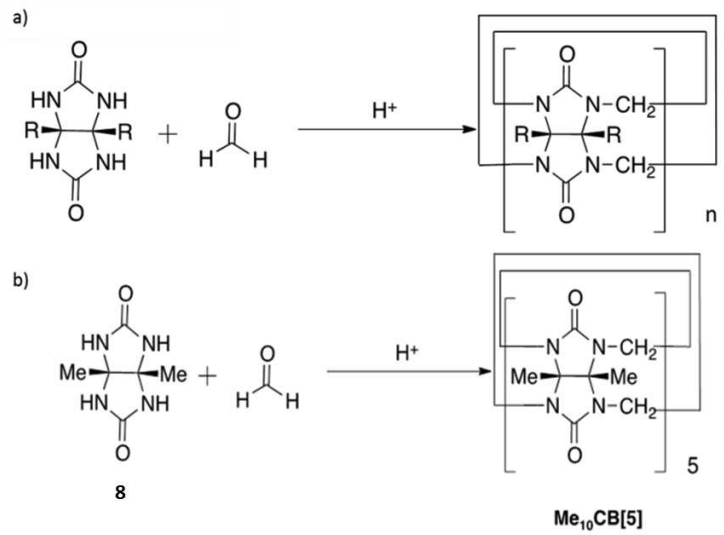

Scheme 2. a) General scheme for functionalization with modified glycoluril units and b) a selected example.[48]

The functionalization can occur also at the methylene bridges.
Isaacs and coworkers reported an example in which the methylene bridged glycoluril hexamer **9** undergoes macrocylization with phthalaldehyde **10** in 9 M H_2SO_4 or concentrated HCl at room temperature to achieve monofunctionalized CB[6] derivative **11** (Scheme 3).[47]

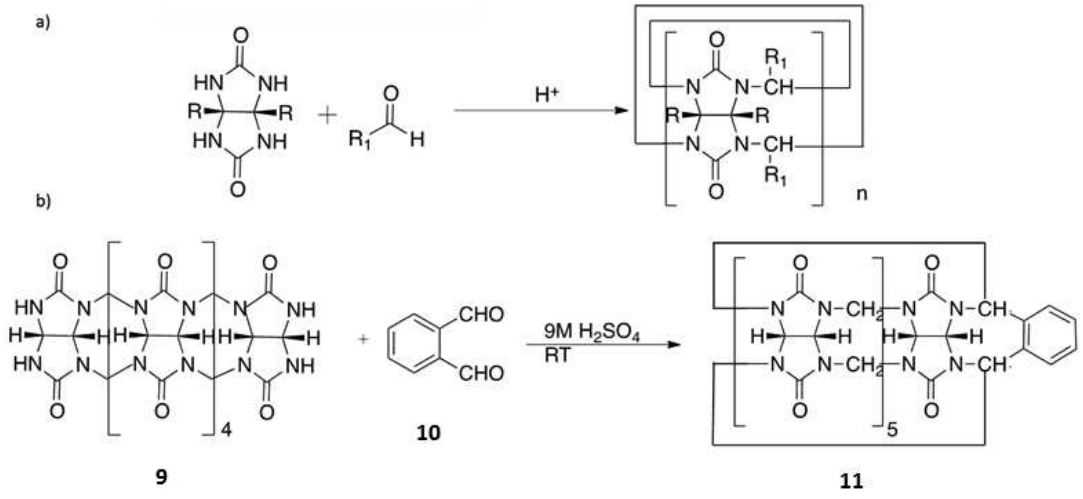

Scheme 3. a) General scheme of functionalization at the methylene bridges and b) a selected example.[47]

Finally, a functionalization directly on the CB surface has been achieved, important for extensive employment in several fields.The first direct method is an oxidation that introduces hydroxyl groups at the equatorial CH positions around CB[6], the perhydroxylation of CB[6] developed by the Kim group,[49] that used these compounds for several applications including membrane protein fishing and stimuli responsive polymer nanocapsules for drug delivery.[50,51]

Reaction of CB[6] with $K_2S_2O_8$ (KPS) in water at 85 °C for 6 h generates perhydroxycucurbit[6]uril (**12**) in 45% yield as a potassium ion complex (Scheme 4).

The new derivative **12** is soluble in DMSO and moderately soluble in DMF. Most importantly, **12** allows further post-functionalization with desired groups by conventional reactions (Scheme 4).

Among these derivatives, perallyloxycucurbit[6]uril (**13**), which can be easily prepared from the reaction of **12** with allyl bromide in the presence of NaH, is useful for further transformation thanks to its good solubility in organic solvents. [49]

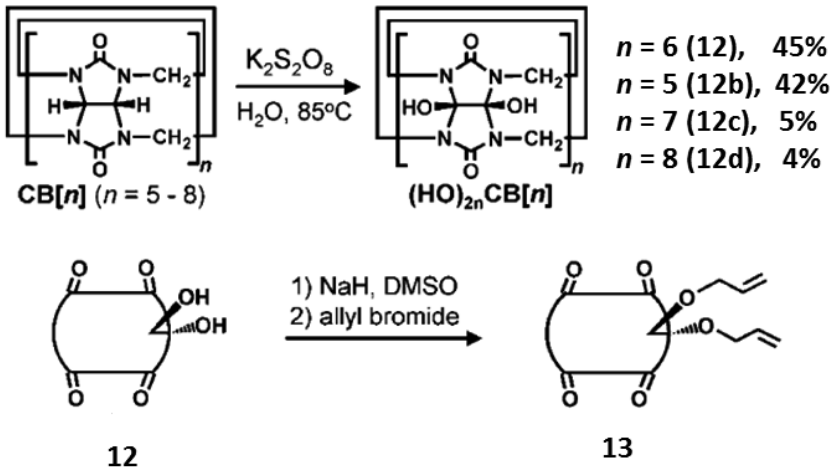

Scheme 4. Perhydroxycucurbit[6]uril **12** and its functionalization.

As mentioned before, spin labelling of cucurbiturils is possible as a result of a proper functionalization of CB[n], but in order to obtain a useful ESR signal the introduction of a single radical probe is desirable.

Therefore, the best strategy for this purpose is the direct monohydroxylation of CB[6] reported by Scherman.[52]

In the route reported by Kim et al., the oxidation with KPS of the CH groups occurred in a stepwise process but while the parent CB[6] molecule has low water solubility (<0.018 mM[22]), partially functionalized-CB[6] (fCB[6]) compounds become more soluble in water, therefore, there is a greater probability for the oxidation process to go on. Thus, the increased rate of functionalization is useful to obtain perhydroxylation fCB[6] (CB[6]-12OH), but in order to get the single functionalization it should be avoided.

In Scherman's approach, the solubility of CB[6] in water is improved before the oxidative reaction, in order to control the stoichiometry of the process and then the final product amount.

In particular, complexation with imidazolium compounds increases the solubility of CB[6] in water[53,54] and their elimination can be readily achieved by refluxing in dichloromethane (DCM).[55] Besides, the proper selection of the alkyl chain length and counterions, can modulate the affinity between imidazolium compounds and CB[6].[56]

The best candidate for the reaction is a bis-ethylimidazolium salt (**14**) linked with an octyl chain (Scheme 5). It shows a binding constant of $4.7 \cdot 10^4$ M^{-1} with CB[6] that allows the complexation process but also the subsequent dissociation from any fCB[6] molecules after the reaction.
Oxidation and purification steps were monitored by ESI-MS, that proved to be suitable compared to ^{1}H NMR and thin layer chromatography.
Effectively, CB[6] and fCB[6] ionise together with guest **14** as a 1 : 1 complex and are detectable as doubly charged ions, moreover, despite the ability of CB[6] to bind several cations the complexity of the mass spectra was reduced due to the imidazolium cations that decrease the ability of CB[6] to bind Na^+, K^+ or H^+ in the gas phase. $(NH_4)_2S_2O_8$ (APS) was used instead of KPS as the oxidizing agent because of its higher solubility in water .
Thus, functionalization of the CB[6], dissolved in water thanks to guest **14**, was performed by addition of APS and subsequent heating at 85 °C. Several fCB[6] compounds could be created with one to twelve hydroxyl groups in the mixture and their ratio depends on the amount of APS used. The task is to yield the monohydroxylated CB[6] avoiding higher order functionalisation, therefore the reaction is controlled so that 50% of the CB[6] molecules do not react with APS.
The separation of MonOH from unreacted CB[6] was obtained by using a macroporous resin, a polystyrene–divinylbenzene (PS–DVB) copolymer resin, MCI GEL CHP20P, with pore sizes between 400-600 Å, in which the aromatic groups determine the weak binding to the OH group of the monofunctionalized CB[6], giving rise to the slow rate of its elution from the resin with respect of CB[6].[57]
In fact, **14** ⊂ CB[6] was first eluted with pure water, followed by **14** ⊂ MonOH.
Refluxing the isolated complex in dichloromethane in the presence of NH_4PF_6[55] allowed to remove the guest, obtaining the monofunctionalized CB[6].
Even though the yield was only 12%, unreacted species can be oxidized again, leading to a continuous process with a much higher total yield.[52]

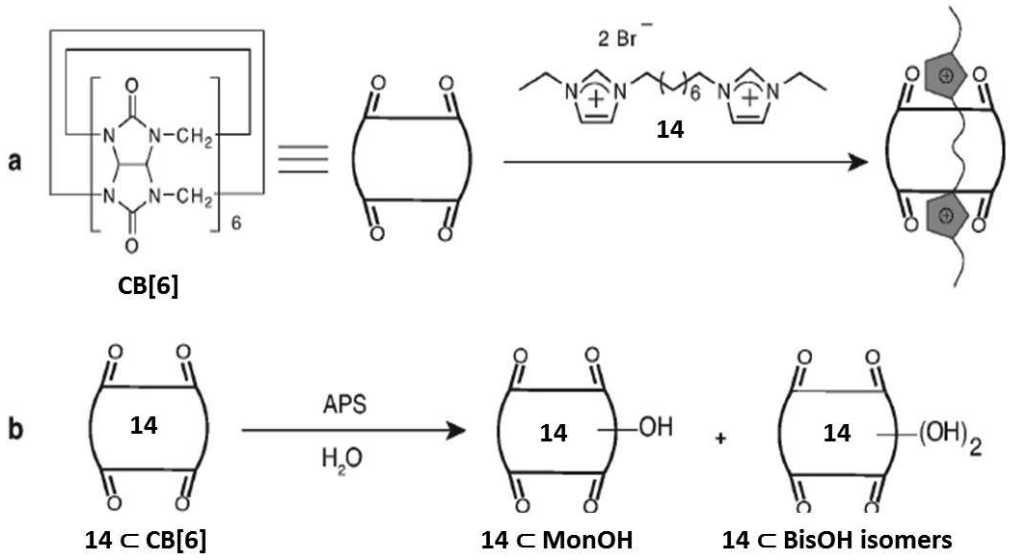

Scheme 5. The procedure of CB[6] functionalization.[52]

The hydroxyl group on MonOH can be post-modified (Scheme 6) by reaction with allyl bromide or propargyl bromide to introduce single alkene or alkyne groups onto the CB[6] surface.
In particular the mono propargylation of CB[6], **16**, is interesting because it allows the ‘‘3+2’’ cycloaddition reaction with suitable compounds carrying an azido moiety (Scheme 6), providing a novel easy strategy for a versatile functionalization of MonOH.[52]

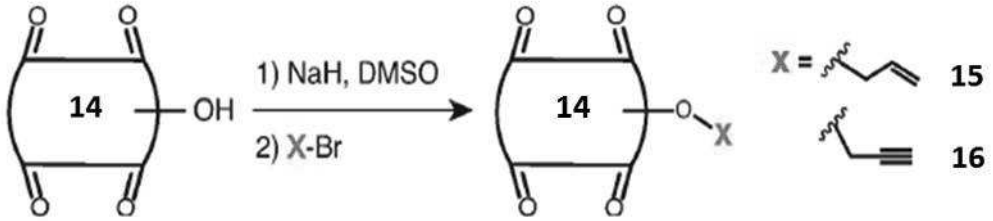

Scheme 6. Modification of MonOH.

According to this strategy, part of my PhD work was focused on the synthesis of **16**,[51] that attracted our attention in order to attach directly to the CB surface a radical function, achieving the first example of paramagnetic cucurbituril **17** (Scheme 8a).
The copper(I)-catalyzed azide–alkyne cycloaddition (example of the so called “click chemistry”) is an efficient synthetic strategy involving azides and terminal alkyne compounds to create carbon-heteroatom bonds forming 1,2,3-triazole units. It provides versatility, simple reaction conditions and good selectivity, resulting in the exclusive formation of the 1,4-disubstituted triazole moiety (Scheme 7).[58,59]

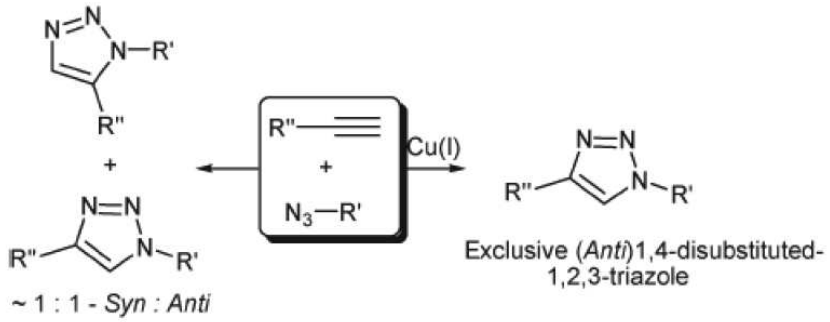

Scheme 7. The Cu(I) catalysed Huisgen ‘click reaction’ results in exclusive formation of the 1,4-triazole derivative, while the thermally induced Huisgen cycloaddition usually results in an approximately 1:1 mixture of 1,4- and 1,5-triazole stereoisomers.

The compound selected to perform the Copper(I)-catalyzed azide–alkyne cycloaddition (CuAAC) was the TEMPO derivative carrying an azido moiety **20**. It was prepared by treatment with *p*-toluenesulfonyl chloride of 4-hydroxy-2,2,6,6-tetramethylpiperidine-*N*-oxide (4-hydroxy-TEMPO) **18**, achieving compound **19**, then subsequent exchange reaction with NaN_3 gave the desired azido-compound **20** (Scheme 8b).

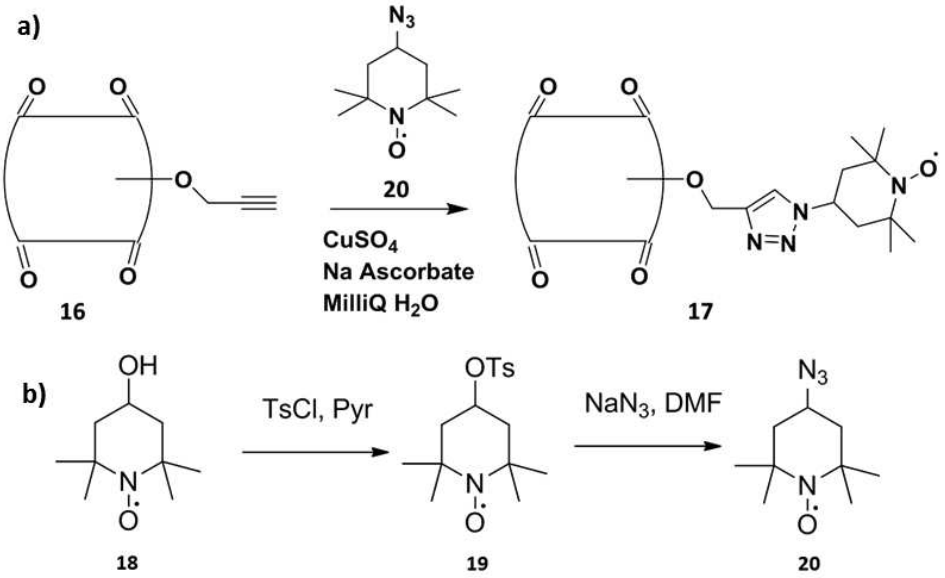

Scheme 8. a) Copper(I)-catalyzed azide–alkyne cycloaddition (CuAAC); b) Synthesis of the TEMPO derivative.

The synthesis of the bis-ethylimidazolium guest was carried out refluxing 1-ethylimidazole **21** and 1,8-dibromooctane **22** in toluene for 12 hours (Figure 10).

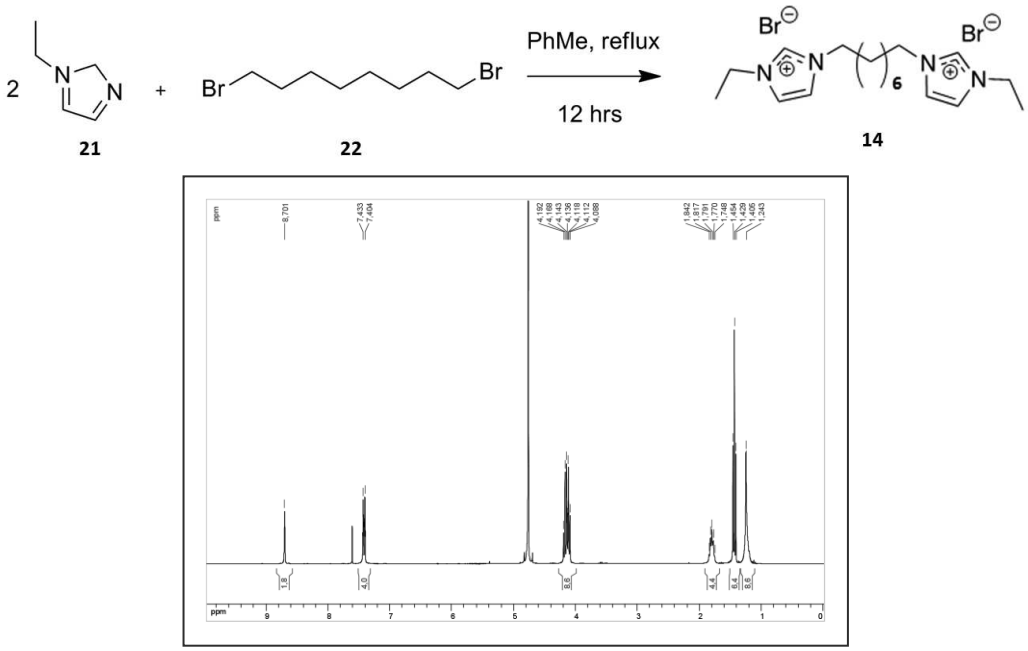

Figure 10. Synthesis and ^{1}H NMR (300 MHz, D_2O) spectrum of compound **14**.

The complexation process of CB[6] and guest (1:1) in water was confirmed by a doubly charged ion in the ESI-MS spectrum (Figure 11 on the left) and, subsequently, the oxidative reaction was performed. Also the monohydroxylated compound was detected by the corresponding dication in the spectrum after 12 hours, together with small signals relative to the starting complex and to

BisOH isomers (Figure 11 on the right). Separation from these undesired species was obtained by using a polystyrene–divinylbenzene (PS–DVB) copolymer resin, MCI GEL CHP20P, with pore sizes between 400-600 Å eluting with Milli-Q H_2O: the unreacted **14** ⊂ CB[6] was eluted first , then few fractions containing the parental CB and increasing amount of the monofunctionalized compound were detected and finally, the pure desired compound was collected.
Importantly, after every separation, the macroporous resin was washed with NaOH solution and MeOH/H_2O mixtures, a process that takes time because pressure can not be applied on the top of the column, but necessary to recycle the resin for a new separation process.

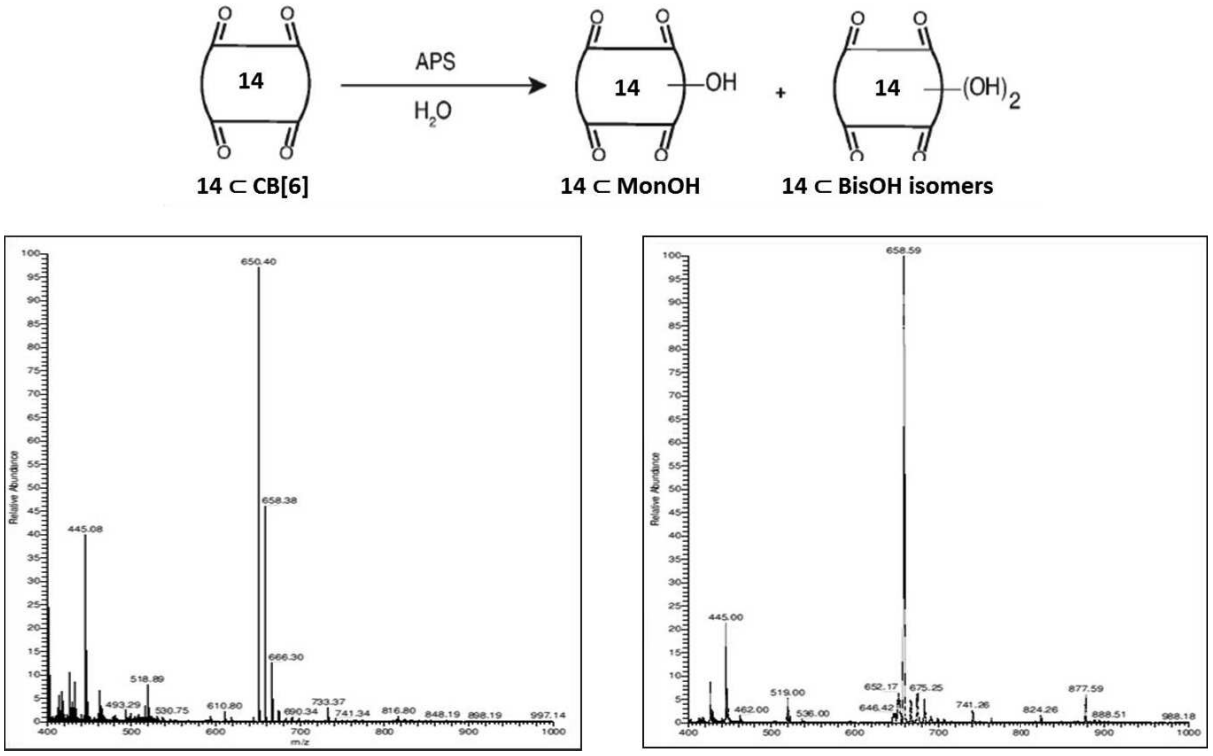

Figure 11. Controlled oxidation and the ESI-MS spectra, relative to the complex **14** ⊂ CB[6] (left) and to the complex **14** ⊂ MonOH (right).

Afterwards, complex **14** ⊂ MonOH was treated with propargyl bromide in the presence of NaH in dimethyl sulfoxide (DMSO) to carry out the post-functionalization of the hydroxyl group (scheme 6, compound 16).
Even in this case, evidence of the formation of **16** was obtained from the ESI-MS spectrum, in which the doubly charged ion relative to the 1:1 complex with the guest was observed (Figure 12).

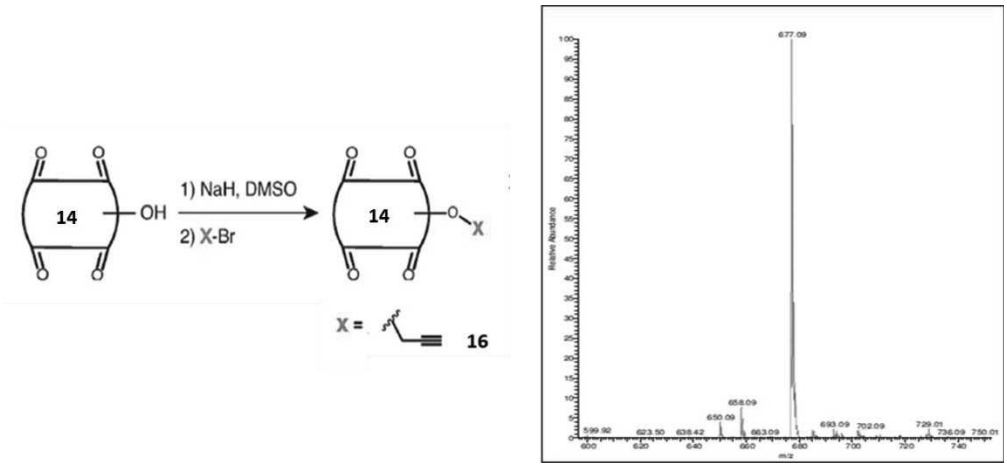

Figure 12. Further functionalization of the OH group.

2.8 Conclusions

In conclusion, the monofunctionalized CB[6] carrying the propargyl group is the best candidate to design a paramagnetic macrocycle since the "click chemistry" provides versatility, simple reaction conditions and good selectivity. Thus, the synthesis of the spin-labelled Cucurbit[6]uril is in progress in our laboratory.

This compound could be introduced, for example, in mechanically interlocked molecules like rotaxanes or catenanes and could create new possibilities for the investigation of novel molecular machines by ESR spectroscopy, providing structural, dynamic and reactivity information of great interest for their development.

References

[1] J. Lagona, P. Mukhopadhyay, S. Chakrabarti, L. Isaacs, *Angew. Chem. Int. Ed.*, **2005**, *44*, 4844-4870.

[2] E. Masson, X. Ling, R. Joseph, L. Kyeremeh-Mensah, X. Lu, *RSC Advances*, **2012**, *2*, 1213-1247

[3] R. Behrend, E. Meyer, F. Rusche, *Justus Liebigs Ann. Chem*., **1905**, *339*, 1-37.

[4] W. A. Freeman, W. L. Mock, N.Y. Shih, *J. Am. Chem. Soc.*, **1981**, *103*, 7367-7368.

[5] A. I. Day, P. Arnold, R. J. Blanch, B. Snushall, *J. Org. Chem.*., **2001**, *66*, 8094-8100.

[6] J. Kim, I. S. Jung, S. Y. Kim, E. Lee, J. K. Kang, S. Sakamoto, K. Yamaguchi, K. Kim, *J.Am. Chem. Soc.*, **2000**, *122*, 540-541.

[7] a) A. I. Day, R. J. Blanch, A. P. Arnold, S. Lorenzo, G. R. Lewis, I. Dance, *Angew. Chem*., **2002**, *114*, 285-287; b) *Angew . Chem. Int. Ed.*, **2002**, *41*, 275-277.

[8] W.-H. Huang, S. Liu, L. Isaacs, *Cucurbit[n]urils, in: Modern Supramolecular Chemistry: Strategies for Macrocycle Synthesis*, ed. F. Diederich, P. J. Stang and R. R. Tykwinski, Wiley-VCH Verlag GmbH & Co., Weinheim, **2008**, *113*.

[9] D. Jiao, N. Zhao, O. A. Scherman, *Chem. Commun.*, **2010**, *46*, 2007-2009.

[10] S. Liu, P. Y. Zavalij, L. Isaacs, *J. Am. Chem. Soc*., **2005**, *127*, 16798-16799.

[11] L. Isaacs, *Chem. Commun*., **2009**, 619-629.

[12] M. J. Pisani, Y. Zhao, L. Wallace, C. E. Woodward, F. R. Keene, A. I. Day, J. G. Collins, *Dalton Trans.*, **2010**, *39*, 2078-2086.

[13] J. W. Lee, S. Samal, N. Selvapalam, H.-J. Kim, K. Kim, *Acc. Chem. Res*., **2003**, *36*, 621-630.

[14] V. Sindelar, K. Moon, A. E. Kaifer, *Org. Lett*., **2004**, *6*, 2665-2668.

[15] W. Wang, A. E. Kaifer, *Supramol. Chem*., **2010**, *22*, 710-716.

[16] H.-J. Buschmann, K. Jansen, C. Meschke, E. Schollmeyer, *J. Solution Chem*., **1998**, *27*, 135-140.

[17] a) G.-L. Zhang, Z.-Q. Xu, S.-F. Xue, Q.-J. Zhu, Z. Tao, *Wuji Huaxue Xuebao*, **2003**, *19*, 655-659.

[18] K. Jansen, H.-J. Buschmann, A.Wego, D. DWpp, C. Mayer, H. J. Drexler, H. J. Holdt, E. Schollmeyer, J. Inclusion Phenom. Macrocyclic Chem. 2001, 39, 357-363.

[19] B. Honig, A. Nicholls, *Science*, **1995**, *268*, 1144-1149.

[20] R. Hoffmann, W. Knoche, C. Fenn, H.-J. Buschmann, *J. Chem. Soc. Faraday Trans*., **1994**, *90*, 1507-1511.

[21] H.-J. Buschmann, E. Cleve, E. Schollmeyer, *Inorg. Chim. Acta*, **1992**, *193*, 93-97.

[22] H.-J. Buschmann, E. Cleve, K. Jansen, E. Schollmeyer, *Anal. Chim. Acta*, **2001**, *437*, 157-163.

[23] H.-J. Buschmann, E. Cleve, K. Jansen, A. Wego, E. Schollmeyer, *J. Inclusion Phenom. Macrocyclic Chem.,* **2001**, *40*, 117-120.

[24] H.-J. Buschmann, K. Jansen, E. Schollmeyer, *Inorg. Chem.Commun*., **2003**, *6*, 531-534.

[25] X. X. Zhang, K. E. Krakowiak, G. Xue, J. S. Bradshaw, R. M. Izatt, *Ind. Eng. Chem. Res*., **2000**, *39*, 3516-3520.

[26] K. Moon, A. E. Kaifer, *Org. Lett*., **2004**, *6*, 185-188.

[27] W. L. Mock, N.-Y. Shih, *J. Org. Chem*., **1986**, *51*, 4440-4446.

[28] H.-J. Buschmann, A. Wego, A. Zielesny and E. Schollmeyer, *J. Inclusion Phenom. Macrocyclic Chem*., **2006**, *54*, 241-246.

[29] S. Liu, C. Ruspic, P. Mukhopadhyay, S. Chakrabarti, P. Y. Zavalij and L. Isaacs, *J. Am.Chem. Soc*., **2005**, *127*, 15959-15967.

[30] M. V. Rekharsky, T. Mori, C. Yang, Y. H. Ko, N. Selvapalam, H. Kim, D. Sobransingh, A. E. Kaifer, S. Liu, L. Isaacs, W. Chen, S. Moghaddam, M. K. Gilson, K. Kim, Y. Inoue, *Proc. Natl.Acad. Sci. U. S. A*., **2007**, *104*, 20737-20742.

[31] S. Moghaddam, C. Yang, M. Rekharsky, Y. H. Ko, K. Kim, Y. Inoue, M. K. Gilson, *J. Am. Chem. Soc.*, **2011**, *133*, 3570-3581.

[32] S. Ghosh, L. Isaacs, *J. Am. Chem. Soc*., **2010**, *132*, 4445-4454.

[33] D. Tuncel, O. Ozsar, H. B. Tiftik, B. Salih, *Chem. Commun*., **2007**, 1369-1371.

[34] V. Sindelar, S. Silvi, A. E. Kaifer, *Chem. Commun*., **2006**, 2185-2187.

[35] V. Sindelar, S. Silvi, S. E. Parker, D. Sobransingh, A. E. Kaifer, *Adv. Funct. Mater*., **2007**, *17*, 694-701.

[36] H. Zhang, Q. Wang, M. Liu, X. Ma, H. Tian, *Org. Lett*., **2009**, *11*, 3234-3237.

[37] D. Sobransingh, A. E. Kaifer, *Org. Lett*., **2006**, *8*, 3247-3250.

[38] D. Tuncel, J. H. G. Steinke, *Chem. Commun.*, **1999**, 1509-1510.

[39] S. Choi, J. W. Lee, Y. H. Ko, K. Kim, *Macromolecules*, **2002**, *35*, 3526-3531.

[40] D. Tuncel, J. H. G. Steinke, *Chem. Commun*., **2001**, 253-254.
[41] U. Rauwald, O. A. Scherman, *Angew. Chem., Int. Ed*., **2008**, *47*, 3950-3953.
[42] Y. Liu, Y. Yu, J. Gao, Z. Wang, X. Zhang, *Angew. Chem., Int. Ed*., **2010**, *49*, 6576-6579.
[43] A. V. Kabanov, S. V. Vinogradov, *Angew. Chem. Int. Ed*., **2009**, *48*, 5418-5429.
[44] L. Yu, J. Ding, *Chem. Soc. Rev*., **2008**, *37*, 1473-1481.
[45] L. Zha, B. Banik, F. Alexis, *Soft Matter*, **2011**, *7*, 5908-5916.
[46] I. Hwang, W. S. Jeon, H.-J. Kim, D. Kim, H. Kim, N. Selvapalam, N. Fujita, S. Shinkai, K. Kim, *Angew. Chem. Int. Ed*., **2007**, *46*, 210-213.
[47] D. Lucas, T. Minami, G. Iannuzzi, L. Cao, J. B. Wittenberg, P. Jr. Anzenbacher, L. Isaacs, *J. Am. Chem. Soc.*, **2011,** *133,* 17966-17976.
[47] A. Flinn, G. C. Hough, J. F. Stoddart, D. J. Williams, *Angew. Chem. Int. Ed. Engl.*, **1992,** *31,* 1475-1476.
[48] S. Y. Jon, N. Selvapalam, D. H. Oh, J. -K. Kang, S.-Y Kim, Y. J. Jeon, J. W. Lee, K. Kimoon, *J. Am. Chem. Soc.*, **2003,** *125,* 10186-10187.
[49] a) E. Kim, D. Kim, H. Jung, J. Lee, S. Paul, N. Selvapalam, Y. Yang, N. Lim, C. G. Park, K. Kim, *Angew. Chem. Int. Ed*., **2010**, *49*, 4405-4408;
b) K. M. Park, D.-W. Lee, B. Sarkar, H. Jung, J. Kim, Y. H. Ko, K. E. Lee, H. Jeon, K. Kim, *Small*, **2010**, *6*, 1430-1441.
[50] a) Y. H. Ko, I. Hwang, D.-W. Lee, K. Kim, *Isr. J. Chem*., **2011**, *51*, 506-514;
b) D.-W. Lee, K. M. Park, M. Banerjee, S. H. Ha, T. Lee, K. Suh, S. Paul, H. Jung, J. Kim, N. Selvapalam, S. H. Ryu, K. Kim, *Nat. Chem*., **2011**, *3*, 154-159;
c) M. Munteanu, S. Choi, H. Ritter, *Macromolecules*, **2009**, *42*, 3887-3891.
[51] N. Zhao, G. O. Lloyd, O. A. Scherman, *Chem. Commun.*, **2012,** *48,* 3070-3072.
[52] L. Liu, N. Zhao, O. A. Scherman, *Chem. Commun*., **2008**, 1070-1072.
[53] V. Kolman, R. Marek, Z. Strelcova, P. Kulhanek, M. Necas, J. Svec, V. Sindelar, *Chem. Eur. J*., **2009**, *15*, 6926-6931.
[54] D. Jiao, N. Zhao, O. A. Scherman, *Chem. Commun*., **2010**, *46*, 2007-2009.
[55] N. Zhao, L. Liu, F. Biedermann, O. A. Scherman, *Chem. Asian J*., **2010**, *5*, 530-537.
[56] M. H. L. Ribeiro, D. M. F. Prazeres, J. M. S. Cabral, M. M. R. Fonseca, *Bioprocess Biosyst. Eng*., **1995**, *12*, 95-102.
[57] H. C. Kolb, M. G. Finn, K. B. Sharpless, *Angew. Chem. Int. Ed*., **2001**, *40*, 2004-2021.
[58] a) V. V. Rostovtsev, L. G. Green, V. V. Fokin, K. B. Sharpless, *Angew. Chem. Int. Ed.*, **2002**, *41*, 2596-99;
b) J. E. Moses, A. D. Moorhouse, *Chem. Soc. Rev*., **2007**, *36*, 1249-1262.

Spin labelled macrocycles: Pillar[n]arenes

Chapter 3. Spin labelled macrocycles: Pillar[n]arenes

3.1 Introduction[1,2]

Great interest in the design and synthesis of new macrocycles has grown considerably in the last years, due to their important applications in supramolecular chemistry. A family of host compounds, however, should have some important features to be interesting and useful, in particular good host-guest complexation properties, easy synthetic strategies and routes to further functionalization.

In 2008, a new class of macrocycles, the pillar[n]arenes, appeared in the literature[3] and since this discovery a rapid development in this field has been reported.

Currently, different members of the pillar[*n*]arene family ("n" identify the number of the hydroquinone units) have been synthesized but those with n = 5 have been most extensively investigated (Figure 1).[4]

Pillar[5]arenes are [1_5]paracyclophane derivatives consisting of 1,4-disubstituted hydroquinones linked by methylene bridges at the 2- and 5-positions. They are characterized by a rigid and highly symmetrical structure that provides them selective binding properties; the cavity of pillar[5]arene (approximately 5.5 Å) is similar to the cavity of α-cyclodextrin (approximately 4.7 Å) and cucurbit[6]uril (approximately 5.8 Å), therefore the inclusion of the same guests involved in binding processes with α-cyclodextrin and cucurbit[6]uril is possible.[5,6]

In particular, the hydroquinone units provide an electron-donating cavity able to form complexes with linear alkanes containing electron-accepting moieties such as amine,[7] ammonium,[8,9] cyano,[10] and halogen[11] groups, and also simple aromatic compounds such as pyridinium and viologen derivatives.[12-20]

Moreover, pillar[n]arenes are soluble in organic solvents and easy to functionalize with different groups on all the monomer units or on one or two positions, which allows to modulate their host-guest binding properties.

Therefore, due to these interesting features, in particular the versatile functionalization, they can be successfully employed in self-assembly and in the construction of supramolecular architectures.

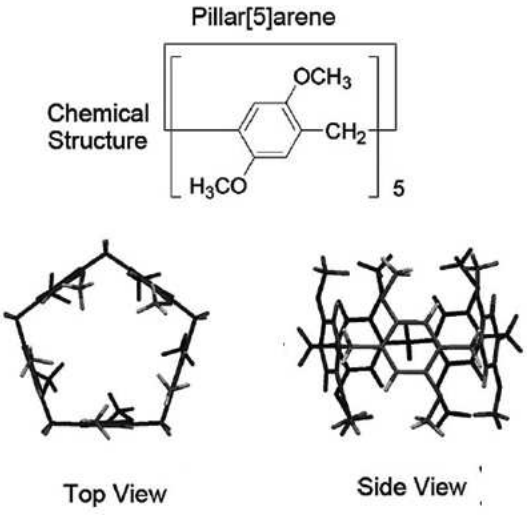

Figure 1. Chemical and X-ray crystal structures of permethylated pillar[5]arene.

3.2 Synthesis

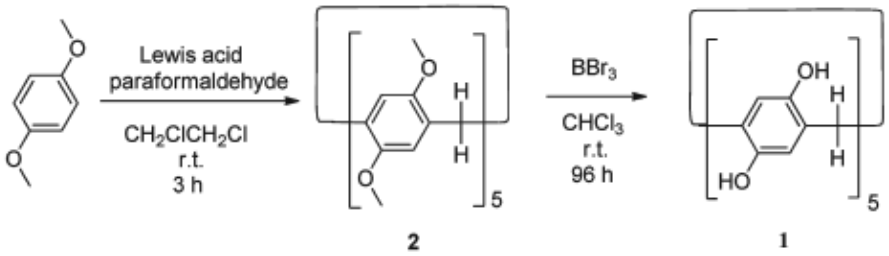

Scheme 1. Synthesis of DMpillar[5]arene (**2**) and Pillar[5]arene (**1**).

The synthesis of pillar[5]arene, **1**, was reported by Ogoshi et al. in 2008.[3] In particular, the condensation of 1,4-dimethoxybenzene with paraformaldehyde and a Lewis acid as a catalyst provides the symmetrical 1,4-dimethoxypillar[5]arene (DMpillar[5]arene), **2** (Scheme 1).
Among various Lewis acids, the most efficient for this reaction proved to be $BF_3{\cdot}O(C_2H_5)_2$, affording, the cyclic pentamer in 22% yield; then pillar[5]arene, **1**, was obtained by deprotection of the methoxy groups of DMpillar[5]arene with a final yield of 7%.

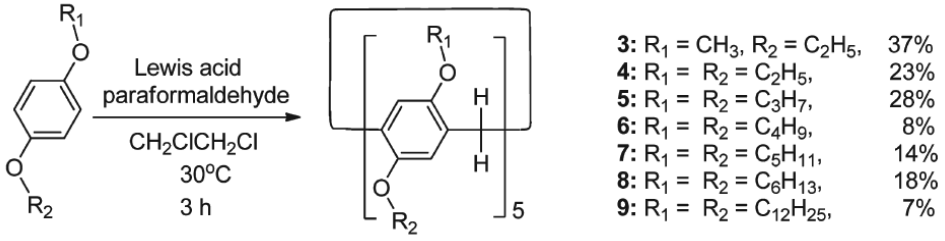

Scheme 2. Synthesis of Alkyl-Substituted Pillar[5]arenes.

Afterwards, studies on the conformational characteristics of pillar[5]arene were performed, in order to investigate how the presence of different substituents could modulate the reaction conditions. In particular, pillar[5]arene derivatives **3-9** carrying various alkyl groups (Scheme 2) have been reported, resulting that long alkyl substituents tend to hinder the cyclization reaction.[21,22]

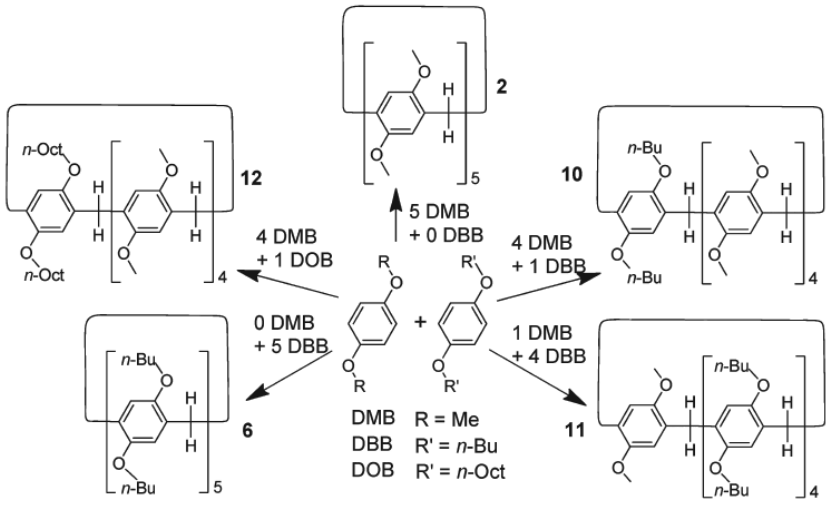

Scheme 3. Preparation of Copillar[5]arenes by oligomerization of different hydroquinone diethers.

Moreover, synthesis of copillar[5]arenes containing different monomers are reported (Scheme 3).[23] For example, from a mixture of 1,4-dimethoxybenzene (DMB) and 1,4-dibutoxybenzene (DBB), copillar[5]arene **10** was obtained in 16% yield. Subsequently, by changing the ratio or the composition of the two different units, compounds **11** and **12** were isolated.

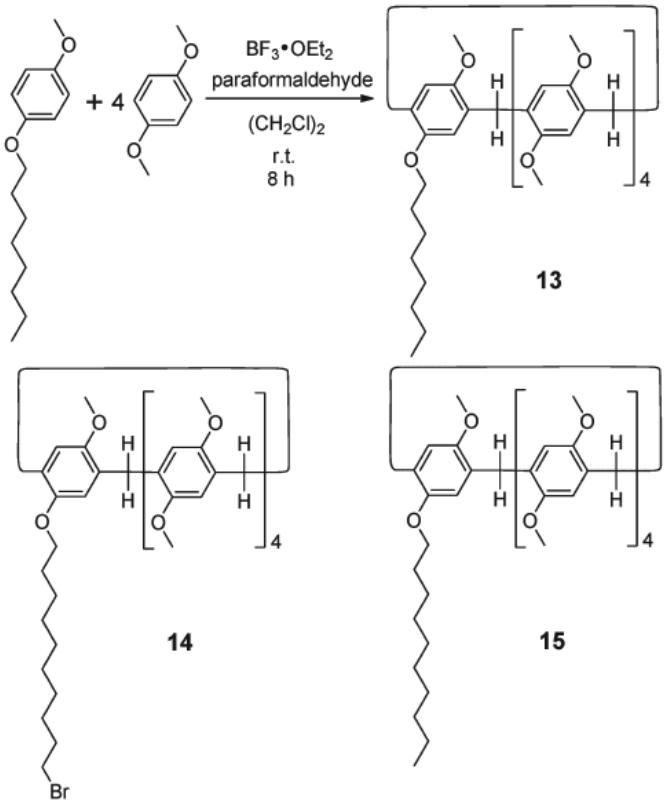

Scheme 4. Synthesis of Copillar[5]arene **13** and chemical structures of Copillar[5]arenes **14** and **15**.

Copillar[5]arene **13** was designed as a monomer for the synthesis of supramolecular polymers and it was obtained by co-oligomerization of 1,4-dimethoxybenzene and 1-methoxy-4 (octyloxy)benzene, in 9% yield (Scheme 4).[24]

Later, copillar[5]arenes **14** and **15** were designed in order to investigate the self-assembly properties of pillararenes.[25]

Further post-functionalization of a copillar[5]arene was performed on compound **16**. It was modified with an azide group and functionalized through copper-catalyzed azide-alkyne cycloaddition reaction (CuAAC; Scheme 5).[26-28]

Recently Ogoshi et al. modified the synthesis of DMpillar[5]arene **2** increasing the amount of paraformaldehyde compared to 1,4-dimethoxybenzene, achieving DMpillar[5]arene, **2**, in a short time (3 min) and in high yield (71%) and pillar[5]arene,**1**, almost in quantitative yield.[29]

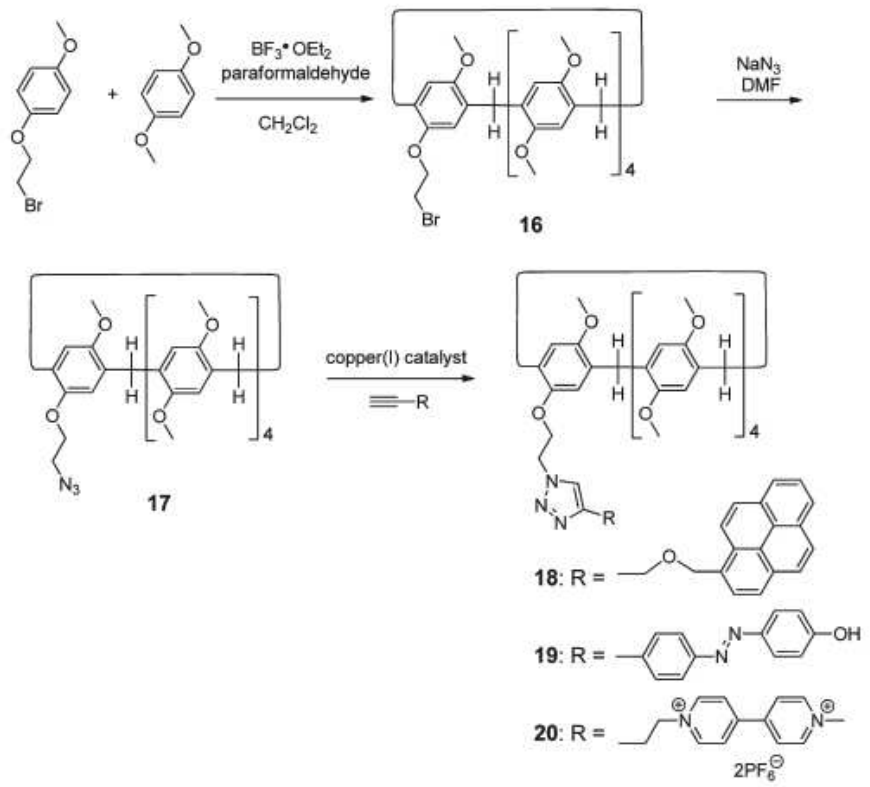

Scheme 5. Synthesis of Copillar[5]arene **16** and its post-modifications.

3.3 Functionalization

The introduction of functional groups can be obtained by using substituted monomers for the cyclization reaction and attractive is the potential further modification of these active moieties.
Hydroxyl groups, for example, are reactive for chemical manipulations and therefore, they can be post-functionalized, affording new properties to the macrocycle.
Consequently, Ogoshi and coworkers exploited the hydroxyl groups of pillar[5]arene **1**, preparing a new fluorescent pillar[5]arene **22** functionalized with phenylethynyl groups (Scheme 6), which exhibited temperature- and solvent-responsive blue-green emission.[30]

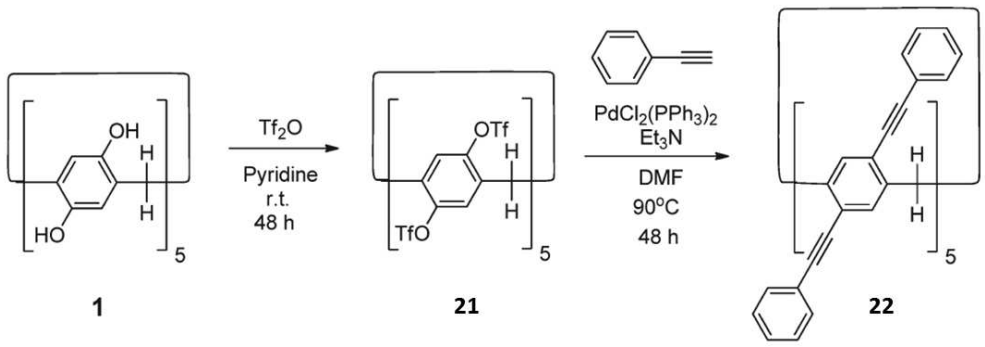

Scheme 6. Synthesis of DPhEpillar[5]arene **22**.

Furthermore, the appropriate introduction of ionic species can provide changes in the solubility, affording water soluble compounds. Negatively charged carboxylate groups with ammonium salt as the counterion afforded successful results (compound **25**, Scheme 7)[12] as well as

trimethylammonium groups that make the cationic macrocycle **26** able to include guests as 1-octanesulfonate in aqueous media (Figure 2).[18]

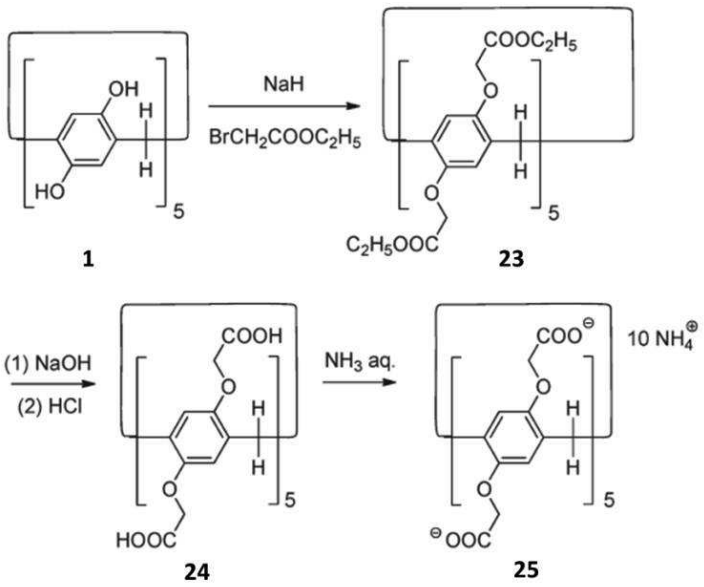

Scheme 7. Synthesis of Water-Soluble Pillar[5]arene **25.**

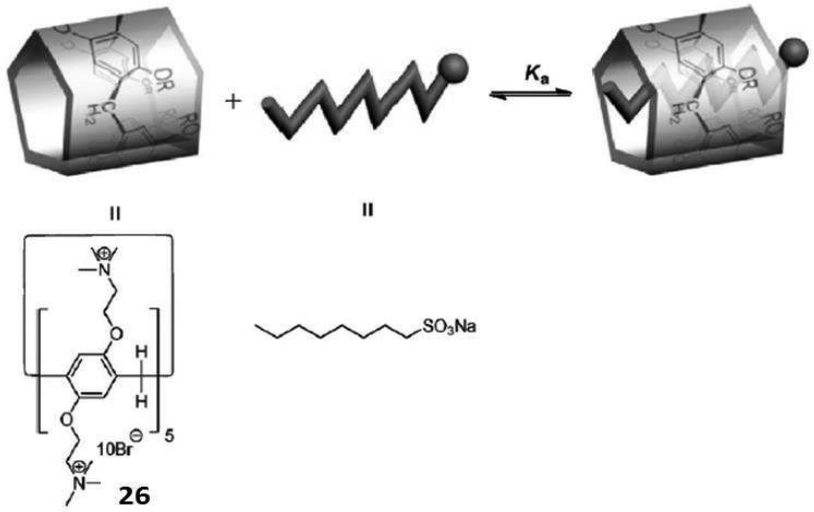

Figure 2. The formation of a host-guest complex from pillar[5]arene **26** and sodium 1-octanesulfonate in water.

Finally, the Copper-(I)-catalyzed azide-alkyne cycloaddition, or "click reaction", represents a simple and versatile synthetic strategy that allows the introduction of several functional groups in pillararenes.[26-28,31]

For example, the treatment of pillar[5]arene **1** with NaH and propargyl bromide yields compound **27**, a useful and versatile macrocycle in which the alkyne groups can be exploited for the "click reaction" with different fragments carrying an azido moiety (Scheme 8).

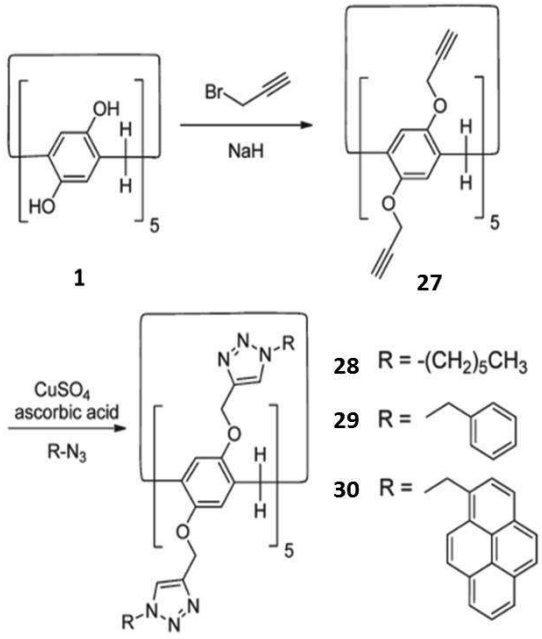

Scheme 8. Synthesis of Pillar[5]arenes **27** employed in "Click Reaction".

3.4 Host-guest binding properties

Complexation processes involving pillar[n]arenes are driven by charge transfer interactions, hydrophobic and electrostatic forces.

Considering the electron-donating cavity, relatively high binding constants (ca. 10^3-10^4 M^{-1}) are reported with typical electron-accepting guests in organic media (Figure 3), suitable for the design and construction of rotaxanes based on pillar[n]arenes.[32]

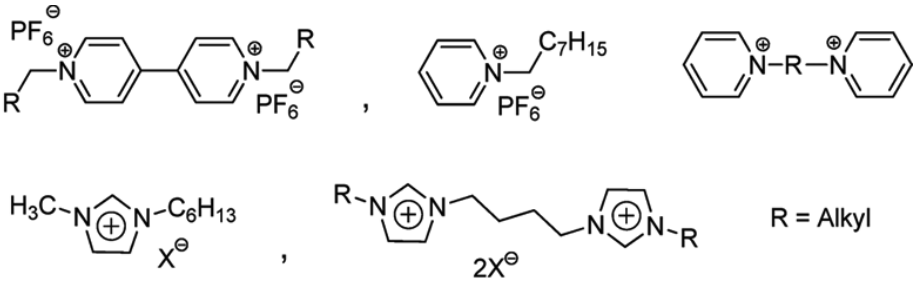

Figure 3. Typical electron-poor guest molecules for pillar[5]arenes.

Ogoshi et al. exploited a trimethyl ammonium group to achieve pillar[5]arene **31** that, due to the interactions between the functional unit and the electron-rich cavity in different organic media, can be observed as a free host in acetone and as a self-inclusion structure in $CDCl_3$ (Figure 4a).[33]

The strong interaction between pillar[5]arene **1** and viologen instead made possible to obtain polyrotaxane **32** by using adamantyl moieties as stopper units (Figure 4b).[34,35]

Recently, supramolecular switches driven by external stimuli based on functionalized pillar[n]arens were investigated. In particular, the photo-responsive pillar[5]arene **19**, obtained by "click reaction"

with an azobenzene unit, was successfully employed to realize a sophisticated architecture by self-assembly, generating a supramolecular switch driven by light stimuli.[27]

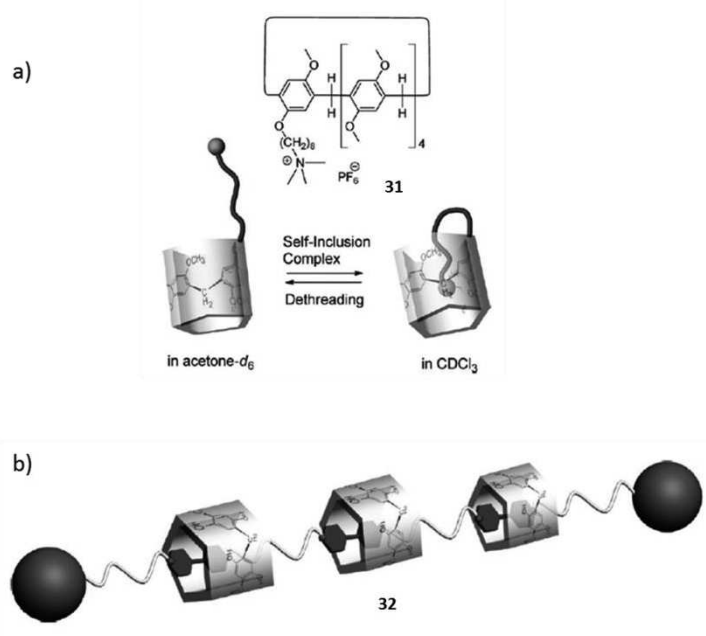

Figure 4. a) Supramolecular structural change of **31** depending on the solvent and b) a pillar[5]arene-based polyrotaxane **32**.

3.5 Spin labelling

Spin labelling of pillar[n]arenes represents a great opportunity to investigate supramolecular systems by Electron Paramagnetic Resonance spectroscopy, considering the potential applications of these macrocycles in host-guest complexes, molecular machines and sophisticated devices.
Effectively, the introduction of stable and persistent radical probes allows the detection of a ESR signal that can be monitored during complexation processes or molecular motion between the components of a supramolecular structure, due to the great sensitivity of this technique towards changes in the radical probe's environment (see Chapter 1).
Therefore, I prepared the first example of a paramagnetic pillar[5]arene based on 2,2,6,6 tetramethylpiperidine *N*-oxide (TEMPO) as the radical probe (Scheme 9).
The monofunctionalization was carried out by following the synthetic strategy reported by Stoddart and co-workers[26] in which the pillar[5]arene is prepared from two different monomers in order to achieve a single functionality in the macrocycle, suitable for further chemical modifications.
Introduction of an azide moiety onto the macrocycle and click reaction with a suitable radical alkyne through CuAAC Huisgen method makes the pillar[5]arene a versatile compound to be functionalized with several different groups.
A similar example is represented by compound **27** (Section 3.3) that, on the contrary, shows the alkyne groups linked to both the edges of the host.
Thus, the reported approach was performed due to its great versatility but also because nitroxide radicals are not apparently reducted in the click reaction conditions (Cu(I) or ascorbate in 10-20% catalytic amounts) , enabling to achieve the spin labelling of different compounds.[36]

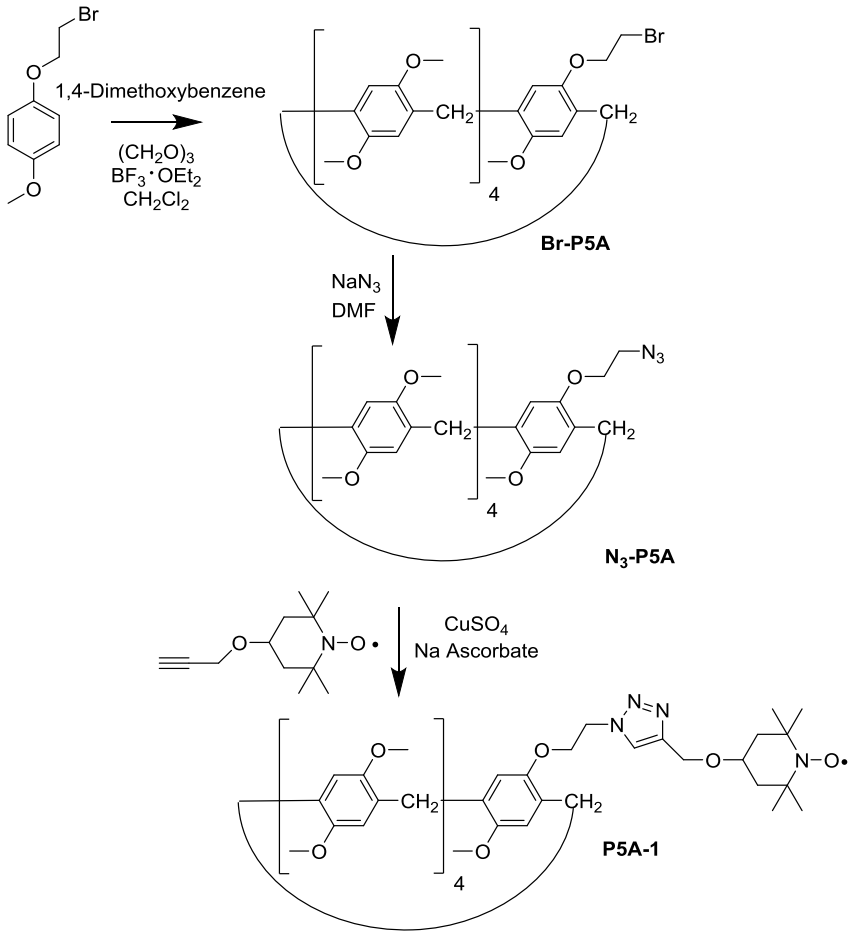

Scheme 9. Synthesis of the spin-labelled pillar[5]arene **P5A-1**.

In details, Scheme 9 reports the synthesis of monofunctionalized pillar[5]arene **P5A-1** by condensation of 5.0 equivalents of 1,4-dimethoxybenzene with 1.0 equivalent of the unsymmetrical hydroquinone derivative 1-(2-bromoethoxy)-4-methoxybenzene and 5.0 equivalents of paraformaldehyde in the presence of $BF_3 \cdot OEt_2$. The bromine atom was substituted with an azide group to create pillar[5]arene derivative **N_3-P5A**, which was functionalized through CuAAC by reaction with the TEMPO alkyne.[37]

The reported host compound was completely characterized by NMR spectroscopy. It should be noted that the presence of the unpaired electron in the molecule negatively affects NMR signals, in particular for protons close to the radical center, determining a low spectral resolution. Considering this, the hydrogens of the TEMPO derivative are not detected and those related to triazole and CH_2-OTEMPO are characterized by broad signals. On the other hand, the macrocycle structure exhibits good spectral resolution due to the larger distance from the radical moiety (Figure 5).

A diamagnetic derivative **P5A-2** carrying the structurally related 2,2,6,6-tetramethylpiperidine unit as substituent was also prepared in order to detect the whole structure. The spectrum in Figure 6, showing the signals (in the box) corresponding to the diamagnetic functional unit attached to the macrocycle, completes the characterization.

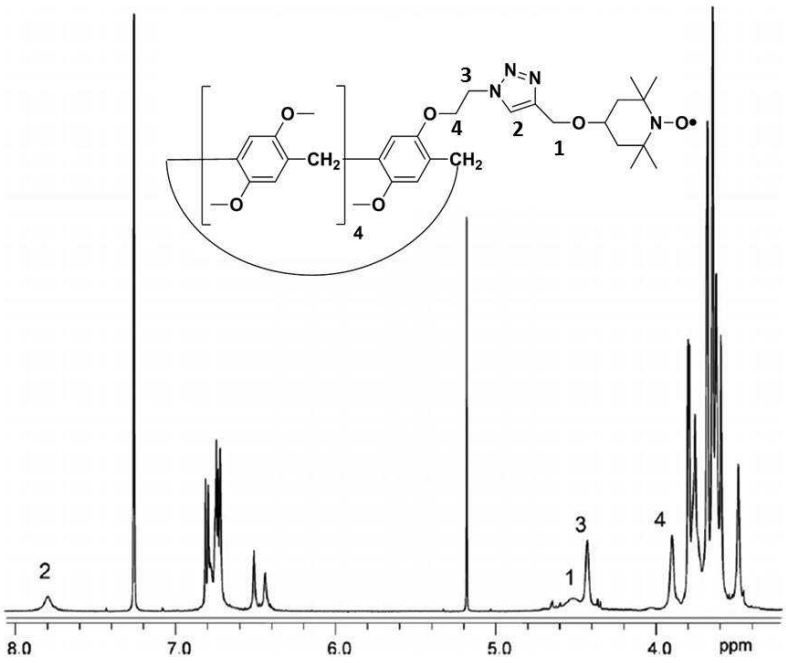

Figure 5. [1]H NMR spectrum ($CDCl_3$, 600 MHz, 298 K) of **P5A-1**.

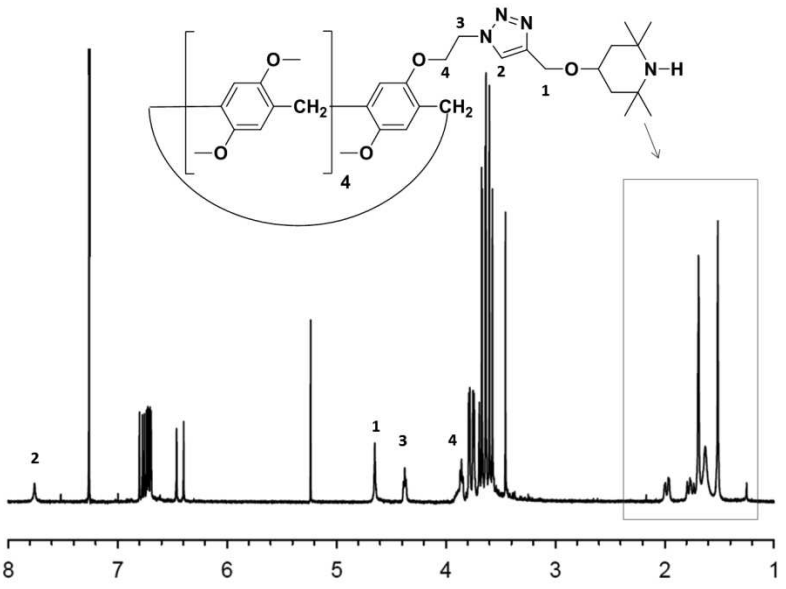

Figure 6. [1]H NMR spectrum ($CDCl_3$, 600 MHz, 298 K) of diamagnetic **P5A-2**.

As mentioned above, the target of my project was the synthesis of a paramagnetic pillar[5]arene that could be employed in different supramolecular architectures, allowing investigations with ESR spectroscopy, therefore, the introduction of the radical moiety should not hinder the binding ability of the reported host.

Consequently, the host-guest complexation properties were investigated by ESR and NMR spectroscopy, in order to observe whether the presence of the paramagnetic side arm could provide differences in the radical pillar[5]arene behavior compared to the unfunctionalized compound, characterized by relatively high binding constants with imidazolium and pyridinium derivatives (ca. 10^3-10^4 M^{-1}).

In particular, 4-methyl-*N*-butylpiridinum-hexafluorophosphate (PF_6) salt shown in Figure 6 was employed as the model guest in our studies with **P5A-1**.

The free paramagnetic compound (Figure 7a) and the related inclusion complex with the model guest (Figure 7b) were detected by recording ESR spectra in deoxygenated $CHCl_3$ solution at room temperature.

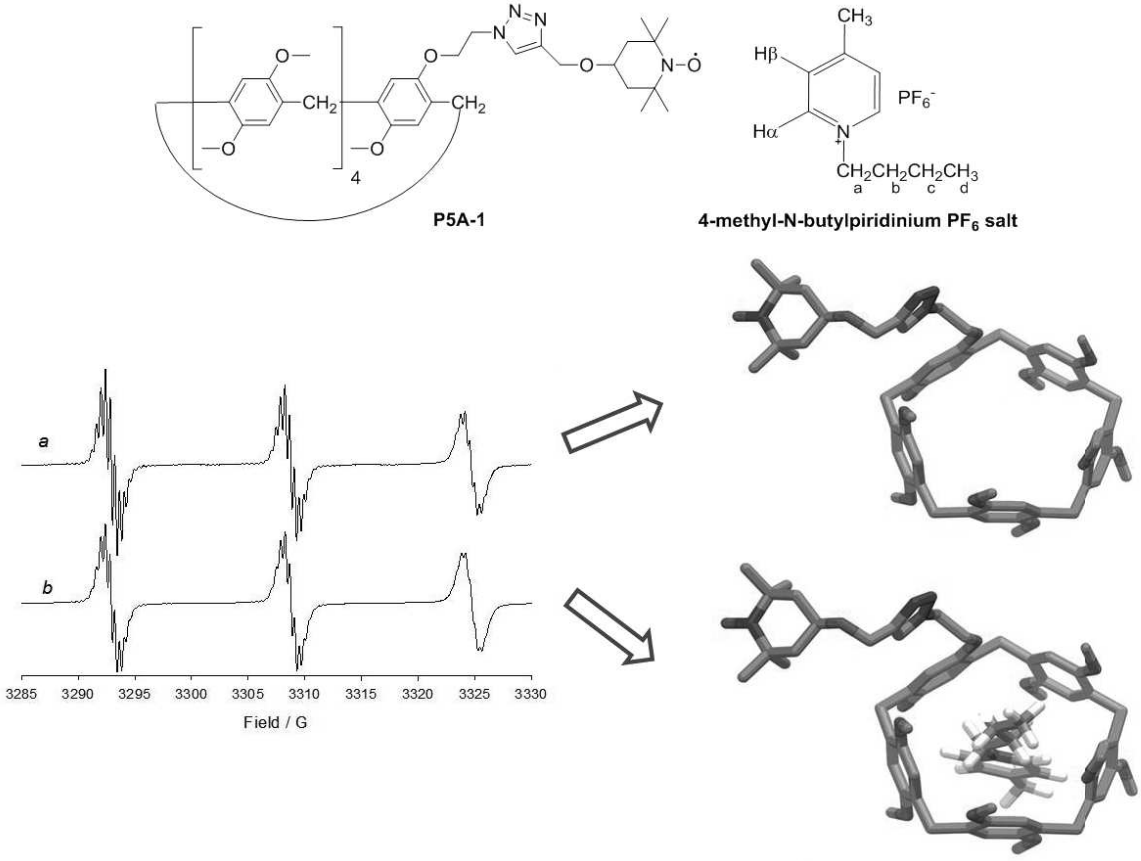

Figure 7. EPR spectra of **4a** (0.1 mM) in a deoxygenated $CHCl_3$ solution recorded at room temperature in the absence (*a*) and in the presence (*b*) of 3 equivalents of 4-methyl-*N*-butylpyridinum PF_6.

The spectrum shows typical nitroxide EPR signals with a(N) = 15.86 G and g = 2.0058, and the highfield line slightly broadened due to restricted tumbling (see Figure 7a). Partially resolved coupling with γ protons (0.40 G) is also evident. EPR spectrum was recorded also in the presence of 4-methyl-N-butylpyridinium PF_6 as the guest molecule.Both free and complexed radicals show very similar ^{14}N hyperfine splittings, a(N) = 15.91 G, which indicates that the complexation does not significantly affect the spin distribution on the nitroxide moiety. This observation also suggests that the radical fragment of the free host is located outside the pillar[5]arene cavity. In fact, a displacement of the nitroxide unit from inside the cavity of the host to the bulk solvent should lead to an appreciable change in the ^{14}N hyperfine splitting, as has been observed in other paramagnetic host–guest complexes.[38]

However, a decrease of the mobility and then of the correlation time (τ) of the paramagnetic host in the presence of the guest is fairly expected and effectively, the broadening of the principal field lines constitutes an evidence of this variation. In the present case probably due to the size of the

model guest, rather small to substantially affect the correlation time of the macrocycle, the slight difference between free and complexed macrocycle does not allow to perform EPR titration experiments to measure a binding constant.
On the contrary, NMR investigations were possible due to the considerablespectral resolution resulting from the protons of the macrocycle and of the radical linker.
In particular, while the protons of the macrocycle did not undergo significantly variations upon the inclusion process, the spectra report an interesting downfield shift for the signals of the side arm compared to those of the free host (Figure 8). This behavior could be indicative of a displacement of the side arm from the original position due to host-guest interaction. .

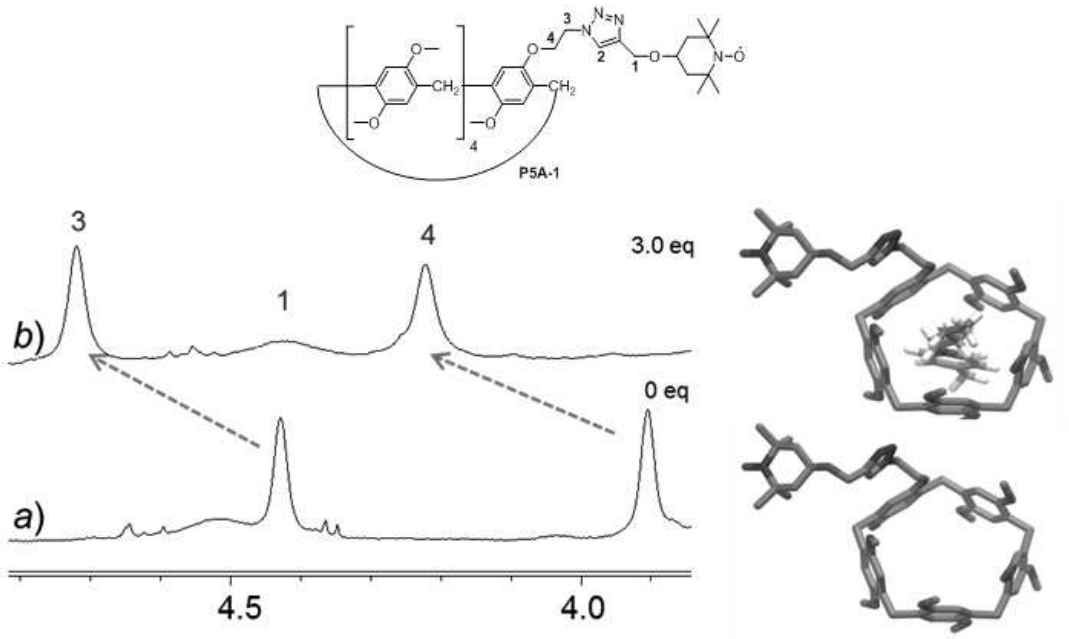

Figure 8. Partial ^{1}H-NMR spectra ($CDCl_3$, 600 MHz, 298 K) of **P5A-1** 2.3 mM, in the presence of *a*) 0 and *b*) 3 equivalents of 4-methyl-*N*-butylpyridinium-PF_6.

In addition, clear and remarkable shifts for some protons of the guest upon the complexation process are detectable
In particular, the remarkable shielding of the aromatic protons Hα (-2.34 ppm) and of the methylene protons Ha and Hb (-3.77 and -3.21 ppm respectively) of the guest molecule (see Figure 7) indicate that these groups are located inside the cavity of the functionalized pillar[5]arene while the methyl group attached in position 4 to the pyridinium, showing a small downfield shift (+0.1 ppm), should stay outside (Table 1).

Guest proton	δ (ppm) free guest	δ (ppm) P5A-1@guest	δ (ppm) P5A-2@guest	δ (ppm) 2@guest
Hα	8.52	6.18	6.23	6.40
Hβ	7.78	7.48	7.45	7.52
CH_3(Pyr)	2.66	2.76	2.70	2.74
Ha	4.52	0.75	0.83	1.83
Hb	1.95	-1.26	-1.22	-0.33
Hc	1.38	0.01	0.01	0.26
Hd	0.96	0.40	0.38	0.51

Table 1. Complex-induced shifts (CIS) of the guest molecule observed in the presence of different macrocycles.

Variations in chemical shift for the protons of the free guest were investigated also with the diamagnetic compound **P5A-2** and the unfunctionalized macrocycle dimethoxypillar[5]arene **2** in order to take into account an overview of the inclusion properties of this molecule.
It should be noted that the unsymmetrical structure of the macrocycle carrying the radical label can afford two different complexes, assuming that the guest could be threaded through the cavity from the spin-labelled side or from the opposite rim.
Although the NMR data reported are not exhaustive to confirm the orientation of the threading, one can notice that the methylene protons in the butyl group exhibit larger chemical shifts upon the inclusion in the cavity of the functionalized compounds **P5A-1** and **P5A-2** than those reported in the parent host **2**, suggesting that part of the butyl chain of the guest could face the side of the functional unit.
Interestingly, the sensitivity of the protons of the guest to the complex formation was exploited to perform a ^{1}H NMR titration of **P5A-1** into a solution of the guest to accurately determine the association constant (Figure 9a).
Spectra recorded in $CDCl_3$ demonstrate the possibility to monitor the inclusion process by following the NMR shifts of selected protons of the guest after the addition of increasing amount of pillar[5]arene.
An association constant (K_{ass}) of 2572 M^{-1} in $CDCl_3$ was calculated from a curve-fitting analysis in which the complexation-induced chemical shifts (CISs) of the aromatic protons Hα and the methylene protons in the butyl chain were reported versus the concentration of the paramagnetic pillar[5]arene (Figure 9b). Besides, a K_{ass} = 2374 M^{-1} for the diamagnetic compound **P5A-2** in similar conditions was achieved (Figure 10a).
These values, compared to the binding constant of 2197 M^{-1} calculated for the unfunctionalized compound **2** with the same guest in chloroform (Figure 10b), suggests that the presence of the radical arm does not decrease the host-guest properties of our host compound.

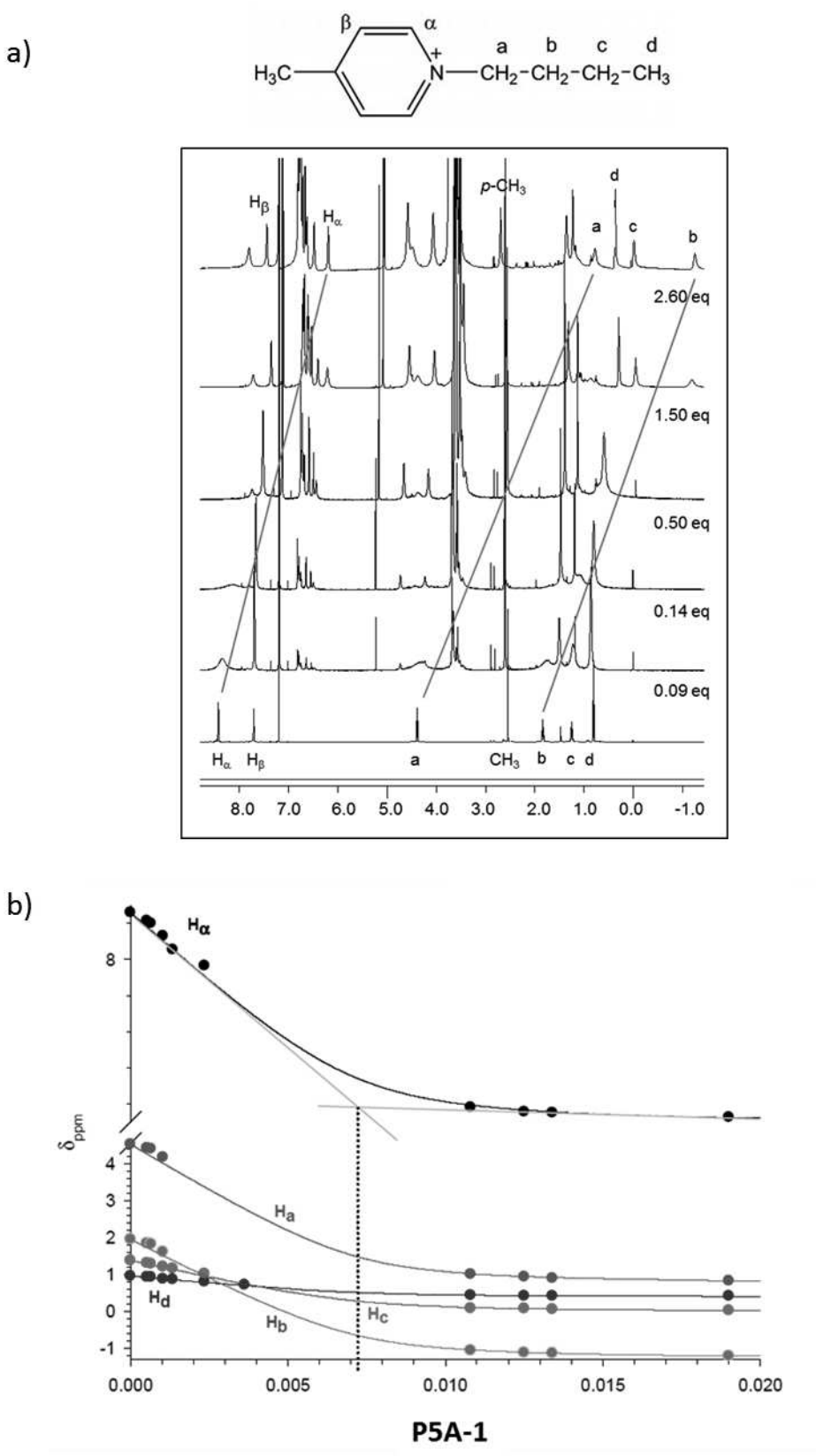

Figure 9. a) ^{1}H NMR titration (600 MHz, $CDCl_3$, 298 K) of **P5A-1** (host) against a 7.23 mM solution of 4-methyl-*N*-butylpyridinum PF_6 (guest); b) plot of the CIS of selected protons of the guest versus the concentration of the paramagnetic host.

In details, from the titration curve important information can be gained.
The lines observed indicate the strictly dependence of the chemical shifts of the guest on the increasing amount of the host.
Moreover, the stoichiometry of the complex can be determined by the molar ratio method[39] applied to the titration curve because the intersect of the asymptotes for the curve corresponding to Hα protons (see Figure 9), related to the concentration of the guest necessary to saturate all binding sites provides the value of 7.1 mM, that corresponds to a stoichiometry of 1:1.

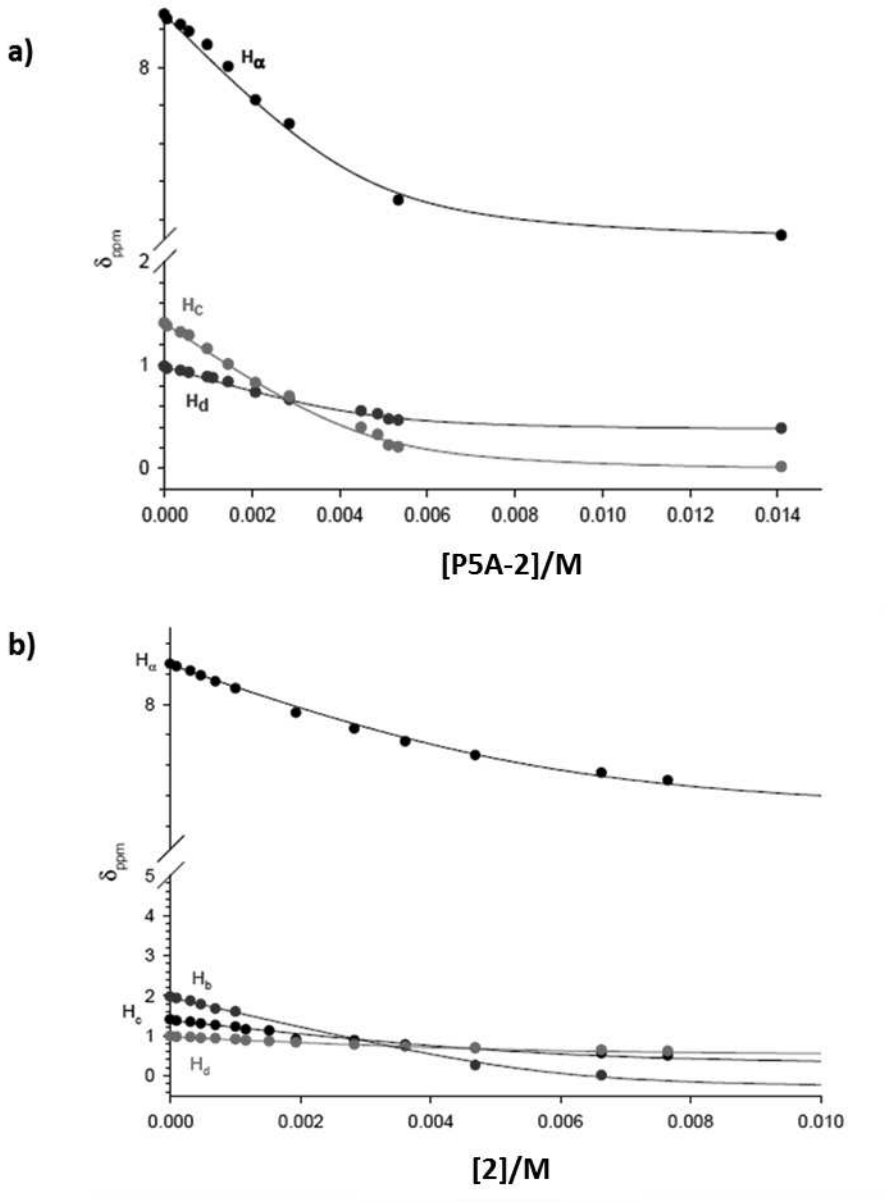

Figure 10. a) Plot of the CIS of selected protons of 4-methyl-*N*-butylpyridinium guest (4.69 mM) versus the concentration of the host **P5A-2** and b) of the shift of selected protons of the guest (5.87 mM) versus the concentration of the **2**.

3.6 Conclusions

The first example of a paramagnetic pillar[5]arene was synthesized in good yields and the related host-guest properties were investigated by using 4-methyl-*N*-butylpyridinium hexafluorophosphate salt, a small molecule taken as the model guest that shows affinity for the pillar cavity due to the electron-poor structure.

In particular, since the presence of the side arm bearing the nitroxide unit does not reduce the binding affinity of the macrocycle for the guest, the reported compound complies with the initial target, the preparation of a host molecule suitable to be employed in host-guest systems, rotaxanes and more complex supramolecular structures, allowing their characterization and the investigation of the molecular motion between the interacting components by the Electron Spin Resonance spectroscopy.

References

[1] M. Xue, Y. Yang, X. Chi, Z. Zhang, F. Huang, *Accounts of Chemical Research*, **2012**, *45*, 1294-1308.

[2] T. Ogoshi, T. Yamagishi, *Eur. J. Org. Chem*., **2013**, 2961-2975.

[3] T. Ogoshi, S. Kanai, S. Fujinami, T. A. Yamagishi, Y. Nakamoto, *J. Am. Chem. Soc.*, **2008**, *130*, 5022-5023.

[4] a) M. Xue, Y. Yang, X. Chi, Z. Zhang, F. Huang, *Acc. Chem. Res.*, **2012**, *45*, 1294-1308; b) P. J. Cragg, K. Sharma, *Chem. Soc. Rev.*, **2012**, *41*, 597-607; c) T. Ogoshi, T. A. Yamagishi, *Eur. J. Org. Chem.*, **2013**, 2961-2975.

[5] a) M. V. Rekharsky, Y. Inoue, *Chem. Rev.*, **1998**, *98*, 1875-1918; b) A. Harada, A. Hashidzume, H. Yamaguchi, Y. Takashima, *Chem. Rev.*, **2009**, *109*, 5974-6023; c) B. H. Han, A. Müller, *Chem. Rev.*, **2006**, *106*, 782-817.

[6] a) J. W. Lee, S. Samal, N. Selvapalam, H. J. Kim, K. Kim, *Acc. Chem. Res.*, **2003**, *36*, 621-630; b) J. Lagona, P. Mukhopadhyay, S. Chakrabarti, L. Isaacs, *Angew. Chem.*, **2005**, *117*, 4922; *Angew. Chem. Int. Ed.*, **2005**, *44*, 4844-4870.

[7] H. Deng, X. Shu, X. Hu, J. Li, X. Jia, C. Li, *Tetrahedron Lett.*, **2012**, *53*, 4609-4612.

[8] C. Han, G. Yu, B. Zheng, F. Huang, *Org. Lett.*, **2012**, *14*, 1712-1715.

[9] M. Ni, Y. Guan, L. Wu, C. Deng, X. Hu, J. Jiang, C. Lin, L. Wang, *Tetrahedron Lett.*, **2012**, *53*, 6409-6413.

[10] X. Shu, S. Chen, J. Li, Z. Chen, L. Weng, X. Jia, C. Li, *Chem. Commun.*, **2012**, *48*, 2967-2969.

[11] X. Y. Shu, J. Z. Fan, J. Li, X. Y. Wang, W. Chen, X. S. Jia, C. J. Li, *Org. Biomol. Chem.*, **2012**, *10*, 3393-3397.

[12] T. Ogoshi, M. Hashizume, T. A. Yamagishi, Y. Nakamoto, *Chem. Commun.*, **2010**, *46*, 3708-3710.

[13] T. Ogoshi, K. Kitajima, T. Aoki, T. Yamagishi, Y. Nakamoto, *J. Phys. Chem. Lett.*, **2010**, *1*, 817-821.

[14] T. Ogoshi, S. Tanaka, T. Yamagishi, Y. Nakamoto, *Chem. Lett.*, **2011**, *40*, 96-98.

[15] C. Li, Q. Xu, J. Li, F. Yao, X. Jia, *Org. Biomol. Chem.*, **2010**, *8*, 1568-1576.

[16] C. Li, L. Zhao, J. Li, X. Ding, S. Chen, Q. Zhang, Y. Yu, X. Jia, *Chem. Commun.*, **2010**, *46*, 9016-9018.

[17] C. Li, X. Shu, J. Li, S. Chen, K. Han, M. Xu, B. Hu, Y. Yu, X. Jia, *J. Org. Chem.*, **2011**, *76*, 8458-8465.

[18] Y. Ma, X. Ji, F. Xiang, X. Chi, C. Han, J. He, Z. Abliz, W. Chen, F. Huang, *Chem. Commun.*, **2011**, *47*, 12340-12342.

[19] X. B. Hu, L. Chen, W. Si, Y. Yu, J. L. Hou, *Chem. Commun.*, **2011**, *47*, 4694-4696.

[20] Q. Duan, W. Xia, X. Hu, M. Ni, J. Jiang, C. Lin, Y. Pan, L. Wang, *Chem. Commun.*, **2012**, *48*, 8532-8534.

[21] T. Ogoshi, K. Kitajima, T. A. Yamagishi, Y. Nakamoto, *Org. Lett*., **2010**, *12*, 636-638.

[22] T. Ogoshi, K. Kitajima, T. Aoki, S. Fujinami, T. A. Yamagishi, Y. Nakamoto, *J. Org. Chem*., **2010**, *75*, 3268-3273.

[23] Z. Zhang, B. Xia, C. Han, Y. Yu, F. Huang, *Org. Lett*., **2010**, *12*, 3285-3287.

[24] Z. Zhang, Y. Luo, J. Chen, S. Dong, Y. Yu, Z. Ma, F. Huang, *Angew. Chem., Int. Ed*., **2011**, *50*, 1397-1401.

[25] Z. Zhang, G. Yu, C. Han, J. Liu, X. Ding, Y. Yu, F. Huang, *Org. Lett*., **2011**, *13*, 4818-4821.

[26] N. L. Strutt, R. S. Forgan, J. M. Spruell, Y. Y. Botros, J. F. Stoddart, *J. Am. Chem. Soc*., **2011**, *133*, 5668-5671.

[27] H. Zhang, N. L. Strutt, R. S. Stoll, H. Li, Z. Zhu, J. F. Stoddart, *Chem. Commun*., **2011**, *47*, 11420-11422.

[28] N. L. Strutt, H. Zhang, M. A. Giesener, J. Lei, J. F. Stoddart, *Chem. Commun*., **2012**, *48*, 1647-1649.

[29] T. Ogoshi, T. Aoki, K. Kitajima, S. Fujinami, T. A. Yamagishi, Y. J. Nakamoto, *Org. Chem*., **2011**, *76*, 328-331.

[30] T. Ogoshi, K. Umeda, T. A. Yamagishi, Y. Nakamoto, *Chem. Commun*., **2009**, 4874-4876.

[31] T. Ogoshi, R. Shiga, M. Hashizume, T. A. Yamagishi, *Chem.Commun*., **2011**, *47*, 6927-6929.

[32] T. Ogoshi, D. Yamafuji, T. Aoki, K. Kitajima, T. Yamagishi,Y. Hayashi, S. Kawauchi, *Chem. Eur. J.*, **2012**, *18*, 7493-7500.

[33] T. Ogoshi, K. Demachi, K. Kitajima, T. A. Yamagishi, *Chem. Commun*., **2011**, *47*, 7164-7166.

[34] T. Ogoshi, Y. Nishida, T. A. Yamagishi, Y. Nakamoto, *Macromolecules*, **2010**, *43*, 3145-3147.

[35] T. Ogoshi, Y. Nishida, T. A. Yamagishi, Y. Nakamoto, *Macromolecules*, **2010**, *43*, 7068-7072.

[36] C. Casati, P. Franchi, R. Pievo, E. Mezzina, M. Lucarini, *J.Am. Chem. Soc.*, **2012**, *134*, 19108-19117.

[37] R. Manoni, P. Neviani, P. Franchi, E. Mezzina, M. Lucarini, *Eur. J. Org. Chem.*, **2014**, 147-151.

[38] P. Franchi, M. Lucarini, G. F. Pedulli, *Curr. Org. Chem.*, **2004**, *8*, 1831-1849.

[39] H.-J. Schneider, A Yatsimirsky, in: *Principle and Methods in Supramolecular Chemistry*, Wiley, Chichester, UK, **2000**, 137-226.

Spin labelled Rotaxanes

Chapter 4. Spin labelled Rotaxanes

4.1 Introduction

Cyclophanes represent a class of synthetic macrocycles based on bridged aromatic molecules with versatile host-guest properties.

The ciclobis (paraquat-p-phenylene) ($CBPQT^{4+}$), member of this family extensively used in supramolecular chemistry, is a tetracationic receptor consisting of two 4,4'-bipyridinium units linked by p-xylylene groups that exhibits exciting binding abilities due to charge-tranfer interactions between the electron-accepting cavity and electron-donating aromatic guests like tetrathiafulvalene (TTF) and 1,5-dioxynaphtalene (DNP) units (Figure 1).[1]

In particular, $CBPQT^{4+}$ has attracted great attention due to the various applications as component of mechanical interlocked structures like rotaxanes[2] and catenanes (Figure 2).[3]

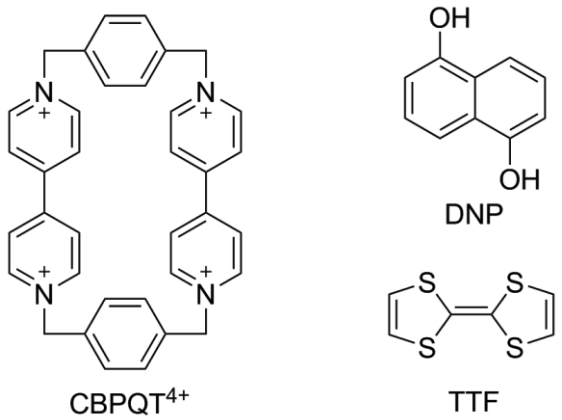

Figure 1. Ciclobis (paraquat-p-phenylene) and the electron-rich guests TTF and DNP.

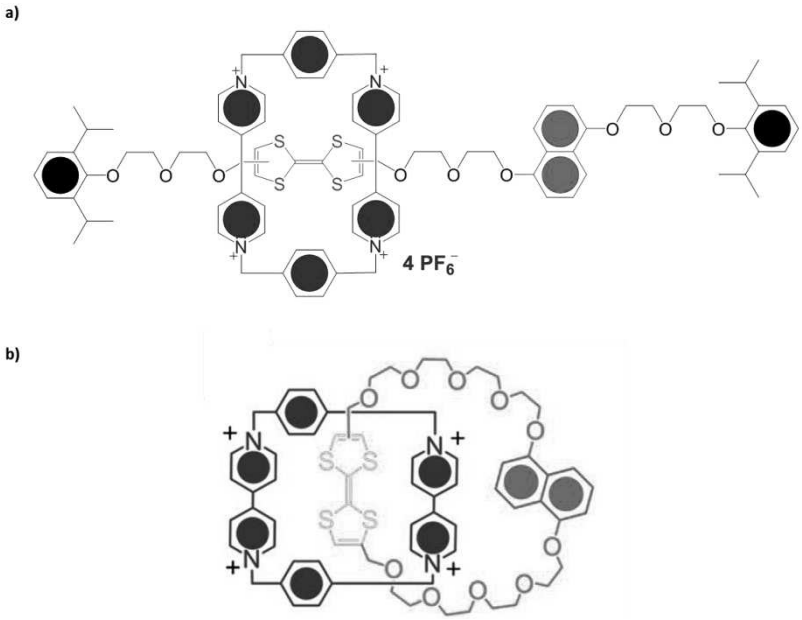

Figure 2. a) Example of rotaxane and b) catenane based on $CBPQT^{4+}$.

4.2 Spin labelling of rotaxanes

The development of ever more sophisticated mechanical interlocked structures requires a deep knowledge of the molecular recognition mechanism that involves the related components and full characterization of the structure.
The introduction of stable and persistent radical groups represents an attractive opportunity that allows the detection and characterization of these systems by the Electron Spin Resonance spectroscopy, a valuable technique that can provide additional information to those obtained by traditional methods.[4]
Spin labelling can involve the macrocycle and/or the linear component of the supramolecular architecture.
In particular, we focused our attention on one of the most studied mechanical interlocked molecules, the bistable [2]rotaxane reported by Stoddart and Heath (Figure 2a), in which the affinity of the $CBPQT^{4+}$ ring for two recognition sites along the thread, TTF and DNP units, affords a molecular switch driven by external stimuli.
Therefore, we prepared and characterized analogous systems containing nitroxide spin labels as stoppers.[5,6]

4.3 [2]rotaxanes containing tetrathiafulvalene or 1,5-dioxynaphtalene molecular stations

The synthesis and characterization of bis-labelled [2]rotaxanes consisting of $CBPQT^{4+}$ as the macrocyclic component, tetrathiafulvalene or 1,5-dioxynaphtalene as recognition sites and bulky nitroxide groups as stoppers are reported in this section.

4.3.1 Synthesis and ^{1}H NMR characterization

Paramagnetic interlocked structures were obtained by following the synthetic strategy reported by Stoddart and coworkers[7] , that exploits the "threading and stoppering approach".
In particular, driven by charge-transfer interactions between the tetracationic ring and the electron-rich molecular station, the complexation process led to the formation of a pseudorotaxane in which the components were, subsequenly, trapped by bulky nitroxide groups.
Functionalization of the linear thread and of TEMPO derivatives employed as stopper units, respectively with azide and alkyne groups, made possible to covalently link these components by exploiting the Copper-(I)-catalyzed azide-alkyne cycloaddition,[8] in order to prevent the pseudorotaxane from dissociation.
The synthetic approach followed to obtain the azide compound containing the DNP molecular station is reported in Scheme 1a.
We first investigated whether the size of TEMPO moiety was suitable to act as a stopper group for the macrocyclic cavity by NMR spectroscopy. In particular, we found that a mixture of the diamagnetic dumbbell **2b**, used to improve the spectral resolution, and $CBPQT^{4+}$ in d_7-dimethylformamide did not show any signals related to complexation processes, therefore, we assumed that TEMPO derivatives could be employed for rotaxanes based on $CBPQT^{4+}$.
Thus, $CBPQT{\bullet}4PF_6$ and DNP diazide **1** were mixed in dimethylformamide at -10°C in order to afford the pseudorotaxane and, subsequently, nitroxide alkyne 4-propargyloxy-TEMPO was added

together with a catalytic amount of $[Cu(MeCN)_4]PF_6$ and (benzyltriazolylmethyl) amine (TBTA) as the stabilizing agent (Scheme 1).

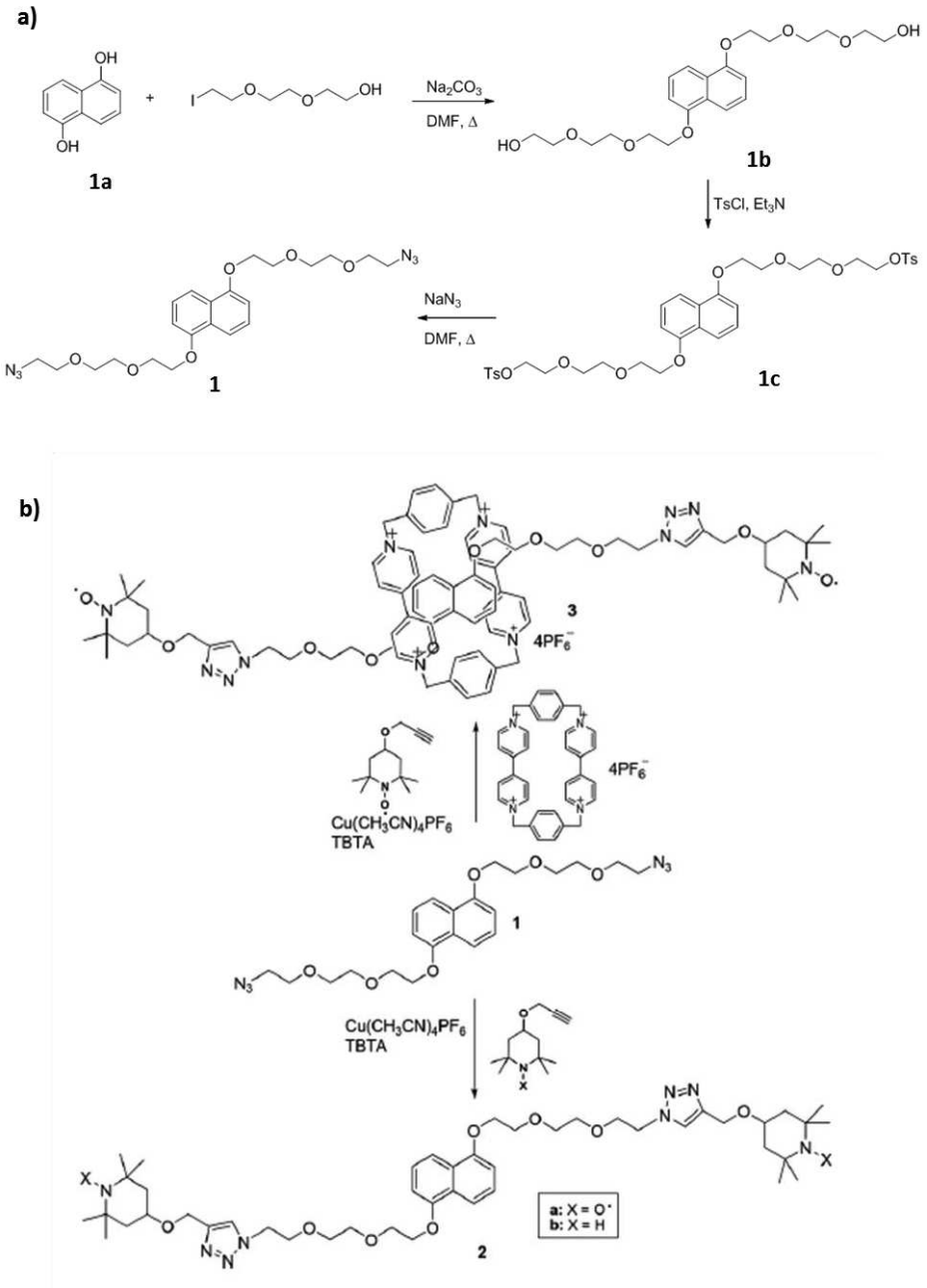

Scheme 1. a) Synthetic approach followed to obtain derivative 1 and b) "click reaction" with TEMPO derivatives.

Nevertheless, the reaction performed did not afford successful results; in particular, the purification process through silica gel chromatography did not allow to collect pure rotaxane fractions but only mixtures containing the desired compound together with the starting materials.

This event could be ascribed to a "partial dethreading" of the ring related to the not sufficiently hindered structure of the stopper moiety that disadvantages the formation of a significant amount of product.

Evaluating these results, we decided to substitute the four methyl groups of the TEMPO derivative and create a more hindered structure carrying cyclohexyl moieties, the spirocyclic paramagnetic derivative **5a** (Scheme 2).

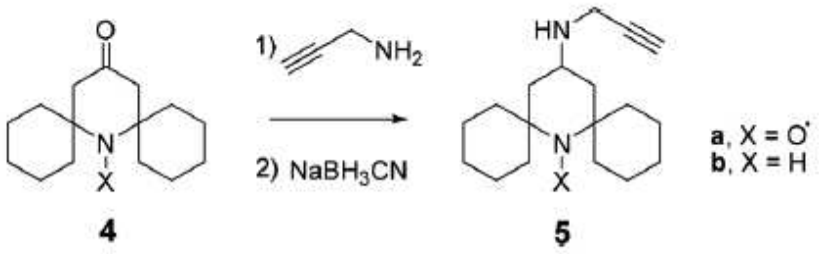

Scheme 2. Synthesis of the spirocyclic stopper **5a**.

The new derivative **5a** was prepared from piperidin-4-one compound **4** and propargylamine in excess without any solvent, followed by the reduction with sodium cyanoborohydride of the related Schiff base.

Afterwards, the rotaxanation process was successfully performed by adding the new bulky stopper to the pseudorotaxane mixture, affording rotaxane **7** in 30% yield (Scheme 3).

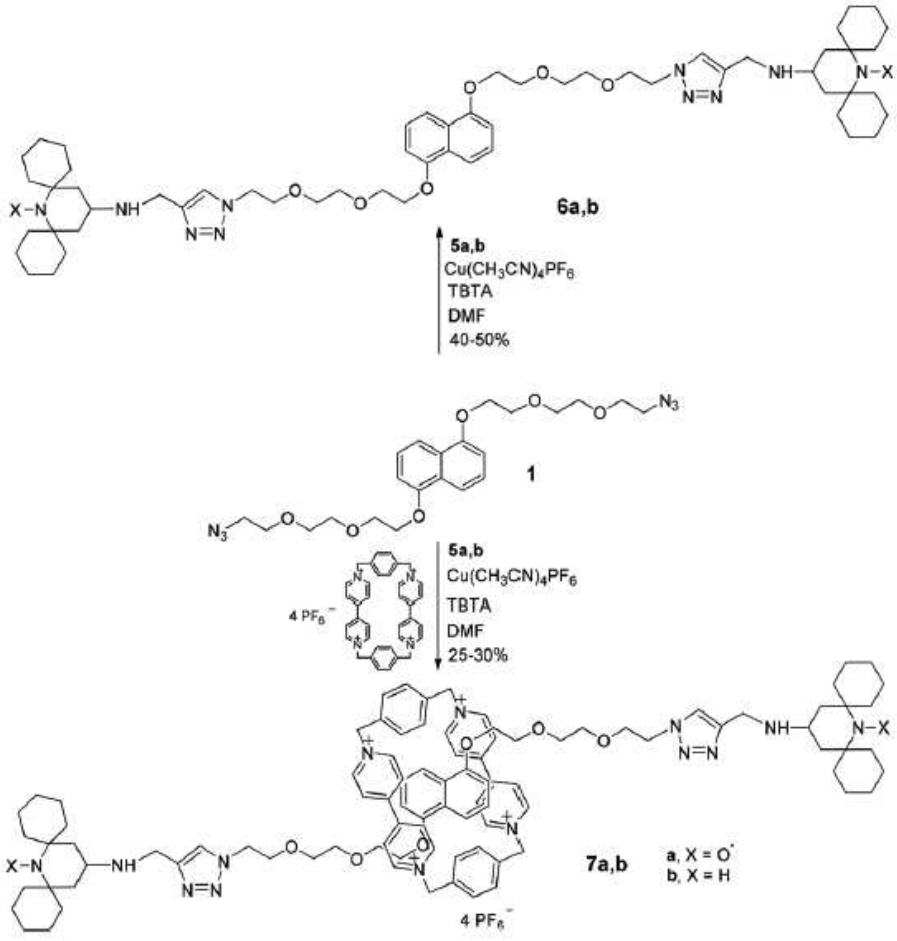

Scheme 3. Synthesis of the DNP-based rotaxane **7**.

The interlocked compound **7a** was detected and characterized by ^{1}H NMR spectroscopy.
Furthermore, due to the lack of signals belonging to the radical fragments, phenylhydrazine was employed in order to achieve in situ reduction of the nitroxide groups, affording the corresponding diamagnetic compound N-hydroxy form, also for dumbbell **6a**.

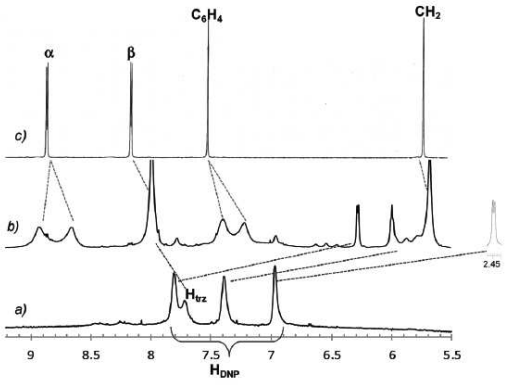

Figure 3. Partial ^{1}H NMR spectra (600 MHz, CD_3CN, 298 K) of (a) dumbbell **6a**; (b) rotaxane **7a**; (c) $CBPQT^{4+}$ host (H_{trz} = triazole proton, H_{DNP} = DNP aromatic protons, α,β = $CBPQT^{4+}$ bipyridinium α and β protons, respectively; C_6H_4 = host p-phenylene protons; CH_2 = host benzyl protons).

Figure 3 shows partial NMR spectra in CD_3CN of dumbbell **6a**, rotaxane **7a** and free $CBPQT^{4+}$ ring. Blue lines underline the remarkable upfield shifts for DNP protons upon the inclusion process in the $CBPQT^{4+}$ cavity, providing evidence of the formation of the interlocked structure. Red lines show the broadening of the macrocyclic signals determined by the slow rotation of the ring trapped in the complex on the ^{1}H NMR time scale at 298K.
$CBPQT^{4+}$ exhibits also a splitting for bipyridinium and p-phenylene groups signals, indicating that the slow exchange process allows the detection of distinct signals for nonequivalent protons.

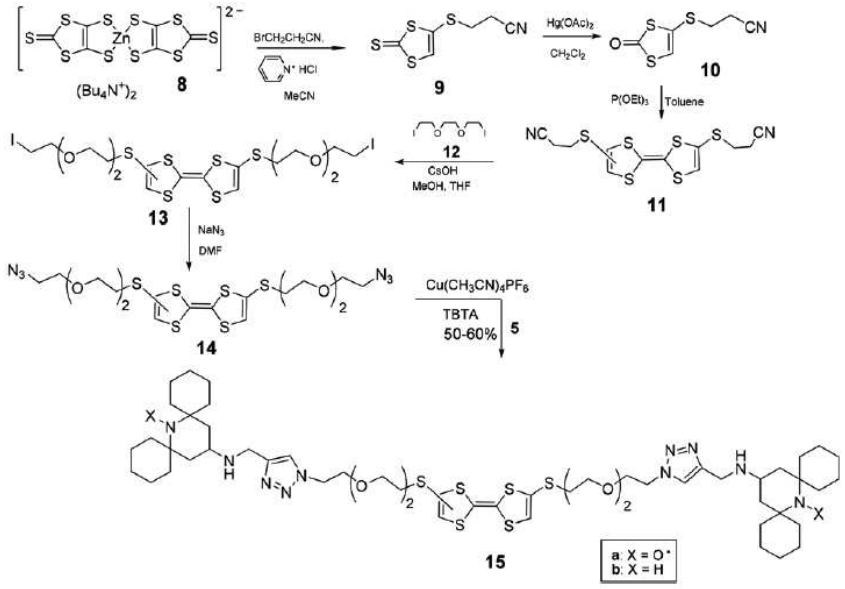

Scheme 4. Synthetic strategy for the TTF component.

Afterwards, we focused on the synthesis of the [2]rotaxane containing the tetrathiafulvalene molecular station.

The synthetic strategy followed to achieve the TTF diazide derivative **14** is reported in Scheme 4.

In particular, $TBA_2[Zn(DMIT)_2]$ [**8**, bis(tetrabutylammonium)bis-(1,3-dithiole-2-thione-4,5 dithiolato)zinc complex)] was reacted with 3-bromopropionitrile affording compound **9**;[9] derivative **10** was then obtained by conventional reactions[9,10] and the coupling in presence of triethylposphite afforded TTF derivative **11**.[10] The substitution of the 2-cyanoethyl groups was achieved by subsequent reaction with cesium hydroxide and diiodo derivative **12**[11] then the azide compound was easily obtained by exchange reaction of **13** with NaN_3.

The desired compound carrying the azide moieties **14** was exploited for the Copper-(I)-catalyzed click reaction with the spirocyclic stopper **5a** leading to the corresponding dumbbell and, under the same conditions employed for DNP-based rotaxane, to the interlocked structure **16a** (Scheme 5).

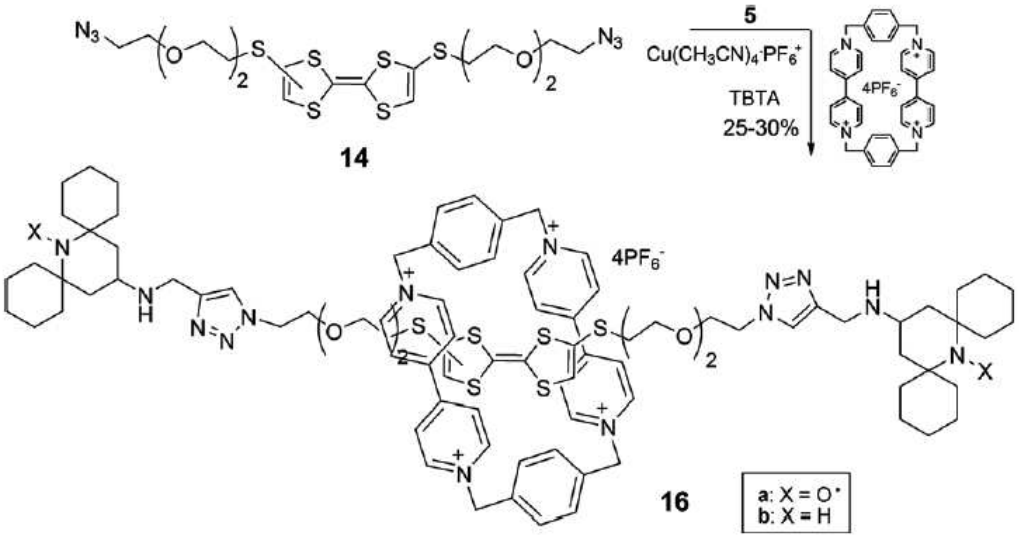

Scheme 5. Synthesis of the TTF-based rotaxane **16**.

In Figure 4 partial ^{1}H NMR spectra of dumbbell **15a** and rotaxane **16a** are reported.

As observed for DNP compound, the considerable shielding observed for the TTF protons clearly identify their inclusion within the ring cavity; on the other hand, a remarkable downfield shift is detected for protons not involved in the complexation process.

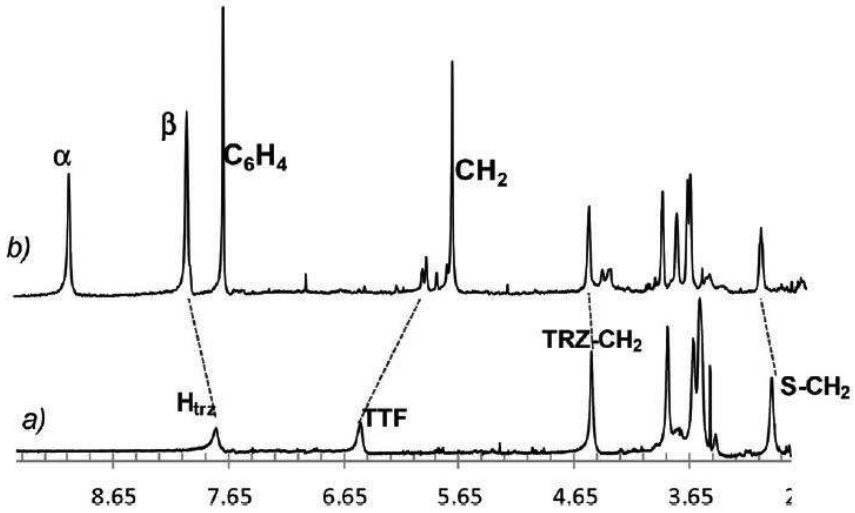

Figure 4. Partial ^{1}H NMR spectra (600 MHz, CD_3CN, 298 K) of (a) dumbbell **15a**; (b) rotaxane **16a**. Htrz = triazole proton, TTF = TTF protons, TRZ-CH_2 = N-methylene protons of the triazole, S-CH_2 = TTF-S-methylene protons, α, β = $CBPQT^{4+}$ bipyridinium α and β protons, respectively; C_6H_4 = host p-phenylene protons; CH_2 = host benzyl protons.

4.3.2 ESR characterization

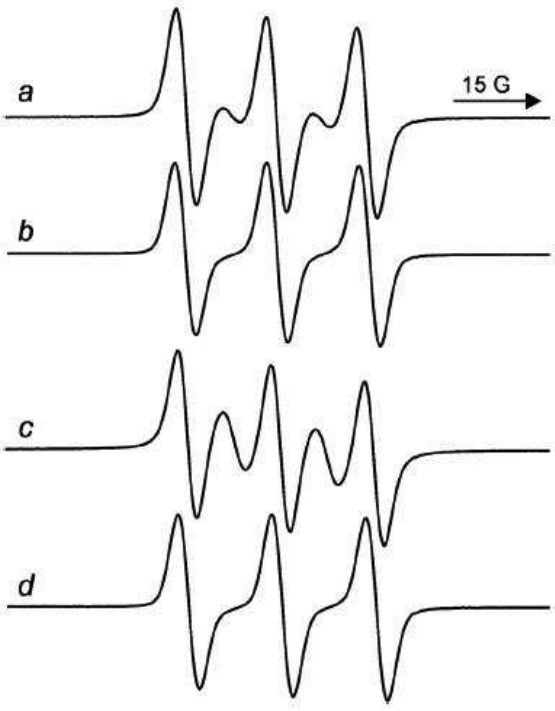

Figure 5. ESR spectra of dumbbells **6a** (a) and **15a** (c) and the corresponding rotaxanes **7a** (b) and **16a** (d) in ACN at 338 K.

Interesting ESR results were achieved with our spin labelled supramolecular systems; in particular, considerable differences in the presence of free and interlocked species were detected (Figure 5).

It should be noted that the ESR spectrum of a mononitroxide is characterized by three lines, originated by the interaction between the unpaired electron and the nitrogen atom.
On the other hand, when two radical centers coexist in the same structure a spin exchange interaction may occur, giving rise to additional lines in the ESR spectrum.
This exchange interaction, measured by the coupling constant J, is operating through space and depends on the frequency of collisions between the paramagnetic moieties.
In particular, a five lines spectrum is expected for a diradical in which the exchange coupling constant J is larger than the hyperfine splitting, a_N.[12]
In our case, the spectrum of dumbbell **6a** (aN = 15.22 G, g = 2.0058) shows five lines, but the intensity ratio of 1 : 2 : 3 : 2 : 1 typical for biradical compounds in which all the conformations exhibit strong exchange between radical moieties, is not detected.
Effectively, we observe a combination of ESR signals typical of biradicals in which the nitroxide radical centers do not communicate (three lines spectrum) and of biradicals where these fragments show exchange coupling interaction (five lines spectrum).
On the other hand, no lines indicating an interaction between the radical stoppers are observed in the [2]rotaxane spectra.
In particular, the ESR spectrum of rotaxane **7a** in ACN at 338 K (aN = 15.30 G, g = 2.0058, see Figure 5b) is characterized by only three lines as expected for a nitroxide biradical in which the radical units do not interact with each other.
The threading of a biradical compound into a macrocyclic cavity significantly reduces the probability of collisions between the nitroxide units and, consequently, ESR spectroscopy can afford interesting information by monitoring complexation processes.
Similar ESR results were also observed with dumbbell **15a** (aN = 15.32 G, g = 2.0058) and rotaxane **16a** (aN = 15.26 G, g = 2.0058) containing the TTF unit (Figure 5). In this case, however, a larger intensity of the exchange lines (the second and the fourth lines) in dumbbell **15a** than in **6a** is observed, due to the greater number of conformations estimated showing a strong spin exchange.[12,13]
Thus, the introduction of paramagnetic groups in supramolecular structures proved to be a rapid and unequivocal method to identify free compounds from interlocked species, useful especially during purification processes.

4.4 Supramolecular Control of Spin Exchange in a Spin-Labelled [2]Rotaxane Incorporating a Tetrathiafulvalene Units

Oligoradicals are employed in many fields of chemistry and related sciences,[14] with some important applications in molecular magnetic materials,[15] as molecular probes[16] and in structural investigations using interspin distance determination[17] for a few examples. Therefore, the accurate modulation of spin exchange interactions, important to extend their potential applications, is a great target in this field.
Mechanical interlocked molecules represent a great opportunity in order to study the spin-spin coupling, due to their ability to vary the relative positions of their components in the structure in response to external stimuli. As an example, the use of spin-spin interactions as driving forces in molecular machines and new structures with improved magnetic properties has been extensively exploited by Stoddart and coworkers. [18]

The introduction of paramagnetic species in rotaxane-like structures allows the monitoring by ESR spectroscopy of the switch mechanism involving the ring compound by tuning the spin exchange interaction.[19]

Tanaka and co-workers reported the tuning of spin-spin coupling interactions between radical fragments by changing their orientation in response to pH changes.[20] Recently, we reported an example of paramagnetic rotaxane functionalized with nitroxide units both at the ring and the dumbbell, affording the switch of the spin exchange by changing the pH.[21] In these examples, however, the paramagnetic centers are not directly involved in the shuttling process. To the best of our knowledge, the use of a magnetic interaction between a radical center formed to induce a movement of the ring and a spin label introduced "ad hoc" to obtain structural information on a mechanical interlocked structure has never been reported.

This section reports the first example of a nitroxide-spin-labelled rotaxane where rotaxanation is proved to have a dramatic effect on through-space spin spin interactions between radical fragments.

As described in section 4.3, the spin-labelled rotaxane **16a** (Scheme 5)[5] is based on the cyclobis(paraquat-p-phenylene) ($CBPQT^{4+}$) ring and contains an interesting recognition site for this macrocycle, the bisthiotetrathiafulvalene (STTFS) unit, system that represents a versatile building block for supramolecular systems.[22]

In fact, TTF unit can be reversibly oxidized (at +0.43 V vs. Ag/AgCl in MeCN) to the TTF•+ radical cation, and then subsequently (at +0.79 V) to the TTF^{2+} dication. As a result, the interaction between the binding site and the tetracationc ring is decreased and $CBPQT^{4+}$ can be exploited to create molecular switches driven by electrochemical stimuli.

The introduction of spin labels at both ends in **16a** made possible to unequivocally detect the formation of the interlocked structure. Moreover, the oxidation of the TTF moiety generated a heterotriradical compound that has never been investigated by continuous-wave X-band EPR (Scheme 6).

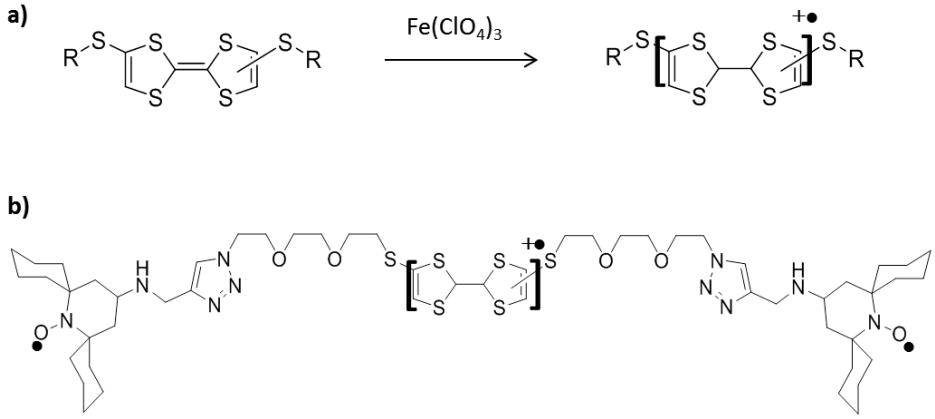

Scheme 6. a) TTF oxidation process and b) the resulting heterotriradical.

We first investigated the EPR properties of the corresponding free dumbbell containing 2,2,6,6-tetramethylpiperidine-N-oxide (TEMPO) derivatives as stopper units **17**, because they offer distinct and sharp signals, providing an easier reading of the spectra.

Figure 6 shows the structure and the relative EPR spectrum recorded in MeCN at 298 K, which exhibits strong spin exchange between the nitroxide units ($J_{NO^{\bullet}-NO^{\bullet}}$).

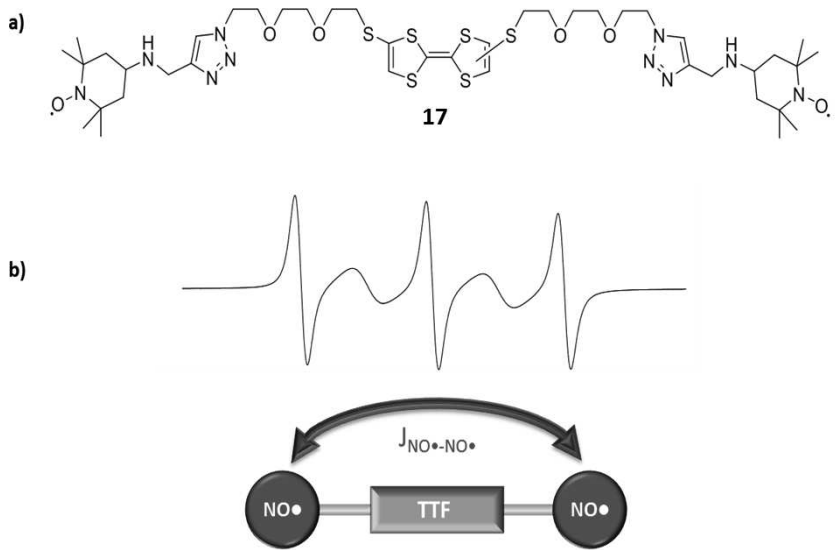

Figure 6. a) Structure of **17** and b) related ESR spectrum showing strong spin exchange.

The TTF unit was then oxidized to TTF•+ by addition of $Fe(ClO_4)_3$. An EPR titration was performed by recording EPR spectra after the addition of increasing amounts of the oxidizing agent. It should be noted that, as a result of the formation of the TTF radical cation form, two different spin exchange interactions contribute to the spectral shape: the interaction between the nitroxide units, that generates the additional lines shown before, and the spin exchange between the nitroxide stoppers with the new radical site, the TTF molecular station (Figure 7).

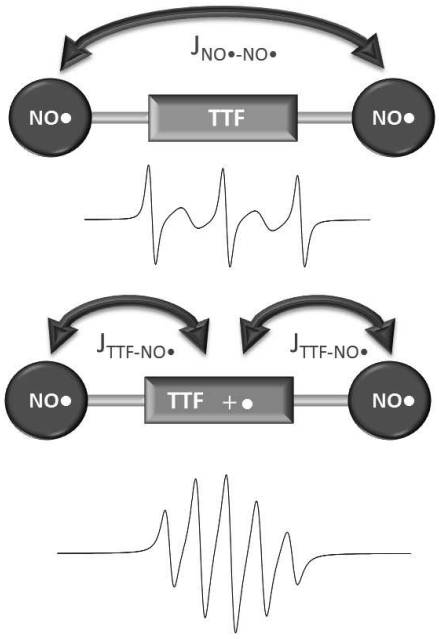

Figure 7. Representation of different kind of interactions expected in the heterotriradical compound.

The EPR titration clearly detects the appearance of new signals generated by the larger contribution of the triradical compound after the addition of the oxidizing agent (Figure 8b).
Moreover, we notice that, at around 1 equivalent of $Fe(ClO_4)_3$, also nitroxide units start to be oxidized to EPR silent species originating a different diradical compound in which a new interaction between the TTF and only one nitroxide unit takes part in the spectrum (Figure 8c).

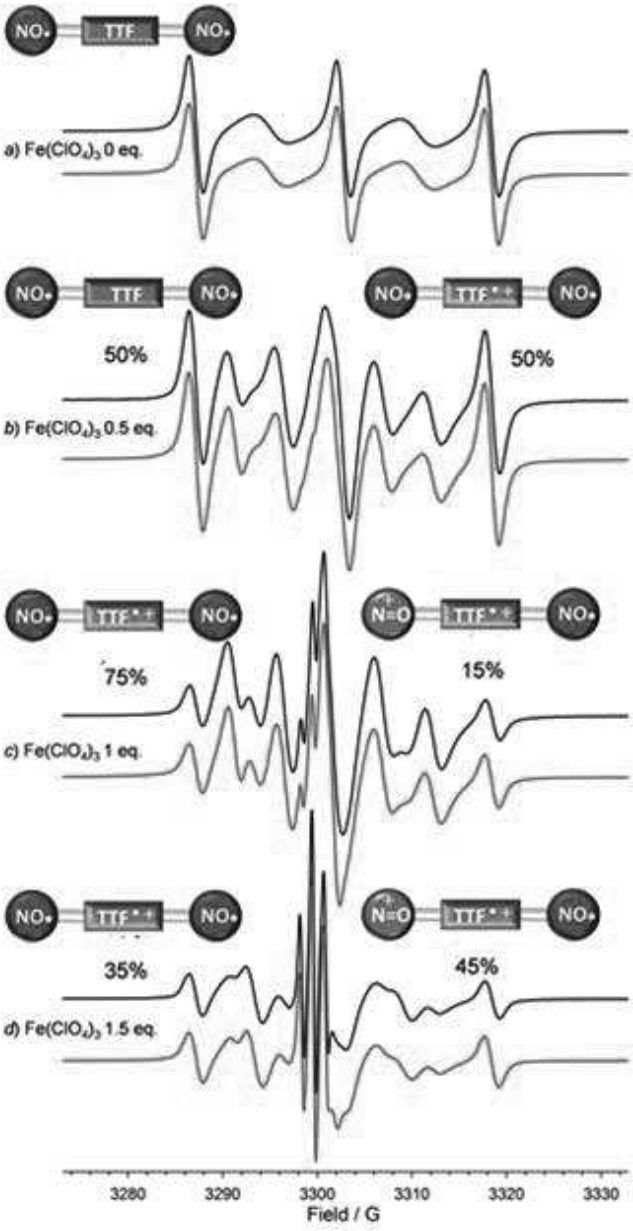

Figure 8. EPR spectra of **17** (0.2 mM) recorded in MeCN at 298 K in the presence of different amounts of $Fe(ClO_4)_3$. Dotted lines represent the corresponding theoretical simulations. Spectra c) and d) were correctly reproduced by also taking into account the presence of some nitroxide (10 %) and TTF•+ monoradicals (20 %).

Similar titration was performed with our more hindered dumbbell and the same species were found, even if with broader signals (Figure 9).

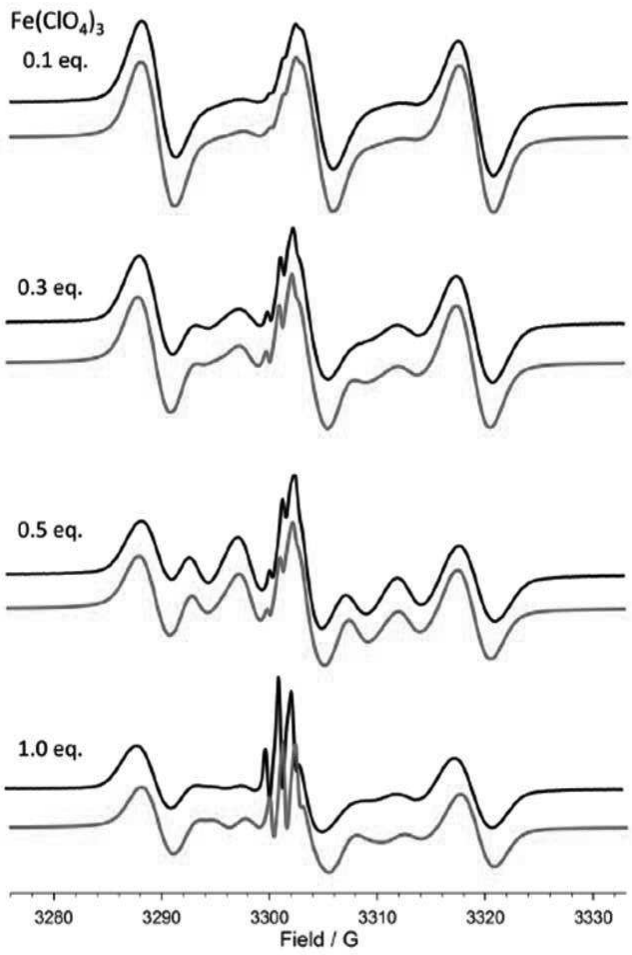

Figure 9. EPR spectra of **15a** (0.2 mM) recorded in ACN at 298 K in the presence of different amounts of $Fe(ClO_4)_3$. In red the corresponding theoretical simulations are reported.

We finally investigated the effect of rotaxanation on the spin exchange (Figure 10). It appeared that the presence of the $CBPQT^{4+}$ ring remarkably changed the shape of the EPR signal of the triradical. In particular, the addition of the oxidant to rotaxane **16a** originates a spectrum which consists of the superimposed signals of a non exchanging dinitroxide compound (a 1:1:1 triplet with a line separation of a_N=15.40 G) and the TTF radical cation (a 1:2:1 triplet with a line separation of a_{2H}=1.30 G) and no lines due to an interaction between the different radical units are visible.
Therefore, in rotaxane **16a** the $CBPQT^{4+}$ ring is stationary on the TTF unit after the oxidation process, as no other binding site is available along the dumbbell. These results are in agreement with previous works[18a,23] on analogous systems in which the position of the $CBPQT^{4+}$ ring was investigated by the value of the oxidation potential of $TTF^{\bullet+}$ to the corresponding dication.
In the present case, the shielding of the radical form provided by rotaxanation turns off the through space interaction between the $TTF^{\bullet+}$ and both nitroxide radicals and spin labelling gives evidence of the position of the ring.

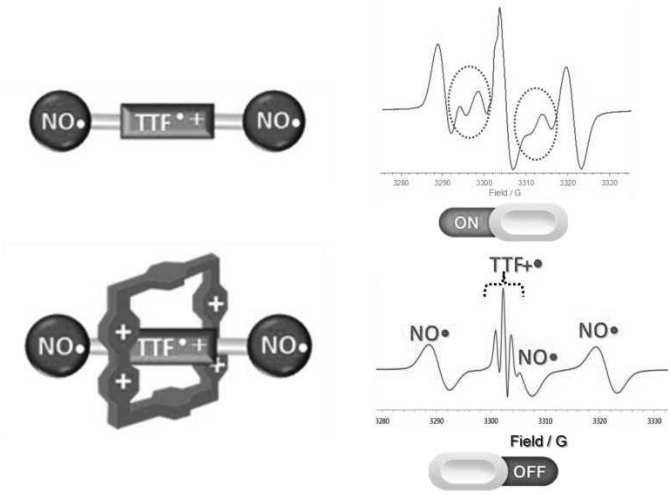

Figure 10. EPR spectra recorded in MeCN at 298 K at a concentration of 0.2 mM of free thread **15a** on the top and the [2]rotaxane **16a** in the presence of 0.5 equiv of $Fe(ClO_4)_3$ on the bottom.

Hence, in order to achieve a full characterization of the spin exchange mechanism, the bistable spin-labelled [2]rotaxane **18**, which incorporates TTF and DNP units and only one nitroxide spin label as stopper, and dumbbell **19** were prepared (see Figure 11). The related synthetic procedures are reported in **Scheme 7**.

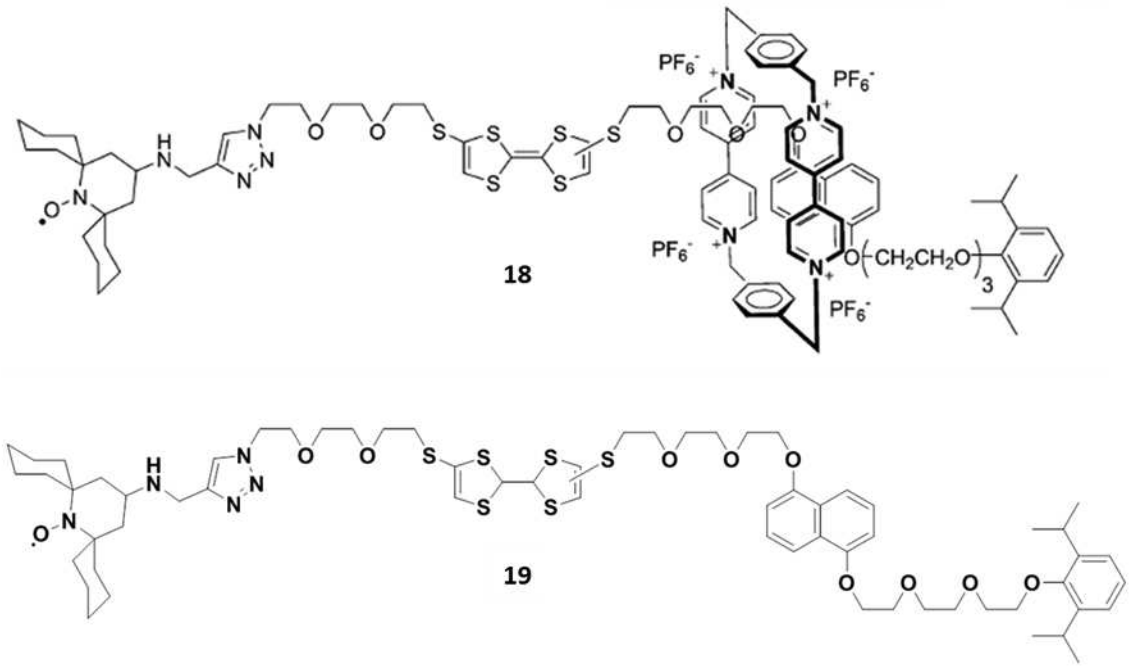

Figure 11. Structures of the bistable spin-labelled [2]rotaxane **18** and the related dumbbell **19.**

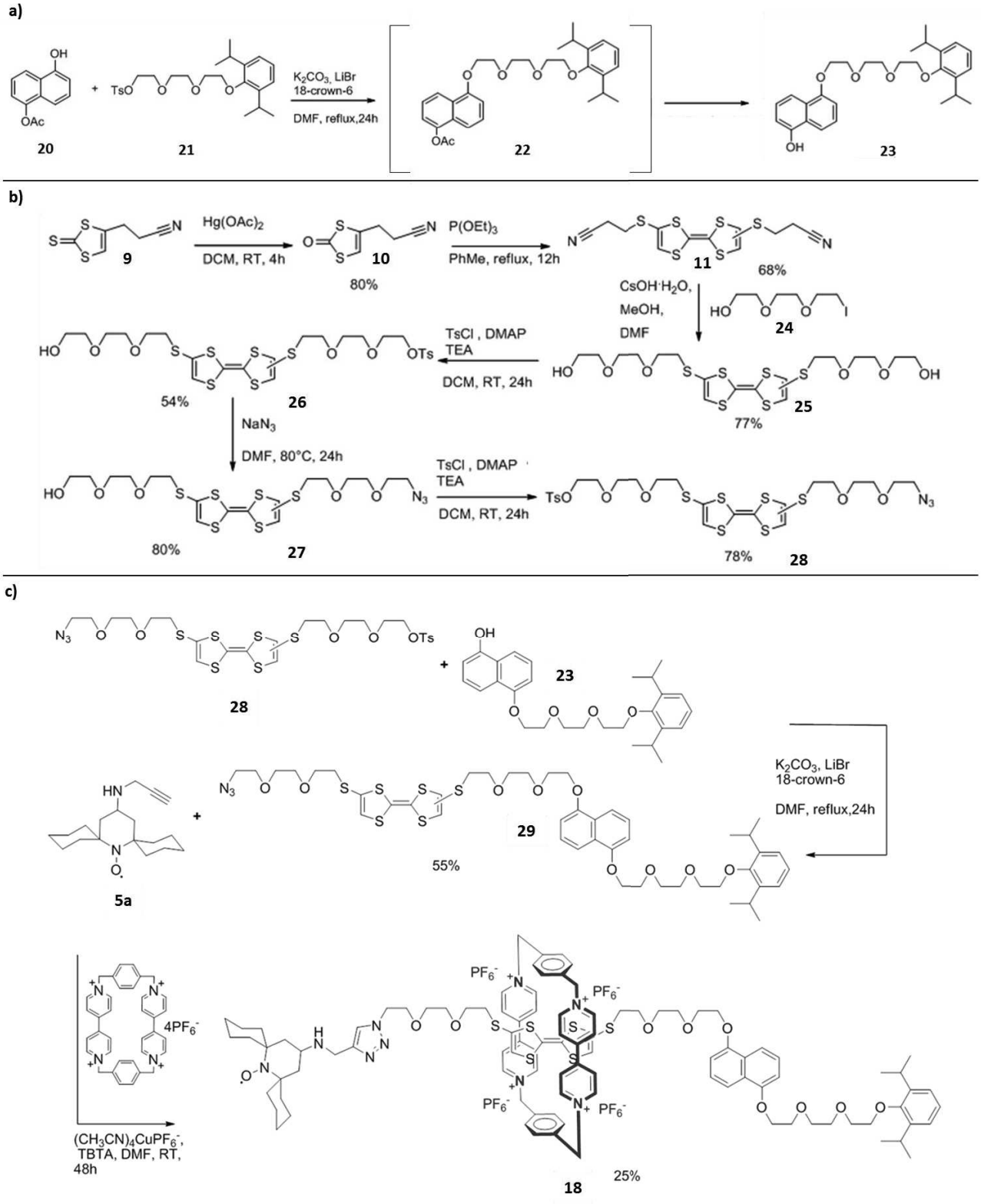

Scheme 7. Synthetic strategies employed for the preparation of a) the DNP molecular station, b) the TTF unit and c) the azide-derivative **29**, employed in the template-directed synthesis afforded by DNP/TTF-CBPQT^{4+} molecular recognition, followed by the copper(I)-catalyzed alkyne–azide cycloaddition reaction (CuAAC) with the nitroxide unit **5a** to obtain rotaxane **18**.

Due to the larger affinities of DNP for the macrocycle compared to STTFS (K=36400 M^{-1}, K=8580 M^{-1} in MeCN, respectively)[24] the $CBPQT^{4+}$ ring primarily resides on the DNP unit, as demonstrated by ^1H NMR spectroscopy (Figure 12).

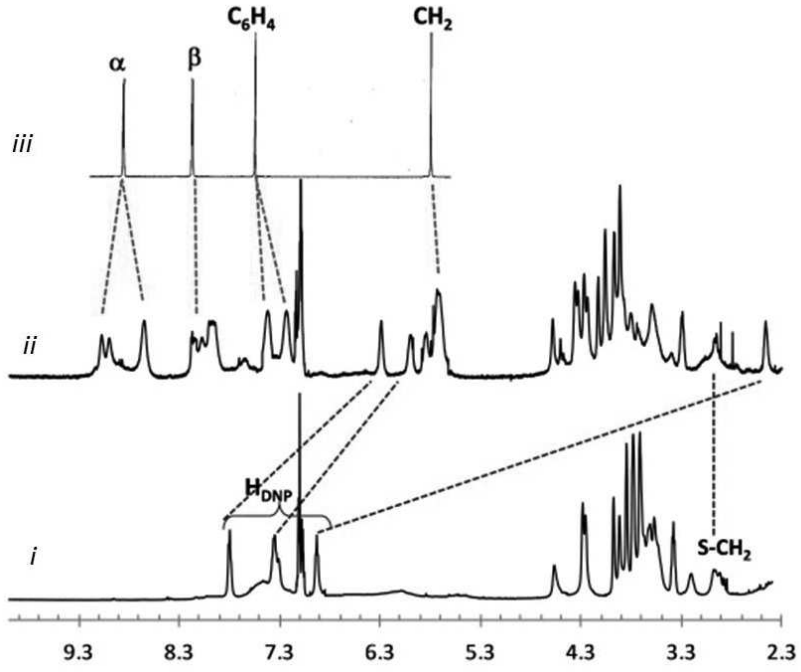

Figure 12. Partial ^1H NMR spectra (600 MHz, CD_3CN, 298 K) of *i*) dumbbell **19**; *ii*) rotaxane **18;** iii) $CBPQT^{4+}$ host. Blue dashed lines point out the remarkable upfield shifts of DNP protons encircled by the $CBPQT^{4+}$ and red dashed lines show the broadening and splitting of the macrocyclic signals due to reduced rotation of $CBPQT^{4+}$ ring in the rotaxane complex. The S-CH_2 protons do not undergo shift, indicating that TTF unit is not involved in the complexation with the host. H_{DNP}= DNP aromatic protons, α, β = $CBPQT^{4+}$ bipyridinium α and β protons, respectively; C_6H_4 = host *p*-phenylene protons; CH_2 = host benzyl protons, S-CH_2 = TTF-S-methylene protons.

Moreover, after the oxidation of the TTF unit to the radical cation form, the ring will quantitatively encircle the DNP unit and a very strong spin-exchange interaction between the close nitroxide fragment and $TTF^{\bullet+}$ is expected. Effectively, strong exchange lines were detected in the EPR spectrum of **18** recorded after the addition of 0.5 equivalents of $Fe(ClO_4)_3$ (Figure 13).

4.5 Conclusions

In conclusion, rotaxanation is proved to have a remarkable effect on through-space spin–spin interactions. Thus, the introduction of radical groups in molecular switches represents an interesting approach for the development of a new generation of poliradicals where the magnetic interactions can be turned on/off by application of an appropriate stimulus. In addition, spin labelling in molecular machines allows to perform structural analysis.
Therefore, spin labelling represents a powerful and valuable technique to enhance our knowledge on the complex mechanism of molecular machines. Experiments in this direction are in progress in our laboratory.

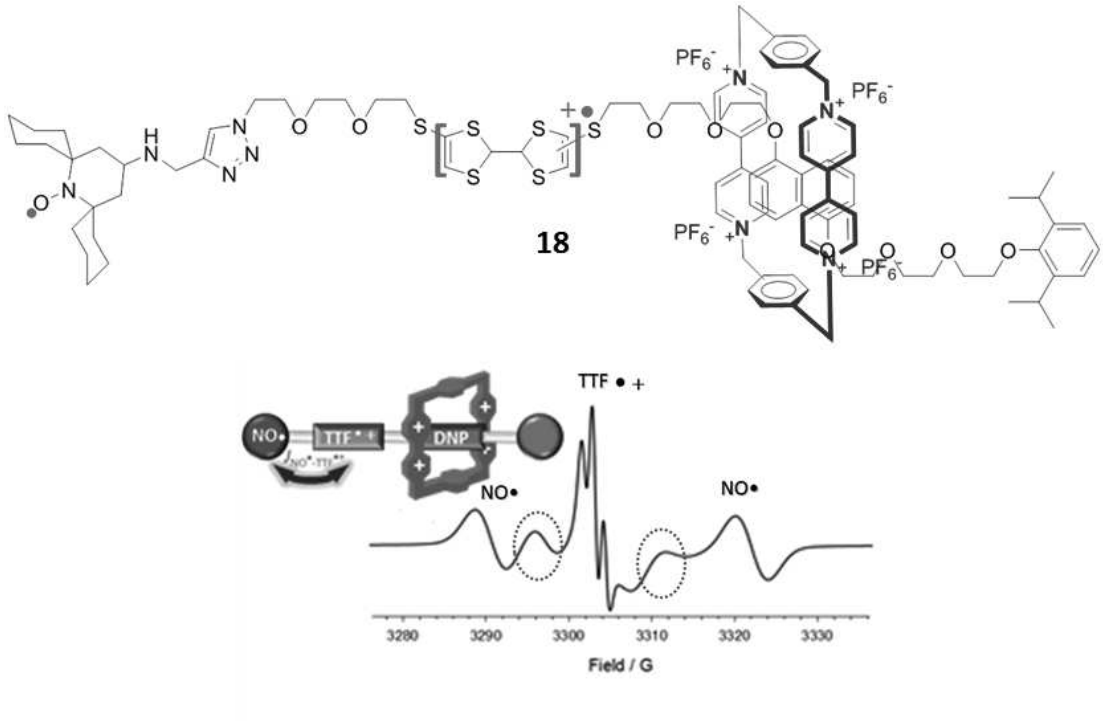

Figure 13. EPR spectrum recorded in MeCN at 298 K at a concentration of 0.2 mM **18** in the presence of 0.5 equiv of $Fe(ClO_4)_3$.

References

[1] a) B. Odell, M. V. Reddington, A. M. Z. Slawin, N. Spencer, J. F. Stoddart, D. J. Williams, *Angew. Chem.,Int. Ed. Engl.*, **1988**, *27*, 1547-1553; b) P. L. Anelli, N. Spencer, J. F. Stoddart, *J. Am. Chem. Soc.*, **1991**, *113*, 5131-5133; c) T. Goodnow, M. V. Reddington, J. F. Stoddart, *J. Am. Chem. Soc.*, **1991**, *113*, 4335-4337; d) M. C. T. Fyfe, J. F. Stoddart, *Acc. Chem. Res.*, **1997**, *30*, 393-401.

[2] J. F. Stoddart, et al., *Acc. Chem. Res*., **2012**, *45*, 1581-1592.

[3] C. Wang, M. A. Alson, L. Fang, D. Benitez, E. Tkatchouk, S. Basu, A. N. Basuray, D. Zhang, D. Zhu, W. A. Goddard, J. F. Stoddart, *PNAS*, **2010**, *107*, 13991-13996.

[4] P. Franchi, M. Lucarini, G. F. Pedulli, *Curr. Org. Chem*., **2004**, *8*, 1831-1849.

[5] R. Manoni, F. Romano, C. Casati, P. Franchi, E. Mezzina, M. Lucarini, Organic Chemistry Frontiers, 2014, 1, 477-483.

[6] F. Romano, R. Manoni, P. Franchi. E. Mezzina, M. Lucarini, *Chem. Eur. J*., **2015**, 2775-2779.

[7] R. W. Dichtel, Š. M. Ognjen, J. M. Spruell, J. R. Heath and J. F. Stoddart, *J. Am. Chem. Soc*., **2006**, *128*, 10388.

[8] J. Luo, C. Pardin, W. D. Lubell, X. X. Zhu, *Chem. Commun*., **2007**, 2136-2138.

[9] C. Jia, D. Zhang, W. Xu and D. Zhu, *Org. Lett*., **2001**, *3*, 1941-1944.

[10] X. Guo, D. Zhang, H. Zhang, Q. Fan, W. Xu, X. Ai, L. Fan and D. Zhu, *Tetrahedron*, **2003**, 4843-4850 and references cited therein; N. Svenstrup, K. M. Rasmussen, T. K. Hansen and J. Becher, *Synthesis*, **1994**, 809-812.

[11] G. Trippé, F. Le Derf, M. Mazari, N. Mercier, D. Guilet, P. Richomme, A. Gorgues, J. Becher and M. Sallé, *C. R. Chim*., **2003**, *6*, 573.

[12] V. N. Parmon, A. I. Kokorin, G. M. Zhidomirov and K. I. Zamarev, *Mol. Phys*., **1975**, *30*, 695.

[13] C. Casati, P. Franchi, R. Pievo, E. Mezzina and M. Lucarini, *J. Am. Chem. Soc*., **2012**, *134*, 19108-19117.

[14] For a recent review, see M. Abe, *Chem. Rev*. **2013**, *113*, 7011-7088.

[15] *Magnetism: Molecules to Materials*, Vols. 1-4 (Eds.: J. S. Miller, M. Drillon), Wiley-VCH, Weinheim, **2001-2003.**

[16] A. I. Smirnov in *Nitroxides: Applications in Chemistry, Biomedicine, and Materials*, (Eds.: G. I. Likhtenshtein, J. Yamauchi, S. Nakatsuji, A. I. Smirnov, R. Tamura), Wiley-VCH, Weinheim, **2008**, 121-160.

[17] As an example, see: a) A. Godt, M. Schulte, H. Zimmermann, G. Jeschke, *Angew. Chem. Int. Ed*. **2006**, *45*, 7560 -7564; *Angew. Chem*. **2006**, *118*, 7722-7726; b) G. Hagelueken, W. J. Ingledew, H. Huang, B. Petrovic-Stojanovska, C. Whitfield, H. ElMkami, O. Schiemann, J. H. Naismith, *Angew. Chem. Int. Ed*., **2009**, *48*, 2904-2906; *Angew. Chem*. **2009**, *121*, 2948-2950.

[18] As an example, see: a) A. Trabolsi, N. Khashab, A. C. Fahrenbach, D. C. Friedman, M. T. Colvin, K. K. Cot, D. Benitez, E. Tkatchouk, J. C. Olsen, M. E. Belowich, R. Carmielli, H. A. Khatib, W. A. Goddard III, M. R. Wasielewski, J. F. Stoddart, *Nature Chem*. **2010**, *2*, 42-49; b) J. C. Barnes, A. C. Fahrenbach, D. Cao, S. M. Dyar, M. Frasconi, M. A. Giesener, D. Bentez, E. Tkatchouk, O. Chernyashevskyy, W. H. Shin, H. Li, S. Sampath, C. L. Stern, A. A. Sarjeant, K. J. Hartlieb, Z. Liu, R. Carmieli, Y. Y. Botros, J. W. Choi, A. M. Z. Slawin, J. B. Ketterson, M. R. Wasielewski, W. A. Goddard III, J. F. Stoddart, *Science*, **2013**, *339*, 429-433.

[19] D. Bardelang, M. Hardy, O. Ouari, P. Tordo in: *Encyclopedia of Radicals in Chemistry, Biology and Materials*, Vol. 4 (Eds.: C. Chatgilialoglu, A. Studer), Wiley, Hoboken, **2012**, 1-51.

[20] Y. Yamada, M. Okamoto, K. Furukawa, T. Kato, K. Tanaka, *Angew. Chem. Int. Ed*., 2012, 51, 709-713; *Angew. Chem*., **2012**, *124*, 733-737.

[21] V. Bleve, C. Schafer, P. Franchi, S. Silvi, E. Mezzina, A. Credi, M. Lucarini, *Chemistry Open*, **2015**; DOI: 10.1002/open.201402073.

[22] J. F. Stoddart, *Chem. Soc. Rev*. **2009**, *38*, 1802-1820.

[23] S. S. Andersen, A. I. Share, B. La Cour Poulsen, M. Korner, T. Duedal, C. R. Benson, S. W. Hansen, J. O. Jeppesen, A. H. Flood, *J. Am. Chem. Soc*., **2014**, *136*, 6373-6384.

[24] a) C. Wang, D. Cao, A. C. Fahrenbach, L. Fang, M. A. Olson, D. C. Friedman, S. Basu, S. K. Dey, Y. Y. Botros, J. F. Stoddart, J. Phys. Org. Chem. 2012, 25, 544– 552; b) A. C. Fahrenbach, C. J. Bruns, D. Cao, J. F. Stoddart, *Acc. Chem. Res*., **2012**, *45*, 158-1592.

Experimental Section

Chapter 5. Experimental section

5.1 General information

All starting materials were obtained from commercial suppliers (Aldrich and Fluka) and were used without further purification. All air- or moisture sensitive reactions were done under an atmosphere of nitrogen. Column chromatography was performed on Aldrich silica gel 230-400 mesh. ^{1}H NMR spectra were recorded on a Bruker AMX (300 MHz) or VARIAN Inova (400-600 MHz) at 25 °C, using D_2O, $CDCl_3$, DMSO-d_6, d_7-dimethylformamide and CD_3CN as solvents and the residual solvent peak as an internal standard. ^{13}C NMR spectra were recorded with the simultaneous decoupling of proton nuclei with a Varian Gemini spectrometer operating at 100 MHz using the solvent peak as the internal standard. Chemical shifts are reported in parts per million (δ scale) and coupling constants are given in Hz. The following abbreviations were used to describe the multiplicities: s, singlet; d, doublet; t, triplet; br., broad; m, multiplet or overlapping peaks. Electrospray Ionization Mass Spectra were obtained on a Micromass ZMD 4000 and on a Thermos LTQ Velos. EPR spectra were recorded on a Bruker ELEXSYS-500 instrument.

5.2 Synthetic procedures

The following are the synthetic procedures used to obtain some of the derivatives described in the previous chapters.

5.2.1 Chapter 2

The general synthetic procedure to obtain CB[6] monofunctionalization and further modification is reported in Scheme 1.[1]
4-*O*-*p*-Toluenesulfonyl-TEMPO (**19**) and 4-azido-TEMPO (**20**) were prepared according to literature procedures.[2]

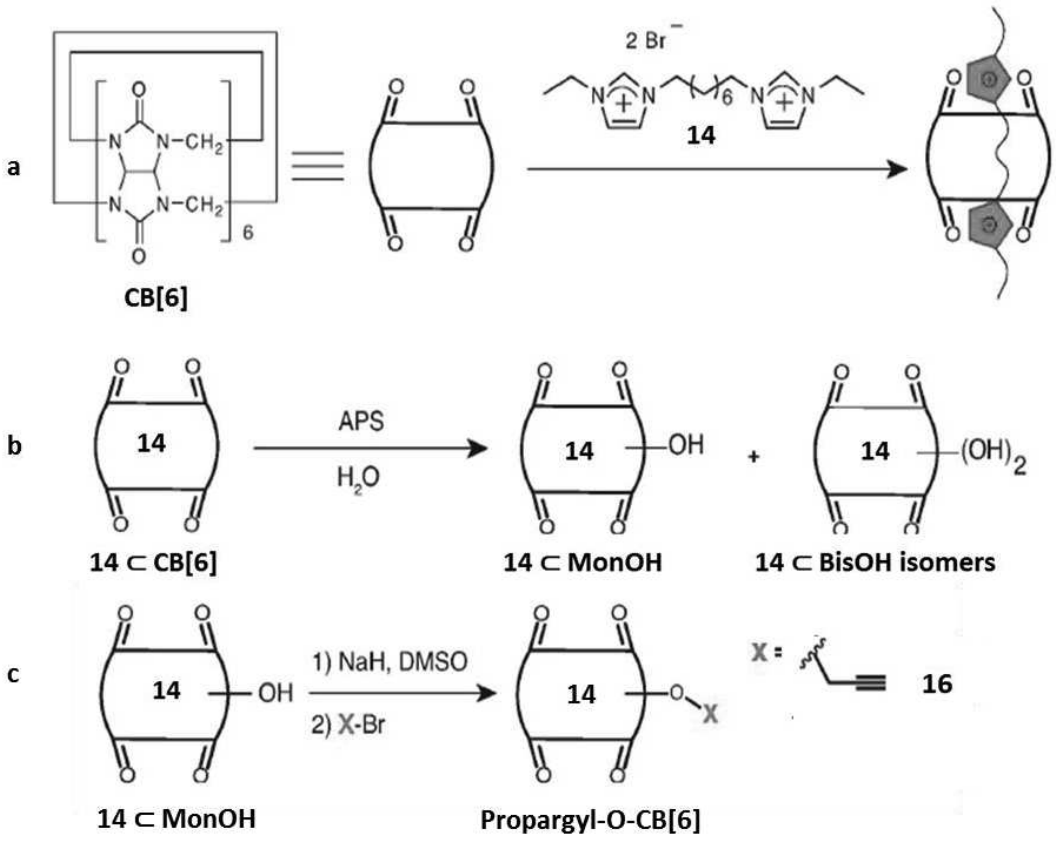

Scheme 1. a-b) CB[6] monofunctionalization strategy and c) synthesis of derivative **16**.

3,3'-(Octane-1,8-diyl)bis(1-ethyl-imidazolium) bromide (1)[1]

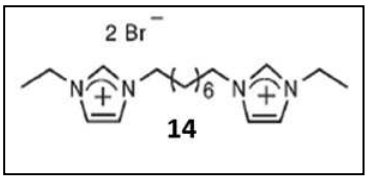

1-Ethylimidazole **21** (5.5 mL, 50 mmol) and 1,8-dibromooctane **22** (5.4 g, 20 mmol) were dissolved in toluene (50 mL) and refluxed for 12 hours: a brown thick material was formed. The solvent was decanted from the insoluble crude mixture, which was then triturated with diethyl ether (5×50 mL) and dried via vacuum to obtain the title compound **14** as a white solid (7.9 g, 85%). ^{1}H-NMR (300 MHz, D_2O, 298K): δ = 8.701 (2H, s), 7.43-7.40 (4H, d), 4.19-4,08 (8H, m), 1.84-1,74 (4H, m), 1.43 (6H, t), 1.24 (8H, m); ESI-MS (positive): *m/z* = 385.1 $[M\text{-}Br]^+$.

CB[6] functionalization: 14 ⊂ MonOH[1]

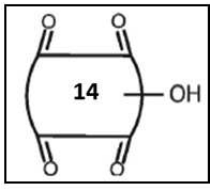

Cucurbit[6]uril (500 mg, 0.5 mmol) and compound **14** (231 mg, 0.5 mmol) were dissolved in 50 mL of bidistilled water at 85 °C. $(NH_4)_2S_2O_8$ (114 mg, 0.5 mmol) was then added and the reaction was stirred at 85 °C for 12 hours. The unsoluble material was removed by filtration. The remaining solution was reduced to 3 mL under vacuum. The sample was ready for resin column separation. ESI-MS (positive): *m/z* = 650 [**14**⊂CB[6]-2Br]$^{2+}$, *m/z* = 658 [**14**⊂MonOH-2Br]$^{2+}$, *m/z* = 666 [**14**⊂BisOH-2Br]$^{2+}$.

Column packing: 80 mL CHP 20P resin was soaked in 100 mL methanol for 15 minutes. The solvent was decanted and the resin was then soaked in bidistilled water (100 mL) for 15 minutes. The H_2O-resin slurry was loaded and packed into a glass column (height = 35 cm, diameter = 2 cm). The resin column was then eluted with bidistilled water (1 L) and ready to use.

Column separation: The prepared sample was loaded onto the resin column. The column was then eluted with an amount of bidistilled water equal to the bed volume of the resin (75 mL) and fractions were collected subsequently (10 mL per fraction). The separation process was monitored by mass spectroscopy. **14**⊂CB[6] was first eluted within fractions 10 to 20 followed by **14**⊂MonOH. There is a small overlap between the two CBs at fraction 20, however the majority of **14**⊂MonOH could be separated within 30 fractions. After 30 fractions, 0.1% (w/w) NaOH was used as the eluent and **14**⊂BisOH was collected subsequently.

14⊂MonOH. ESI-MS: *m/z* = 658 [**14**⊂MonOH-2Br]$^{2+}$, partial ^{1}H-NMR: see Figure 1.

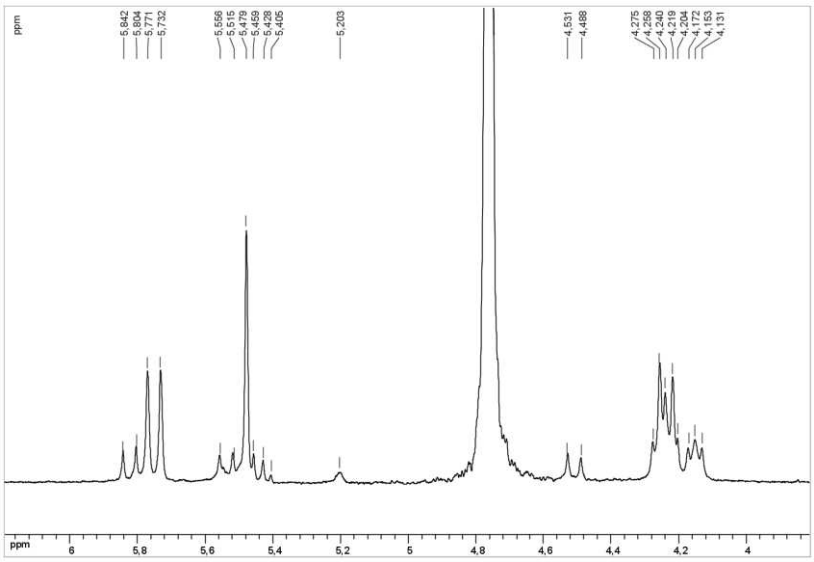

Figure 1. Partial ^{1}H-NMR spectrum (400 MHz, D_2O) for **14**⊂MonOH.

Column Regeneration: The column was washed with 1% (w/w) NaOH (400 mL) and bidistilled water until neutral. The resin was then washed with 400 mL 50% MeOH, 400 mL MeOH, 400 mL 50% MeOH, 400 mL 20% MeOH and 1 L bidistilled water respectively and ready for the next separation.

MonOH: 14⊂MonOH fractions from the column separation were collected and dried under vacuum to give a white solid which was then triturated with MeOH (3×45 mL). The residue was refluxed in DCM in the presence of NH_4PF_6 for 48 hours. The solvent was then decanted and the sediment was washed with MeOH (3×45 mL), and dried under vacuum to give MonOH as a white solid (60 mg, 12%). ^{1}H-NMR (400 MHz, D_2O): see Figure 2. ESI-MS (positive, in presence of $CsCl_2$): *m/z* = 639 $[MonOH+2Cs]^{2+}$.

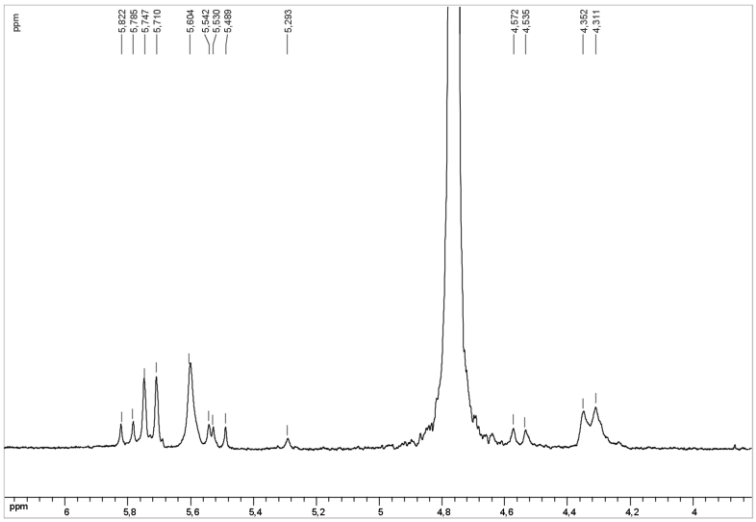

Figure 2. ^{1}H-NMR spectrum for MonOH.

Propargyl-O-CB[6] (16)[1]

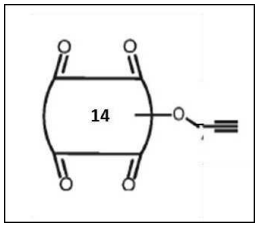

To a solution of **14⊂**MonOH (20 mg) in anhydrous DMSO (1.5 mL), NaH (10 mg, 0.4 mmol) was added and stirred at room temperature for 15 minutes. Propargyl bromide (0.5 mL, 4.4 mmol) was added subsequently at 0 °C and the reaction mixture was stirred at room temperature for 12 hours. The reaction was then diluted with 50 mL diethyl ether and filtered. The remaining solid was triturated with MeOH (3×50mL) and dried under vacuum to give a yellow solid (8 mg,

38.5%). ^{1}H-NMR (600 MHz, D_2O, 298K): See Figure 3. ESI-MS (positive): *m/z* = 677 [**14**⊂**16**−2Br]$^{2+}$.

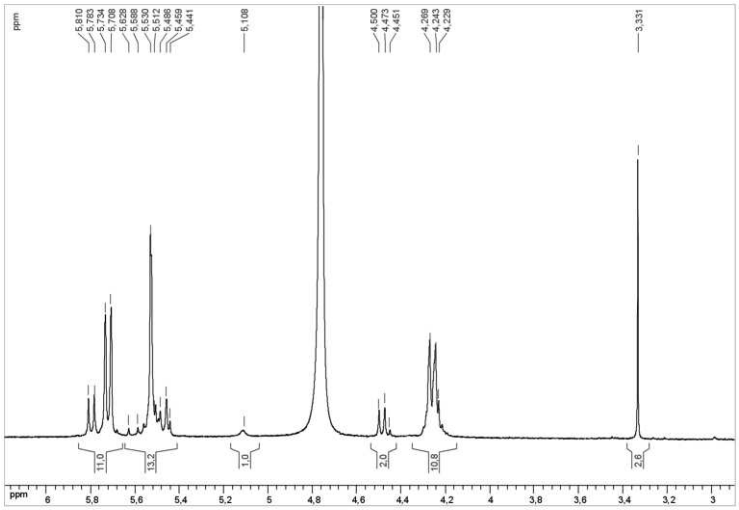

Figure 3. ^{1}H-NMR spectrum of derivative **16**.

5.2.2 Chapter 3

In Scheme 2 the synthesis of derivative **P5A-1** (a) and Dimethoxypillar[5]arene (**2**, b) are reported.

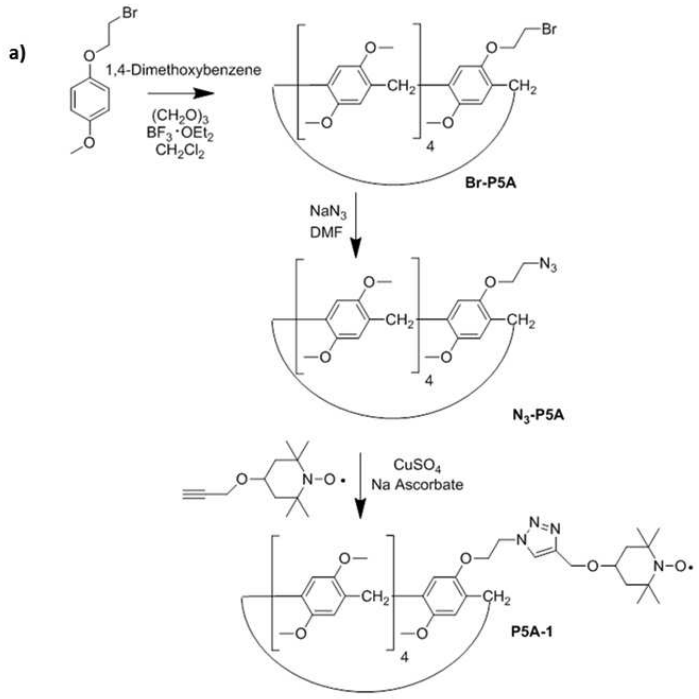

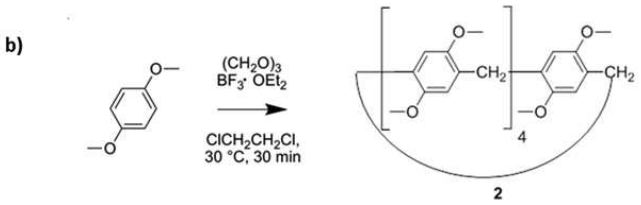

Scheme 2. Synthesis of a) **P5A-1** and b) **2** derivatives.

Br-Pillar[5]arene[3]

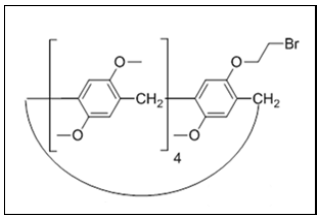

Metaformaldehyde (0.563 g, 18.1 mmol) was added to a solution of 1,4-dimethoxybenzene (2.50 g, 18.1 mmol) and 1-(2-bromoethoxy)-4-methoxybenzene () (0.871 g, 3.59 mmol) in dry CH_2Cl_2 (50 mL) under nitrogen atmosphere. Boron trifluoride etherate [(BF_3•OEt_2), 2.4 mL, 18 mmol] was then added to the solution: the resulting mixture turns to deep green after 10 minutes of stirring. The mixture was stirred at room temperature for 3 h. MeOH (25 mL) was added and the reaction mixture was concentrated under vacuum. The crude material was dissolved in CH_2Cl_2 (50 mL) and the insoluble part was filtered out. The remaining solution was then washed with aqueous $NaHCO_3$ (2 × 25 mL) and H_2O (25 mL). The organic layer was dried (Na_2SO_4), concentrated under vacuum, and subjected to silica gel chromatography (1:2 hexanes / CH_2Cl_2) to give **Br-P5A** (250 mg, 8 %). ^{1}H-NMR (300 MHz, $CDCl_3$): See Figure 4. ESI-MS (positive): *m/z* = 865-867 [**Br-P5A**+Na]$^+$.

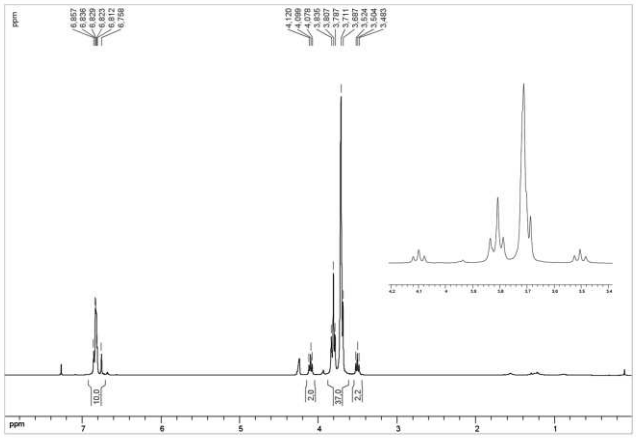

Figure 4. ^{1}H-NMR spectrum of **Br-P5A.**

N3-P5A[3]

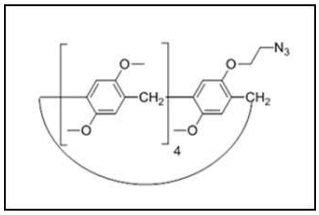

Sodium azide (65 mg, 1.00 mmol) was added to a solution of **Br-P5A** (0.57 g, 0.71 mmol) in dry *N,N*-dimethylformamide (50 mL). The reaction mixture was stirred at 80°C for 12 h, cooled to room temperature and added to CH_2Cl_2 (100 mL). The solution was washed with H_2O (2 × 50 mL) and brine (2 × 50 mL), and dried (Na_2SO_4). The organic layer was removed under vacuum to give **N_3-P5A** (0.53 g, 93%). ^{1}H-NMR (300 MHz, $CDCl_3$): See Figure 5. ESI-MS (positive): *m/z* = 828 [**N_3-P5A**+Na]$^+$.

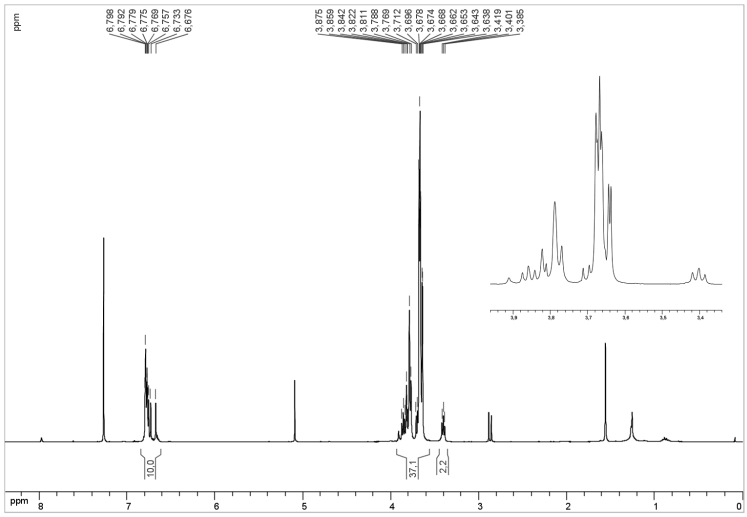

Figure 5. ^{1}H-NMR spectrum of **N_3-P5A**.

Pillar[5]arene 1 (P5A-1)[4]

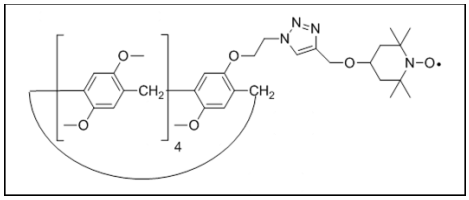

Copper sulfate pentahydrate ($CuSO_4$·5H2O; 3.5 mg, 0.014 mmol) in MeOH (2 mL) was added to a solution of **N_3-P5A** (0.072 g, 0.09 mmol) and 4-(propargyloxy)-TEMPO (0.025 g, 0.12 mmol) in Me_2CO (5 mL). Sodium ascorbate was then added and the solution was stirred for 18 h at 40

°C. The reaction mixture was cooled to room temperature and the solvent removed under vacuum. The remaining solid was added to CH_2Cl_2 (15 mL) and washed with aqueous NH_4Cl (2 x 15 mL) and H_2O (2 x 15 mL). The organic layer was dried ($MgSO_4$), concentrated under vacuum and subjected to silica gel chromatography (CH_2Cl_2 and then CH_2Cl_2/MeOH, 9:1) to give **P5A-1** (0.064 g, 70%). ^{1}H NMR (600 MHz, $CDCl_3$, 298 K): δ = 7.81 (s, 1H), 6.82 (s, 1 H), 6.81 (s, 1 H), 6.77–6.80 (m, 1 H), 6.76 (s, 1 H), 6.75 (s, 1 H), 6.74 (s, 1 H), 6.73 (br. s, 2 H), 6.52 (s, 1 H), 6.45 (s, 1 H), 4.53 (br. s, 2 H), 4.44 (br. s, 2 H), 3.91 (br. s, 2 H), 3.82 (s, 2H), 3.81 (s, 2 H), 3.77 (m, 6 H), 3.70 (s, 3 H), 3.65 (s, 3 H), 3.66 (br. s, 9 H), 3.64 (m, 6 H), 3.61 (s, 3 H), 3.50 (br. s, 3 H) ppm. ^{1}H NMR (600 MHz, [d_6]DMSO, 298 K): δ = 8.23 (br. s, 1 H), 6.60–6.90 (m, 10 H), 4.77 (br. s, 2 H), 4.30–4.60 (m, 2 H), 4.28 (br. s, 2H), 3.40–3.90 (m, 37 H) ppm. ^{13}C NMR (100 MHz, $CDCl_3$, 298 K): δ = 151.05, 150.48, 150.36, 150.28, 150.24, 150.21, 150.18, 150.12, 148.40, 144.13, 128.15, 128.08, 128.01, 127.89, 127.80, 127.75, 127.56, 127.28, 127.11, 123.18, 114.75, 113.78, 113.75 113.55, 113.50, 113.34, 113.27, 66.63, 59.74, 55.57, 55.49, 55.43, 55.26, 55.13, 49.36, 29.90, 29.32, 29.23, 28.81 ppm. ESI-MS (positive): m/z = 1017.4 $[M+H]^+$, 1039.5 $[M+Na]^+$. $C_{58}H_{71}N_4O_{12}$ (1016.22): calcd. C 68.55, H 7.04, N 5.51; found C 68.20, H 6.99, N 5.70. The ^{1}H NMR spectrum of *N*-hydroxylamine of **P5A-1** (**P5A-1-OH**) was also recorded after in situ reduction of the sample containing the pillar nitroxide **P5A-1** by using phenylhydrazine. ^{1}H NMR (600 MHz, [d_6]DMSO, 298 K): δ = 8.17 (s, 1 H), 6.73–6.81 (m, 9 H), 6.68 (s,1 H), 4.75 (t, J = 4.8 Hz, 2 H), 4.51 (s, 2 H), 4.26 (t, J = 4.8 Hz, 2H), 3.62–3.70 (m, 34 H), 3.46 (s, 3 H), 1.85 (d, J = 11.5 Hz, 2 H),1.23 (t, J = 11.5 Hz, 2 H), 1.04 (s, 6 H), 0.98 (s, 6 H) ppm.

Pillar[5]arene 2 (P5A-2)[4]

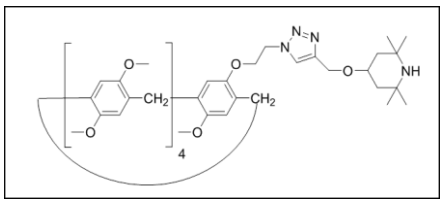

Copper sulfate pentahydrate ($CuSO_4 \cdot 5H_2O$, 3.5 mg, 0.014 mmol) in MeOH (2 mL) was added to a solution of **N_3-P5A** (0.072 g, 0.09 mmol) and 4-propargyloxy-2,2,6,6-tetramethylpiperidine (0.021 g, 0.108 mmol) in Me_2CO (5 mL). Sodium ascorbate was then added and the solution stirred for 24 h at 40 °C. The reaction mixture was cooled to room temperature and the solvent was removed under vacuum. The remaining solid was added to CH_2Cl_2 (15 mL) and washed with aqueous NH_4Cl (2 x 15 mL) and H_2O (2 x 15 mL). The organic layer was dried ($MgSO_4$), concentrated under vacuum and subjected to silica gel chromatography (CH_2Cl_2 and then CH_2Cl_2/MeOH, 9:1) to give **P5A-2** (0.054 g, 60 %). ^{1}H NMR (600 MHz, $CDCl_3$, 298 K): δ = 7.75 (s, 1 H), 6.81 (s, 1 H), 6.78 (s, 1 H), 6.76 (s, 1 H), 6.74 (s, 1 H), 6.73 (s, 1 H), 6.72 (s, 1 H), 6.71 (br. s, 2 H), 6.70 (s, 1 H), 6.48 (s, 1 H), 6.41 (s, 1 H), 4.65 (s, 2 H), 4.40 (t, J =m4.8 Hz, 2 H), 3.88 (t, J = 4.8 Hz, 2 H), 3.87–3.91 (m, 1 H), 3.80 (s, 2 H), 3.79 (s, 2 H), 3.76 (s, 2 H), 3.75 (s, 2 H), 3.70 (s, 2 H), 3.68 (s, 3 H), 3.67 (s, 3 H), 3.63–3.66 (m, 9 H), 3.62 (m, 3 H), 3.61 (s, 3 H),3.59 (s, 3 H), 3.47 (s, 3 H), 1.98 (br. d, J = 12 Hz, 2 H) 1.77 (dd, J = 12, 10 Hz, 2 H), 1.7 (s, 6 H), 1.52 (s, 6 H) ppm. ^{13}C NMR (100 MHz, $CDCl_3$, 298 K): δ = 151.67, 151.15, 151.03, 150.95,

150.85, 150.76, 150.69, 149.03, 144.91, 128.85, 128.80, 128.61, 128.50, 128.39, 128.28, 127.88, 127.73, 123.91, 115.31, 114.44, 114.24 114.15, 113.91, 69.81, 67.11, 61.69, 57.65, 56.16, 55.99, 55.95, 55.82, 55.65, 50.03, 40.71, 30.40, 29.95, 29.71, 29.35, 26.80 ppm. ESI-MS (positive): *m/z* = 1000.5 $[M+H]^+$. $C_{58}H_{72}N_4O_{11}$ (1001.23): calcd. C 69.58, H 7.25, N 5.60; found C 68.90, H 7.12, N 5.45.

Dimethoxypillar[5]arene (2)[5]

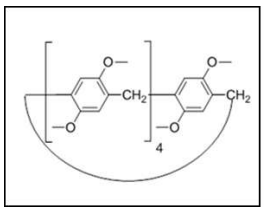

This is a modified procedure from a previous synthetic approach.[6] To a solution of 1,4-dimethoxybenzene (1.38 g, 10 mmol) in 1,2-dichloroethane (20 mL) was added metaformaldehyde (0.93 g, 30 mmol). Then, boron trifluoride diethyl etherate [$BF_3O(C_2H_5)_2$, 1.25 mL, 10 mmol] was added to the solution, and the mixture was stirred at 30 °C for 30 min (the resulting mixture turns to deep green after 10 minutes of stirring). The solution was poured into methanol, and the resulting precipitate was collected by filtration. The obtained solid was recrystallized from chloroform/acetone (1:1 v/v) to yield 0.6 g of DMpillar[5]arene **2** as a while solid (Yield: 40 %). ^{1}H-NMR (300 MHz, $CDCl_3$): See Figure 6. ESI-MS (positive): *m/z* = 773 [**2**+Na]$^+$.

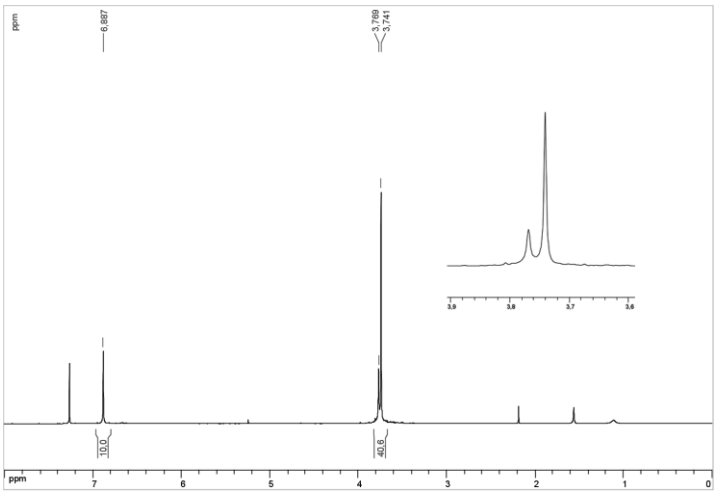

Figure 6. ^{1}H-NMR spectrum of **2**.

5.2.3 Chapter 4

Section 4.3

Synthetic procedures to obtain paramagnetic rotaxanes are reported in this section.
Compounds **5a**,[7] **5b**,[8] **1**,[9] **1b**,[10] **1c**,[11] **9**,[12] **10**,[13] **11**,[13] **13**,[14]were synthesized according to literature procedures.

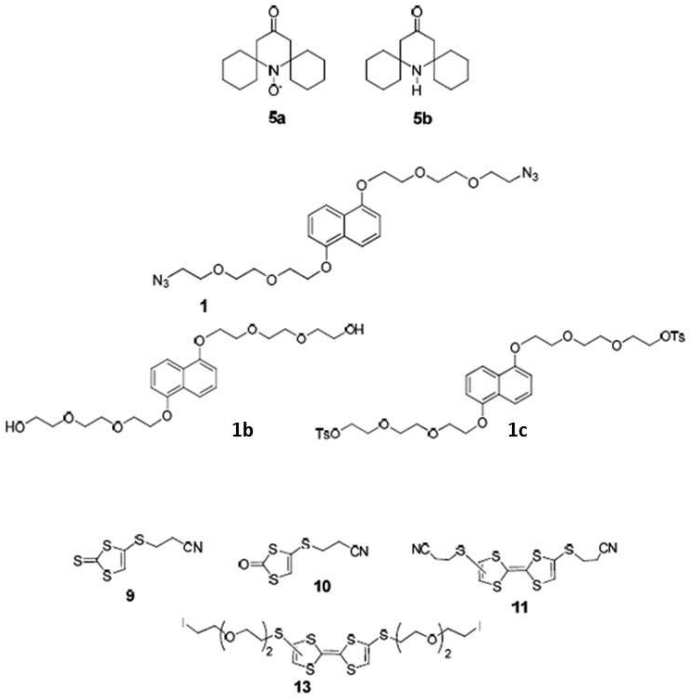

Dumbbell 2a

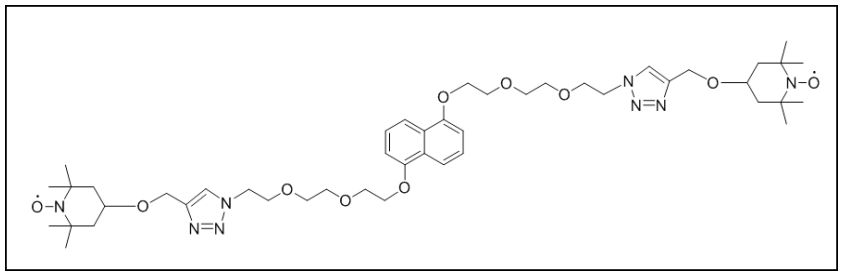

To a solution of diazide **1** (0.012 g, 0.025 mmol), 4-propargyloxy-TEMPO (0.013 g, 0.063 mmol) in DMF (1 mL), TBTA (0.003 mg, 0.0054 mmol) and $Cu(CH_3CN)_4PF_6$ (0.0054 mmol, 0.002 g). Purification of the crude mixture by a silica gel column using CH_2Cl_2–MeOH 90 : 10 affords the biradical **2a** (0.0123 g, 0.014 mmol) in 55% yield. ^{1}H NMR (600 MHz, d_6-DMSO): δ 3.59 (br s), 3.64 (s, 4H), 3.84 (br s), 4.23 (br s), 4.39 (br s), 4.52 (br s), 7.00 (br s), 7.39 (br s), 7.73 (br s), 8.01 (br s). The ^{1}H NMR spectrum of bis-*N*-hydroxy amine of **2a** (**2a-OH**) was

recorded after *in situ* reduction of the sample containing the dinitroxide **2a** by using phenylhydrazine. ^{1}H NMR (600 MHz, d_6-DMSO): δ 1.00 (s, 12H), 1.04 (m, 12H), 1.23 (t, J = 11.0 Hz, 4H), 1.85 (d, J = 11.0 Hz, 4H), 3.55-3.68 (m, 8H), 3.78-3.88 (m, 10H), 4.20-4.26 (m, 4H), 4.46 (s, 4H), 4.50 (t, J = 5Hz, 4H), 6.97 (d, J = 8.0 Hz, 2H), 6.98 (s, 2H), 7.37 (t, J = 8.0 Hz), 7.71 (d, J = 8.0 Hz, 2H), 8.00 (s, 2H). ESI-MS: m/z = 895.5 $[M+H]^+$. Elemental analysis: calculated for $C_{46}H_{70}N_8O_{10}$ C, 61.72; H, 7.88; N, 12.52. Found: C, 61.64; H, 7.97; N, 12.45.

Dumbbell 2b

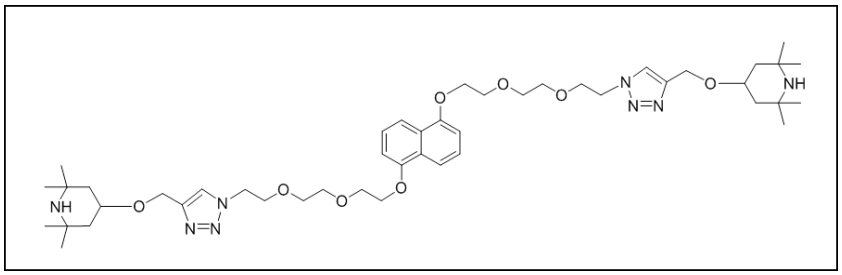

To a solution of diazide **1** (0.049 g, 0.1 mmol) and 4-propargyloxy-TMP (0.042 g, 0.215 mmol) in DMF (5 mL), tris(benzyltriazolylmethyl)amine (TBTA) (0.011 mg, 0.02 mmol) and $Cu(CH_3CN)_4PF_6$ (0.007 g, 0.02 mmol) were added, and the resulting mixture was stirred at room temperature for 24 h, at which time the solvent was evaporated. Purification of the crude mixture by a silica gel column using CH_3CN–H_2O–30% NH_3 90 : 10 : 2 affords **2b** (0.052 g, 0.06 mmol) in 60% yield. ^{1}H NMR (600 MHz, d_6-DMSO): δ 0.92 (t, J = 11.0 Hz, 4H), 1.02 (s, 12H), 1.07 (m, 12H), 1.82 (dd, J = 11.0 and 3.0 Hz, 4H), 3.56–3.60 (m, 4H), 3.62–3.66 (m, 4H), 3.74–3.78 (m, 2H), 3.81–3.86 (m, 8H), 4.23 (br s, 4H), 4.54 (s, 4H), 4.50 (t, J = 5.2 Hz, 4H), 6.98 (d, J = 8.0 Hz, 2H), 7.37 (t, J = 8.0 Hz), 7.71 (d, J = 8.0 Hz, 2H), 8.00 (s, 2H). ESI-MS (positive): m/z = 433.0 $[M+2H]^{2+}$. Elemental analysis: calculated for $C_{46}H_{72}N_8O_8$ C, 63.86; H, 8.39; N, 12.95. Found: C, 63.64; H, 8.45; N, 12.81.

Stopper 5a

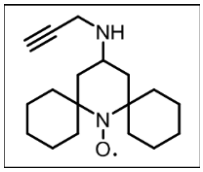

Ketone **4a** (0.2 g, 0.8 mmol) was treated with propargylamine (1.02 mL, 16 mmol) under inert N_2 atmosphere at room temperature and the mixture kept under magnetic stirring until disappearance of the ketone. After ca. 8 h methanol (5 mL), tetrahydrofurane (THF, 5 mL) and sodium cyanoborohydride (0.11 g, 1.76 mmol) in two portions were added and the mixture was stirred for 3 h at room temperature. After aqueous work-up with 5 M HCl and then with 5M

NaOH until pH = 10, the aqueous phase was extracted with CH_2Cl_2 (3 x 20 mL), the combined organic extracts were dried (Na_2SO_4), and the solvent evaporated. The crude product was chromatographed (SiO_2, ethyl acetate and then cyclohexane/ethyl acetate 8:2) to give 162 mg (70% yield) of **5a** as an orange solid. ESI-MS (positive): *m/z* = 312.23 $[M+Na]^+$. EPR: (a_N = 16.64 G, g = 2.0057). ^{1}H NMR (600 MHz, CD_3CN): δ 2.40 (s, 1H), 3.20 (br s, 2H).
The ^{1}H NMR spectrum of *N*-hydroxy amine of **5a** (**5a-OH**) was also recorded after *in situ* reduction of the sample containing the nitroxide **5a** by using phenylhydrazine.^{1}H NMR (600 MHz, CD_3CN): δ 0.74 (t, *J* = 12.3 Hz, 2H), 1.00-1.20 (m, 2H), 1.19 (d, *J* = 12.9 Hz, 2H), 1.33-1.45 (m, 6H), 1.50-1.70 (m, 12H), 2.35 (d, *J* = 12.3 Hz, 2H), 2.40 (s, 1H), 2.80-2.88 (m, 1H), 3.42 (s, 2H).

Stopper 5b

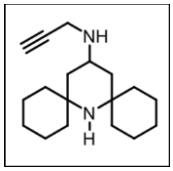

The above procedure was followed using **4b** (0.4 g, 1.7 mmol) as the starting ketone. The crude product was chromatographed (SiO_2, ethyl acetate/methanol 9:1, then methanol: 30% NH_3 99:1) to give 335 mg (72% yield) of **5b** as a white solid. **5b**: ESI-MS (positive): *m/z* = 275.44 $[M+H]^+$. ^{1}H NMR (600 MHz, d_6-DMSO): δ 0.60 (t, *J* = 12.0 Hz, 2H). 1.22-1.29 (m, 4H), 1.30-1.35 (m, 8H), 1.50-1.59 (m, 8H), 1.89 (d, *J* = 12.0 Hz, 2H), 2.94 (tt, *J* = 12.0 and 3.3 Hz, 1H), 2.99 (t, *J* = 2.2 Hz, 1H), 3.34 (d, *J* = 2.2 Hz, 2H).

Dumbbell 6a

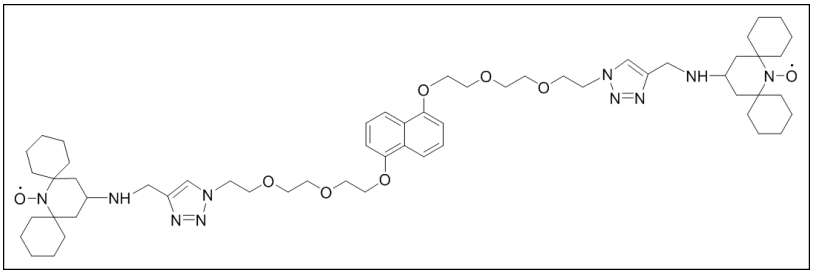

To a solution of diazide **1** (0.016 g, 0.034 mmol) and alkyne functionalized nitroxide **5a** (0.024 g, 0.084 mmol) in DMF (1 mL), $Cu(CH_3CN)_4PF_6$ (0.002 g, 0.006 mmol) and TBTA (0.003 g, 0.006 mmol) were added, and the resulting mixture was stirred at room temperature for 24 h, at which time the solvent was evaporated. Purification of the crude mixture by a silica gel column using CH_2Cl_2–MeOH 90 : 10 affords biradical **6a** (0.018 g, 50% yield). ^{1}H NMR (600 MHz, CD_3CN): δ 3.61 (br s, 4H), 3.68 (br s, 4H), 3.80–3.90 (m, 8H), 4.26 (br s, 4H), 4.46 (br s, 4H), 6.95 (br s, 2H), 7.38 (br s, 2H), 7.70 (br s, 1H), 7.79 (br s, 2H). The ^{1}H NMR spectrum of bis-*N*-hydroxy amine of **6a** (**6a-OH**) was also recorded after *in situ* reduction of the sample containing

the dinitroxide **6a** by using phenylhydrazine. ^{1}H NMR (600 MHz, d_6-DMSO): δ 0.75-0-85 (m, 4H), 0.90-1.00 (m, 4H), 1.10-1.16 (m, 4H), 1.20-1.35 (m, 12H), 1.40-1.60 (m, 16H), 1.75-1.84 (m, 4H), 1.85-1.95 (m, 4H), 2.36 (d, *J* = 11.0 Hz, 4H), 2.75-2.82 (m, 2H), 3.58 (br s, 4H), 3.64 (br s, 4H), 3.82 (br s, 6H), 3.85 (br s, 6H), 4.24 (br s, 4H), 4.51 (br s, 4H), 6.97 (s, 2H), 6.98 (d, *J* = 8.0 Hz, 2H), 7.37 (t, *J* = 8.0 Hz, 2H), 7.71 (d, *J* = 8.0 Hz, 2H), 7.97 (s, 2H). ESI-MS: *m/z* = 1054.4 $[M+H]^+$. Elemental analysis: calculated for $C_{58}H_{88}N_{10}O_8$ C, 66.13; H, 8.42; N, 13.30. Found: C, 65.96; H, 8.35; N, 13.38.

Dumbbell 6b

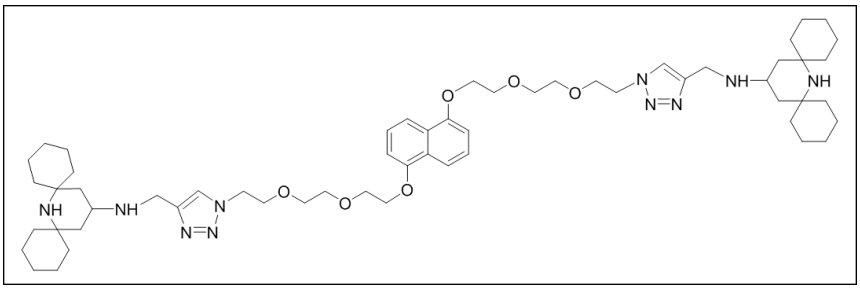

The above procedure was followed using diazide **1** (0.016 g, 0.034 mmol) and alkyne functionalized amine **5b** (0.024 g, 0.084 mmol) in DMF (1 mL), $Cu(CH_3CN)_4PF_6$ (0.002 g, 0.006 mmol) and TBTA (0.003 g, 0.006 mmol). Purification of the crude mixture by a silica gel column using CH_2Cl_2-MeOH 90 : 10 and then CH_2Cl_2-MeOH–30% NH_3 90 : 10 : 1 affords **6b** (0.0135 g, 39% yield). ^{1}H NMR (600 MHz, d_6-DMSO): δ 0.62 (t, J = 11.7 Hz, 4H), 1.10–1.70 (m, 40H), 1.90 (d, J = 11.7 Hz, 4H), 2.68–2.78 (m, 2H), 3.54–3.60 (m, 4H), 3.60–3.68 (m, 4H), 3.74 (s, 4H), 3.81 (t, J = 5.0 Hz, 4H), 3.82–3.84 (m, 4H), 4.20–4.26 (m, 4H), 4.48 (t, J = 5.0 Hz, 4H), 6.98 (d, J = 8.0 Hz, 2H), 7.37 (t, J = 8.0 Hz, 2H), 7.71 (d, J = 8.0 Hz, 2H), 7.87 (s, 2H). ESI-MS (positive): *m/z* = 1024.2 $[M+H]^+$. Elemental analysis: calculated for $C_{58}H_{90}N_{10}O_6$ C, 68.07; H, 8.86; N, 13.69. Found: C, 68.15; H, 8.80; N, 13.59.

Rotaxane 7a

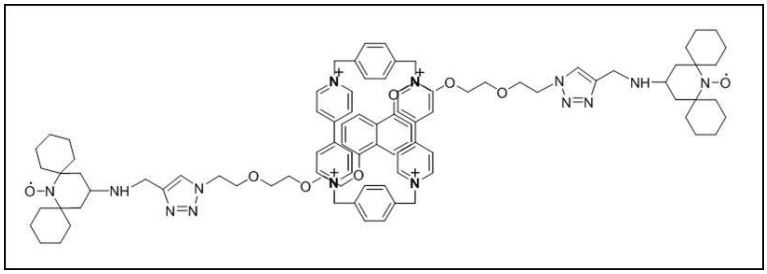

DNP diazide derivative **1** (0.012 g, 0.025 mmol), CBPQT·$4PF_6$ (0.022 g, 0.02 mmol) and the alkyne functionalized stopper **5a** (0.018 g, 0.062 mmol) were dissolved in DMF (0.200 mL) at

−10 °C under a N_2 atmosphere, forming a deep purple solution. TBTA (0.002 g, 0.004 mmol) and $Cu(CH_3CN)_4PF_6$ (0.0014 g, 0.004 mmol) were added to the solution and the resulting mixture was stirred at room temperature for 48 h, at which time the solvent was evaporated. The crude reddish solid was purified by column chromatography (SiO_2: 1% w/v NH_4PF_6 solution in Me_2CO, i.d. 10 mm, h 19.5 cm). The purple fractions in Me_2CO were collected, concentrated to a minimum volume, and the product was precipitated from this solution through the addition of an excess of cold water. The resulting solid was collected by filtration, and washed with H_2O to remove the excess of NH_4PF_6 to afford the [2]rotaxane **7a**·4PF6 as a purple powder (0.0162 g, 30% yield). ^{1}H NMR (600 MHz, CD_3CN): δ 2.42 (d, J = 7.2 Hz, 2H), 3.90 (br s, 8H), 4.01 (br s, 8H), 4.21 (br s, 4H), 4.30 (br s, 4H), 4.57 (br s, 4H), 5.67 (br s, 8H), 5.94–6.02 (m, 2H), 6.27 (d, J = 7.2 Hz, 2H), 7.21 (br s, 4H), 7.38 (br s, 4H). 7.98 (br s, 10H), 8.65 (br s. 4H), 8.92 (br s, 4H). The ^{1}H NMR spectrum of bis-*N*-hydroxy amine of **7a** (**7a-OH**) was recorded after *in situ* reduction of the sample containing the dinitroxide **7a** by using phenylhydrazine.
^{1}H NMR (600 MHz, CD_3CN): δ 1.06-1.12 (m, 8H), 1.22-1.40 (m, 16H), 1.50-1.70 (m, 20H), 1.85-1.90 (m, 4H), 2.41 (d, *J* = 8.4 Hz, 2H), 2.48-2.53 (m, 4H), 3.90 (br s, 8H), 3.98-4.06 (m, 8H), 4.21 (br s, 4H), 4.30 (br s, 4H), 4.55 (t, *J* = 5.4 Hz, 4H), 5.67 (br s, 8H), 5.98 (t, *J* = 7.8 Hz, 2H), 6.27 (d, J 7.2 Hz, 2H), 7.21 (br s, 4H), 7.38 (br s, 4H), 7.98 (bs, 10H), 8.65 (bs. 4H), 8.92 (bs, 4H). ESI-MS (positive): *m/z* = 2154.8 $[M+H]^+$. Elemental analysis: calculated for $C_{94}H_{120}F_{24}N_{14}O_8P_4$ C, 52.42; H, 5.62; N, 9.10. Found: C, 52.39; H, 5.70; N, 8.97. UV-Vis: λmax = 504 nm, ε = 4184 L mol^{-1} cm^{-1} in acetonitrile (ACN) at 298 K.

Rotaxane 7b

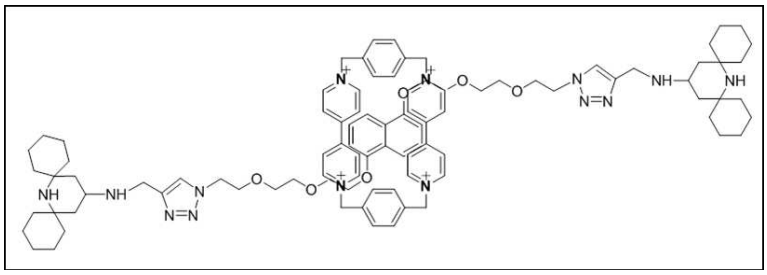

The above procedure was followed using the DNP derivative **1** (0.016 g, 0.034 mmol), CBPQT·4PF_6 (0.026 g, 0.027 mmol), the alkyne functionalized stopper **5b** (0.024 g, 0.085 mmol), DMF (0.200 mL), TBTA (0.0031 g, 0.006 mmol) and $Cu(CH_3CN)_4PF_6$ (0.0021 g, 0.006 mmol). The resulting [2]rotaxane **7b**·4PF6 was obtained as a purple powder (0.0186 g, 25% yield). ^{1}H NMR (600 MHz, d_6-DMSO): δ 1.12–1.20 (m, 4H), 1.34–1.48 (m, 8H), 1.50–1.70 (m, 28H), 1.80–1.90 (m, 4H), 2.08–2.18 (m, 4H), 2.31 (d, J = 7.8 Hz, 2H), 2.70–2.76 (m, 2H), 3.86–3.90 (m, 8H), 3.96–4.06 (m, 8H), 4.21 (m, 4H), 4.30 (m, 4H), 4.55–4.70 (m, 4H), 5.78 (br s, 8H), 5.84 (t, J = 7.8 Hz, 2H), 6.15 (d, J = 7.8 Hz, 2H), 7.63–7.78 (m, 8H), 8.09 (s, 8H), 8.24 (s, 2H), 9.11 (d, J = 6.5 Hz, 8H). ESI-MS (positive): *m/z* = 2124.8 $[M+H]^+$. Elemental analysis: calculated for $C_{94}H_{122}F_{24}N_{14}O_6P_4$ C, 53.16; H, 5.79; N, 9.23. Found: C, 52.99; H, 5.89; N, 9.15.

4,4'-bis((2-(2-(2-azidoethoxy)ethoxy)ethyl)thio)-2,2'-bi(1,3-dithiolylidene) (14)

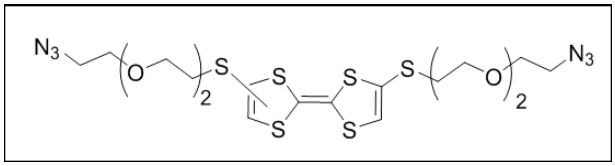

4,4'-Bis((2-(2-(2-iodoethoxy)ethoxy)ethyl)thio)-2,2'-bi(1,3-dithiolylidene) (**13**, 0.200 g, 0.294 mmol) and sodium azide (0.382 g, 5.88 mmol) were dissolved in DMF (3 mL) and heated to 80° C for 24 h. The crude reaction mixture was partitioned between 50 mL of H_2O and CH_2Cl_2, and the aqueous phase was washed with CH_2Cl_2 (3 x 25 mL). The combined organic extracts were washed with brine, dried ($MgSO_4$), and the solvent evaporated. The crude product was chromatographed (SiO_2, CH_2Cl_2 eluent) to give 135 mg (90% yield) of **14** as a pale yellow solid. ^{1}H NMR (600 MHz, d_6-DMSO): δ 2.98 (t, J = 6.3 Hz, 4H), 3.39 (t, J = 4.8 Hz, 4H), 3.55 (br s, 8H), 3.55-3.65 (m, 8H), 6.88 (s, 2H). ESI-MS (positive): m/z = 581.9 $[M+H]^+$, 604.9 $[M+Na]^+$.

Dumbbell 15a

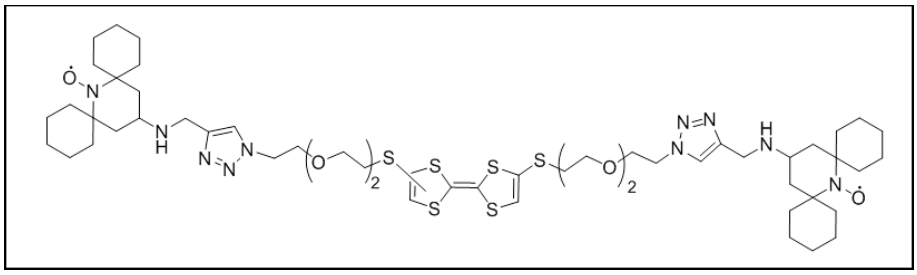

To a solution of the diazide TTF derivative **14** (0.021 g, 0.036 mmol) and alkyne functionalized nitroxide **5a** (0.026 g, 0.09 mmol) in DMF (1 mL), $Cu(CH_3CN)_4PF_6$ (0.0022 g, 0.006 mmol) and TBTA (0.0031 g, 0.006 mmol) were added, and the resulting mixture was stirred at room temperature for 24 h, at which time the solvent was evaporated. Purification of the crude mixture by a silica gel column using CH_2Cl_2–MeOH 90 : 10 affords biradical **15a** (0.021 g, 50% yield). ^{1}H NMR (600 MHz, CD_3CN): δ 2.93 (br s, 4H) 3.56 (br s, 8H), 3.61 (br s, 4H), 3.69 (br s, 4H), 3.83 (br s, 4H), 4.48 (br s, 4H), 6.50 (br s, 2H), 7.71 (br s, 2H). The ^{1}H NMR spectrum of bis-*N* hydroxy amine of **15a** (**15a-OH**) was recorded after *in situ* reduction of the sample containing the dinitroxide **15a** by using phenylhydrazine. ^{1}H NMR (600 MHz, CD_3CN): δ 0.78-0-90 (m, 4H), 1.00-1.11 (m, 4H), 1.22-1.32 (m, 12H), 1.33-1.46 (m, 8H), 1.50-1.68 (m, 16H), 1.84-1.92 (m, overlapped with CHD_2CN signal), 2.72-2.79 (m, 2H), 2.91-2.98 (m, 4H), 3.50-3.73 (m, 12H), 3.83 (br s, 4H), 3.89 (br s, 4H), 4.48 (br s, 4H), 6.54 (br s, 2H), 7.74 (br s, 2H). ESI-MS (positive): m/z = 1161.6 $[M+H]^+$. Elemental analysis: calculated for $C_{54}H_{84}N_{10}O_6S_6$ C, 55.83; H, 7.29; N, 12.06; S, 16.56. Found: C, 55.72; H, 7.33; N, 11.98; S, 16.44.

Dumbbell 15b

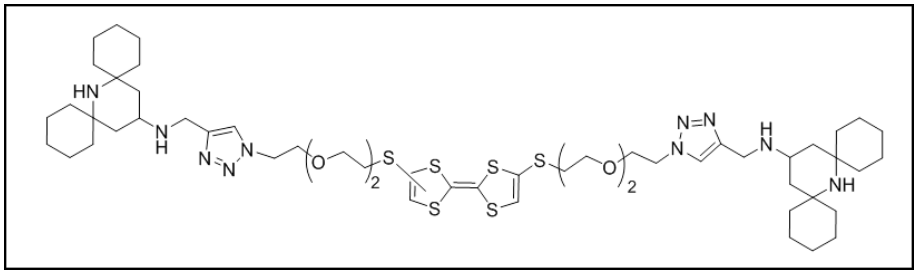

The above procedure was followed using the diazide TTF derivative **14** (0.021 g, 0.036 mmol), alkyne **5b** (0.026 g, 0.09 mmol) in DMF (1 mL), $Cu(CH_3CN)_4PF_6$ (0.0022 g, 0.006 mmol) and TBTA (0.0031 g, 0.006 mmol). Purification of the crude mixture by a silica gel column using CH_2Cl_2–MeOH–30% NH_3 70 : 30 : 1 affords biradical **15b** (0.015 g, 36%). ^{1}H NMR (600 MHz, CD_3CN): δ 0.70 (t, J = 12 Hz, 4H), 1.26–1.44 (m, 20H), 1.50–1.66 (m, 20H), 2.01 (dd, J = 12.0 and 2.4 Hz, 4H), 2.84 (tt, J = 12.0 and 2.4 Hz, 2H), 2.94 (t, J = 6.0 Hz, 4H), 3.51–3.56 (m, 8H), 3.59 (t, J = 6.1 Hz, 4H), 3.81 (t, J = 5.0 Hz, 4H), 3.86 (s, 4H), 4.47 (t, J = 5.0 Hz, 4H), 6.54 (s, 2H), 7.68 (s, 2H). ESI-MS (positive): *m/z* = 1131.5 $[M+H]^+$. Elemental analysis: calculated for $C_{54}H_{86}N_{10}O_4S_6$ C, 57.31; H, 7.66; N, 12.38; S, 17.00. Found: C, 57.72; H, 7.33; N, 12.26; S, 17.11.

Rotaxane 16a

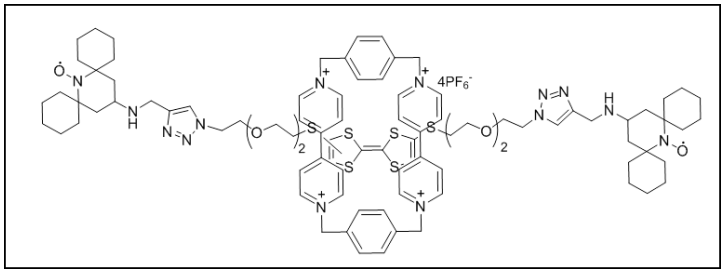

TTF diazide derivative **14** (0.012 g, 0.02 mmol), CBPQT·$4PF_6$ (0.017 g, 0.015 mmol) and the alkyne functionalized stopper **5a** (0.014 g, 0.051 mmol) were dissolved in DMF (0.200 mL) at room temperature under a N_2 atmosphere, forming a green solution. TBTA (0.0018 g, 0.003 mmol) and $Cu(CH_3CN)_4PF_6$ (0.0013 g, 0.003 mmol) were added to the solution and the resulting mixture was stirred at room temperature for 48 h, at which time the solvent was evaporated. The crude solid was purified by column chromatography (SiO_2: 1% w/v NH_4PF_6 solution in Me_2CO, i.d. 10 mm, h 19.5 cm). The green fractions in Me_2CO were collected, concentrated to a minimum volume, and the product was precipitated from this solution through the addition of an excess of cold water. The resulting solid was collected by filtration, and washed with water to remove the excess of NH_4PF_6 to afford the [2]rotaxane **16a**·4PF6 as a green powder (0.0114 g, 25%). ^{1}H NMR (600 MHz, CD_3CN): δ 3.07–3.13 (m, 4H), 3.66–3.76 (m, 12H), 3.83 (bs, 4H), 3.92–3.97 (m, 4H), 4.58 (br s, 4H), 5.74 (s, 8H), 5.96 (s, 1H), 6.00 (s, 1H), 7.71 (br s, 8H), 8.02 (br s, 10H), 9.02 (br s, 8H). The ^{1}H NMR spectrum of bis-*N*-hydroxy amine of **16a** (**16a-OH**)

was also recorded after *in situ* reduction of the sample containing the dinitroxide **16a** by using phenylhydrazine. ^{1}H NMR (600 MHz, CD_3CN): δ 0.78-0-90 (m, 4H), 1.20-1.77 (m, 40H), 1.90-2.00 (m, overlapped with water signal), 2.78-2.81 (m, 2H), 3.03-3.10 (m, 4H), 3.68-3.76 (m, 12H), 3.76-3.82 (m, 4H), 3.90-3.96 (m, 4H), 4.50-4.56 (m, 4H), 5.75 (s, 8H), 5.96 (s, 1H), 6.00 (s, 1H), 7.00(s, 2H), 7.74 (s, 8H), 8.04-8.10 (m, 10H), 9.07-9.15 (m, 8H). ESI-MS (positive): *m/z* = 2263.4 $[M+H]^+$. Elemental analysis: calculated for $C_{90}H_{116}F_{24}N_{14}O_6P_4S_6$ C, 47.78; H, 5.17; N, 8.67; S, 8.50. Found: C, 47.65; H, 5.25; N, 8.37; S, 8.40. UV-Vis: λmax = 796 nm, ε = 4780 L mol^{-1} cm^{-1} in ACN at 298 K.

Rotaxane 16b

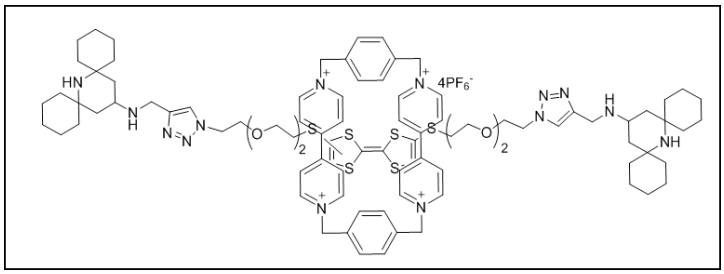

The above procedure was followed using the TTF derivative **14** (0.01 g, 0.017 mmol), CBPQT·$4PF_6$ (0.015 g, 0.013 mmol), the alkyne functionalized stopper **5b** (0.011 g, 0.042 mmol), DMF (0.200 mL), TBTA (0.0013 g, 0.002 mmol) and $Cu(CH_3CN)_4PF_6$ (0.0009 g, 0.002 mmol). The resulting [2]rotaxane **16b**·$4PF_6$ was obtained as a green powder (0.0129 g, 30%). ^{1}H NMR (600 MHz, d_6-DMSO): δ 1.10–1.20 (m, 4H), 1.30–1.45 (m, 12H), 1.52–1.72 (m, 28H), 1.82–1.89 (m, 4H), 2.10–2.16 (m, 4H), 2.70–2.76 (m, 2H), 3.13 (br s, 4H), 3.65–3.70 (m, 8H), 3.80–3.86 (m, 4H), 3.92 (br s, 4H), 4.46 (br s, 4H), 4.66 (br s, 4H), 5.82 (br s, 8H), 6.23 (s, 2H), 7.78 (s, 8H), 8.23 (s, 2H), 8.40–8.48 (m, 8H), 9.40–9.48 (m, 8H). ESI-MS (positive): *m/z* = 2233.4 $[M+H]^+$. Elemental analysis: calculated for $C_{90}H_{118}F_{24}N_{14}O_4P_4S_6$ C, 48.43; H, 5.33; N, 8.78; S, 8.62. Found: C, 48.20; H, 5.25; N, 8.67; S, 8.50.

Section 4.4

Synthetic procedures to obtain the bistable [2]rotaxane **18** and the free dumbbell **19** are reported in this section.
Compounds **20**,[15] **21**,[16] **24**,[17] were synthesized according to literature procedures.

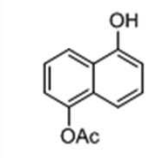

20

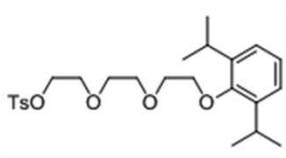

21

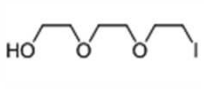

24

Synthesis of compound 23[18]

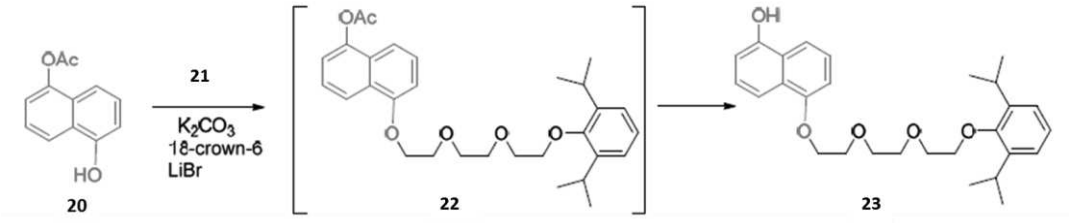

A solution of **21** (1.83 g, 3.94 mmol), 1-acetoxy-5-hydroxynaphalene **20** (0.399 g, 1.97 mmol), K_2CO_3 (0.817 g, 5.91 mmol), 18-crown-6 (0.052 g, 0.197 mmol), and LiBr (0.0085 g, 0.0986 mmol) in DMF (11mL) was heated under N_2 atmosphere at reflux for 24 h. After cooling down to room temperature, the reaction mixture was filtered and the solid was washed with dichloromethane (20 mL) and the combined organic filtrate was concentrated in vacuo. The residue was dissolved in dichloromethane (20 mL), washed with brine (2×10 mL), dried ($MgSO_4$), and the solvent evaporated. The crude product was chromatographed (SiO_2, h 5 cm, i.d. 5.5 mm cyclohexane/ethyl acetate 9:1). Fractions containing two close bands (products **22** and **23)** were subjected to a further chromatography (SiO_2, h 16 cm, i.d. 4.5 mm cyclohexane/ethyl acetate 1:1) to give 0.112 g of **22**, and 0.149 g (16% yield) of **23** as a pale yellow oil. The yield was not optimized. **23**: ^{1}H NMR (600 MHz, CD_3CN): δ 1.16 (d, *J* = 7.0 Hz, 12H), 3.39 (heptet *J* = 7.0 Hz, 2H), 3.69-3.72 (m, 2H), 3.75-3.79 (m, 4H), 3.84-3.87 (m, 2H), 3.94-3.97 (m, 2H), 4.24-4.27 (m, 2H), 6.89 (d, *J* = 7.7 Hz, 2H), 6.91 (d, *J* = 7.5 Hz, 1H), 7.04-7.11 (m, 3H), 7.27 (t, *J* = 7.7 Hz, 1H), 7.34 (t, *J* = 8.0 Hz, 1H), 7.55 (s, 1H), 7.75 (d, *J* = 8.6 Hz, 1H), 7.77 (d, *J* = 8.3 Hz, 1H). ESI-MS: *m/z* 451.0 $[M-H]^-$,487.0 $[M+Cl]^-$.

2-[2-[2-[2-[[2-[4-[[2-[2-[2-(2-hydroxyethoxy)ethoxy]ethoxy]ethyl]thio]-1,3-dithiol-2-ylidene]-1,3-dithiol-4-yl]thio]ethoxy]ethoxy]ethoxy]-ethanol (25)[19]

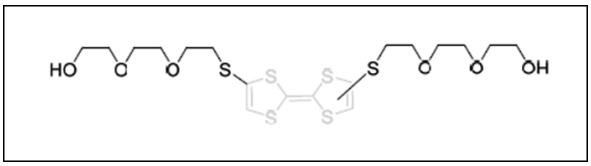

To a stirred solution of compound **11**[20] (0.14 g, 0.374 mmol) in dry degassed *N*,*N*-dimethylformamide (DMF) (4.3 mL) was added a solution of cesium hydroxide monohydrate (0.155 g, 0.923 mmol) in dry degassed methanol (1.4 mL) dropwise over 20 min under N_2. The color changed from orange to brown and the stirring was continued for another 30 min. 2-(2-(2-Iodoethoxy)ethoxy)ethan-1-ol **24** (1.6 g, 6.15 mmol) was then added dropwise, and the brown solution was stirred for 24 h before it was concentrated *in vacuo*. The residue was dissolved in dichloromethane (20 mL), washed with brine (2x10 mL), dried ($MgSO_4$), and the solvent evaporated. The crude product was chromatographed (SiO_2, ethyl acetate and then ethyl acetate/MeOH 9:1) to give 0.135 g (78% yield) of **25** as a brown yellow oil. ^{1}H NMR (600 MHz, CD_3CN): δ 2.72 (t, *J* = 6.0 Hz, 1H), 2.73 (t, *J* = 6.0 Hz, 1H), 2.95 (t, *J* = 6.0 Hz, 4H), 3.48 (t, *J* =

6.0 Hz, 4H), 3.55-3.58 (m, 8H), 3.64 (t, *J* = 6.0 Hz, 4H), 6.57 (s, 2H). ESI-MS: *m/z* = 554.25 $[M+Na]^+$.

Compound 26[20]

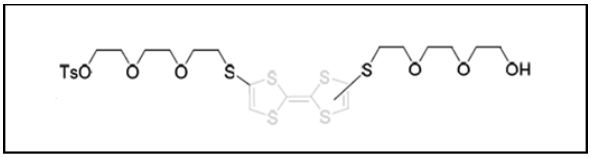

TsCl (0.027 g, 0.144 mmol) dissolved in anhydrous CH_2Cl_2 (1.5 mL) was added dropwise over a period of 5 min to an ice-cooled solution of **25** (0.086 g, 0.161 mmol), Et_3N (0.0356 g, 0.352 mmol, 50 mL) and DMAP (0.008 g, cat.) in anhydrous CH_2Cl_2 (1 mL). The reaction mixture was stirred overnight (0°C to rt), whereupon it was washed with satured $NaHCO_3$ solution, brine, dried ($MgSO_4$), and the solvent evaporated. The crude product was chromatographed over silica gel column eluting with cyclohexane/ethyl acetate 6:4 and then ethyl acetate. The second band containing the desired product was collected and concentrated to give 0.060 g (54% yield) of **26**. ^{1}H NMR (600 MHz, CD_3CN): δ 2.44 (s, 3H), 2.68 (t, *J* = 6.0 Hz, 1H), 2.92 (t, *J* = 6.1 Hz, 2H), 2.95 (t, *J* = 6.1 Hz, 2H), 3.46-3.50 (m, 6H), 3.56 (s, 4H), 3.57-3.62 (m, 6H), 3.63 (t, *J* = 6.1 Hz, 2H), 4.09-4.12 (m, 2H), 6.53 (s, 1H), 6.56 (s,1H), 7.44 (d, *J* = 7.8 Hz, 2H), 7.78 (d, *J* = 7.8 Hz, 2H). ESI-MS: *m/z* = 709.65 $[M+Na]^+$.

Compound 27

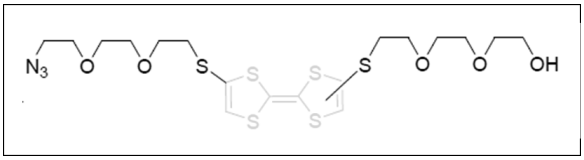

Compound **26** (0.172 g, 0.25 mmol) and sodium azide (0.162 g, 2.5 mmol) were dissolved in DMF (20 mL) and heated to 80° C for 24 h. After removal of the solvent *in vacuo* the crude was partitioned between 50 mL of water and CH_2Cl_2, and the aqueous phase was washed with CH_2Cl_2 (3×25 mL). The combined organic extracts were washed with brine, dried ($MgSO_4$), and the solvent evaporated to give 0.112 g (80% yield) of **27**. ^{1}H NMR (600 MHz, CD_3CN): δ 2.69 (*br* t, *J* = 4.4 Hz, 1H), 2.95 (t, *J* = 6.1 Hz, 4H), 3.34-3.38 (m, 2H), 3.49 (t, *J* = 4.4 Hz, 2H), 3.55-3.60 (m, 10H), 3.61-3.66 (m, 6H), 6.55 (s, 1H), 6.57 (s, 1H). ESI-MS: *m/z* = 580.58 $[M+Na]^+$.

Compound 28

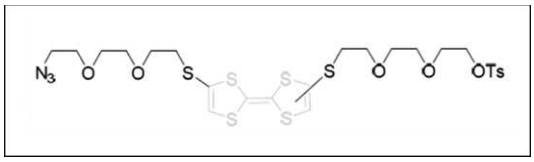

TsCl (0.152 g, 0.8 mmol) dissolved in anhydrous CH_2Cl_2 (6 mL) was added dropwise over a period of 15 min to an ice-cooled solution of **27** (0.112 g, 0.2 mmol), Et_3N (0.081 g, 0.8 mmol, 112 mL) and DMAP (0.008 g, cat.) in anhydrous CH_2Cl_2 (7 mL). The reaction mixture was stirred overnight (0°C to rt), whereupon it was washed with satured $NaHCO_3$ solution, brine, dried ($MgSO_4$), and the solvent evaporated. The crude product was chromatographed over silica gel column eluting with cyclohexane/ethyl acetate 6:4. The band containing the desired product was collected and concentrated to give 0.110 g (78% yield) of **28**. ^{1}H NMR (600 MHz, CD_3CN): δ 2.44 (s, 3H), 2.92 (t, *J* = 6.1 Hz, 2H), 2.94 (t, *J* = 6.1 Hz, 2H), 3.36 (t, *J* = 5.0 Hz, 2H), 3.47-3.50 (m, 4H), 3.56-3.66 (m, 12H), 4.09-4.12 (m, 2H), 6.54 (s, 2H), 7.44 (d, *J* = 8.0 Hz, 2H), 7.78 (d, *J* = 8.0 Hz, 2H). ESIMS: *m/z* = 735.0 $[M+Na]^+$.

Compound 29[18]

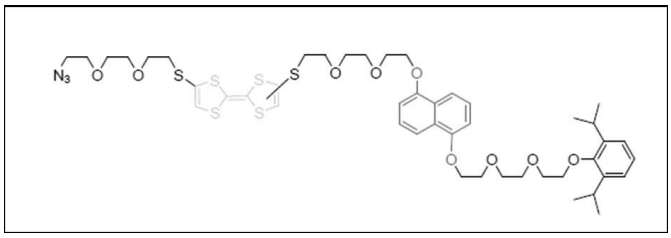

A solution of **28** (0.119 g, 0.167 mmol), 5-monosubstituted-1-hydroxynaphtalene **23** (0.0756 g, 0.167 mmol), K_2CO_3 (0.046 g, 0.057 mmol), 18-crown-6 (0.005 g, 0.0189 mmol), and LiBr (0.005 g, 0.0576 mmol) in acetonitrile (25 mL) was heated under N_2 atmosphere at reflux for 16 h. After cooling down to room temperature, the reaction mixture was filtered and the solid was washed with dichloromethane (20 mL) and the combined organic filtrate was concentrated in vacuo. The residue was dissolved in dichloromethane (50 mL), washed with brine (2×20 mL), dried ($MgSO_4$), and the solvent evaporated. The crude product was chromatographed (SiO_2, h 15 cm, i.d. 3mm cyclohexane/ethyl acetate 1:1) to give 0.084 g of **29** (50.7 % yield) as a pale yellow oil. ^{1}H NMR (600 MHz, CD_3CN): δ 1.16 (d, *J* = 7.2 Hz, 12H), 2.89-2.94 (m, 4H), 3.34 (t, *J* = 4.8 Hz, 2H), 3.38 (quint. *J* = 7.2 Hz, 2H), 3.53-3.57 (m, 4H), 3.59-3.65 (m, 8H), 3.68-3.73 (m, 4H), 3.76-3.80 (m, 4H), 3.84-3.86 (m, 2H), 3.91-3.93 (m, 2H), 3.97-3.99 (m, 2H), 4.25-4.28 (m, 2H), 4.28-4.31 (m, 2H), 6.49 (s, 1H), 6.51 and 6.53 (s, 1H, cis-trans), 6.93 (d, *J* = 8.4 Hz, 1H), 6.94 (d, *J* = 8.4 Hz, 1H), 7.05-7.12 (m, 3H), 7.36 (t, *J* = 8.4 Hz, 1H), 7.38 (t, *J* = 8.4 Hz, 1H), 7.80 (d, *J* = 8.4 Hz,1H), 7.81 (d, *J* = 8.4 Hz, 1H). ESI-MS: *m/z* = 991.0 $[M+H]^+$, 1013.9 $[M+Na]^+$, 1030.1 $[M+K]^+$.

Dumbbell 19

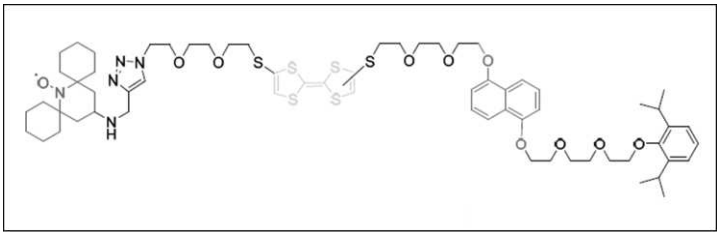

To a solution of azide **29** (0.013 g, 0.013 mmol) and alkyne functionalized nitroxide **5a** (0.0048 g, 0.0166 mmol) in acetonitrile (0.15 mL), $Cu(CH_3CN)_4PF_6$ (0.0007 g, 0.0019 mmol) and TBTA (0.001 g, 0.0019 mmol) were added at room temperature under N_2 atmosphere, and the resulting mixture was stirred at room temperature for 72 h, at which time the solvent was evaporated. Purification of the crude by silica gel column using acetone affords radical **19** (0.0083 g, 50% yield). ^{1}H NMR (600 MHz, CD_3CN): δ 1.16 (d, J = 6.8 Hz, 12H), 2.89-3.02 (m, 4H), 3.16-3.26 (m, 2H), 3.35-3.41 (m, 2H), 3.49-4.00 (m, 24H), 4.20-4.32 (m, 4H), 4.50-4.60 (m, 2H), 6.89-6.96 (m, 2H), 7.04-7.13 (m, 3H), 7.27-7.60 (m, 3H), 7.76-7.82 (m, 2H). ESI-MS: *m/z* = 1280.5 $[M+H]^+$.

Rotaxane 18

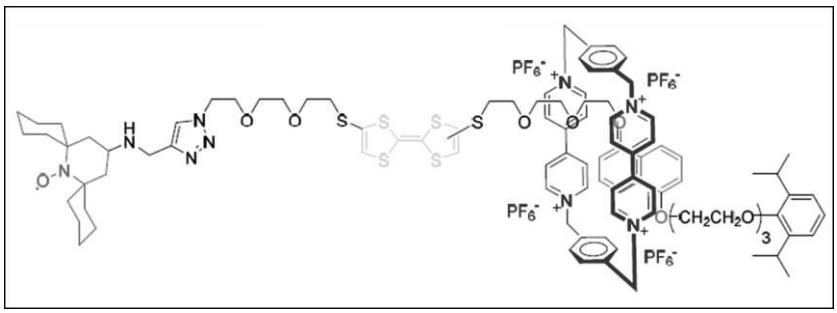

Azide derivative **29** (0.018 g, 0.018 mmol), CBPQT•$4PF_6$ (0.020 g, 0.018 mmol) and the alkyne functionalized stopper **5a** (0.0065 g, 0.0225 mmol) were dissolved in DMF (0.141 mL) at -10 °C under N_2 atmosphere, forming a brown solution. TBTA (0.00145 g, 0.0027 mmol) and $Cu(CH_3CN)_4PF_6$ (0.001 g, 0.0027 mmol) were added to the solution and the resulting mixture was stirred at room temperature for 48 h, at which time the solvent was evaporated. The crude solid was purified by column chromatography (SiO_2: 1% w/v NH_4PF_6 solution in Me_2CO, i.d. 10 mm, h 16 cm). The fractions in Me_2CO containing the desired product were collected, concentrated to a minimum volume, and the product was precipitated from this solution through the addition of an excess of cold water. The resulting solid was collected by filtration, washed with water (35 mL) to remove the excess of NH_4PF_6, and dried by vacuum pump to afford the [2]rotaxane **18** as a brown-reddish powder (0.019 g, 44% yield). ^{1}H NMR (600 MHz, CD_3CN): δ 1.10 (d, J = 6.5 Hz, 12H), 2.44 (*br* s, 2H), 2.88-3.10 (m, 4H), 3.25-3.30 (m, 2H), 3.45-4.14 (m, 24H), 4.20-4.38 (m, 6H), 4.54-4.62 (m, 2H), 5.60-5.90 (m, 8H), 5.92-6.05 (m, 2H), 6.23-6.32

(m, 2H), 7.05-7.12 (m, 3H), 7.15-7.27 (m, 4H), 7.30-7.45 (m, 4H), 7.90-8.20 (m, 9H), 8.98-9.01 (m, 2H) 9.02-9.10 (m, 2H). ESI-MS: *m/z* = 2382.7 $[M+H]^+$, 2236.9 $[M-PF_6]^+$.

References

[1] N. Zhao, G. O. Lloydb and O. A. Scherman *Chem. Comm.*., **2012**, *48*, 3070-3072.

[2] a) M. Mannini, S. Cicchi, D. Berti, A. Caneschi, A. Brandi, L. Lascialfari, L. Sorace, *ChemPlusChem*., **2013**, *78*, 149-156; b) N. G. Bushmakina, A. Y. Misharin, *Synthesis*, **1986**, 966.

[3] N. L. Strutt, R. S. Forgan, J. M. Spruell, Y. Y. Botros, J. F. Stoddart , *J. Am. Chem. Soc.,* **2011**, *133*, 5668-5671

[4] R. Manoni, P. Neviani, P. Franchi, E. Mezzina, M. Lucarini, *Eur. J. Org. Chem.*, **2014**, 147-151.

[5] T. Ogoshi, T. Aoki, K. Kitajima, S. Fujinami, T. Yama *J. Org. Chem.*., **2011**, *76*, 328-331.

[6] T. Ogoshi, S. Kanai, S. Fujinami, T. Yamagishi and Y. Nakamoto, *J. Am. Chem. Soc.*, **2008**, *130*, 5022-5023.

[7] A. Rajca, V. Kathirvelu, S. K. Roy, M. Pink, S. Rajca, S. Sarkar, S. S. Eaton and G. R. Eaton, *Chem. Eur. J.*, **2010**, *16*, 5778-5782.

[8] K. Sakai, K. Yamada, T. Yamasaki, Y. Kinoshita, F. Mito and H. Utsumi, *Tetrahedron,* **2010**, *66*, 2311-2315.

[9] W. R. Dichtel, O. Ŝ. Miljanic´, J. M. Spruell, J. R. Heath and J. F. Stoddart, *J. Am. Chem. Soc.,* **2006**, *128*, 10388-1039.

[10] S. J. Rowan and J. F. Stoddart, *Org Lett.*, **1999**, *1*, 1913-1916

[11] P. R. Ashton, J. Huff, S. Menzer, I. W. Parsons, J. A. Preece, J. F. Stoddart, M. S. Tolley, A. J. P. White and D. J. Williams, *Chem. Eur. J.*, **1996**, *2*, 31-44.

[12] C. Jia, D. Zhang, W. Xu and D. Zhu, *Org. Lett.*, **2001**, *3*, 1941-1944.

[13] X. Guo, D. Zhang, H. Zhang, Q. Fan, W. Xu, X. Ai, L. Fan and D. Zhu, *Tetrahedron*, **2003**, 4843-4850.

[14] G. Trippé, F. Le Derf, M. Mazari, N. Mercier, D. Guilet, P. Richomme, A. Gorgues, J. Becher and M. Sallé, *C. R. Chimie* **2003**, *6,* 573-580.

[15] J. Becher, O. A. Matthews, M. B. Nielsen, F. Raymo, J. F. Stoddart, *Synlett*, **1999**, 330-332.

[16] T. Ikeda, M.Higuchi, *Tetrahedron*, **2011**, *67*, 3046-3052.

[17] S. Arumugam, V. V. Popik, *J. Am. Chem. Soc.*, **2011**, *133*, 15730-15736.

[18] D. W. Steuerman, H. -R. Tseng, A. J. Peters, A. H. Flood, J. O. Jeppesen, K. A. Nielsen, J. F. Stoddart, J. R. Heath, *Angew. Chem. Int. Ed.*, **2004**, *43*, 6486-6491.

[19] a) T. Akutagawa, T. Ohta, T. Hasegawa, T. Nakamura, C. A. Christensen, J. Becher, *PNAS,* **2002**, *99*, 5028-5033; b) M. B. Nielsen, Z.-T. Li, J. Becher, *J. Mater. Chem.*, **1997**, *7*, 1175-1187; c) J. G. Hansen, K. S. Bang, N. Thorup, J. Becher, *Eur. J. Org. Chem.*, **2000**, 2135-2144. X. Guo, D. Zhang, H. Zhang, Q. Fan, W. Xu, X. Ai, L. Fan, D. Zhu, *Tetrahedron*, **2003**, *59*, 4843-4850.

[20] C. P. Collier, J. O. Jeppesen, Y. Luo, J. Perkins, E. W. Wong, J. R. Heath, J. F. Stoddart, *J. Am. Chem. Soc.,* **2001**, *123*, 12632-12641. **2001**, *123*, 12632-12641.